Characterisation of the Non-Canonical Translation Initiation Factor eIF4E-3 as a Merlin Interacting Protein in *Drosophila melanogaster*

by

Kirsten Julia Arnold

A thesis submitted in partial fulfillment of the requirements for the degree of

Master of Science

in

Medical Sciences – Medical Genetics

University of Alberta

Abstract

Merlin is a tumour suppressor protein, the loss of which is linked to the inherited nervous system tumour syndrome Neurofibromatosis type 2 as well as sporadic tumour development. It is related to the ERM (ezrin-radixin-moesin) protein family, which is involved in linking the cytoskeleton to membrane associated proteins and thereby coordinating processes such as cell shape and polarity. However, Merlin's activity as a tumour suppressor is not clearly defined, nor is it clear why tumours form primarily in the nervous system although Merlin is broadly expressed. Merlin has numerous interacting partners, and a possible explanation for nervous system specific tumour development is that one or more Merlin interacting proteins modifies its tumour suppressor activity in these cell types. In *Drosophila melanogaster*, a non-canonical translation initiation factor eIF4E-3 was previously identified as genetically interacting with Merlin. In this study, the interaction between Merlin and eIF4E-3 was further characterised in the nervous system and male germline of *Drosophila* as eIF4E-3 expression appears to be restricted to these tissues. Thus, eIF4E-3 may be a candidate for cell type specific modification of Merlin activity. Merlin and eIF4E-3 genetically interact to affect the abundance of neuroblasts in the larval central brain, morphology of the mature testis, and subcellular localisation of eIF4E-3 and Merlin in spermatocytes. Preliminary evidence indicates that Merlin and eIF4E-3 may be able to both increase and decrease translation of transcripts identified as bound to both proteins *in vivo*, suggesting multiple translational regulatory complexes including Merlin and eIF4E-3 may be formed.

Preface

This thesis is an original work by Kirsten Julia Arnold. No part of this thesis has been previously published.

Acknowledgements

A multitude of thanks goes to my supervisor, Dr. Sarah Hughes, for supporting and encouraging me through the ups and downs of my thesis work and beyond. If not for her positivity and her patience, I would have been lost within the turns this project has taken. I am so grateful to have had the opportunity to first experience research in her lab during my undergraduate degree, and moreover to have been able to spend the past few years in the lab as a graduate student, learning about a very specific aspect of biology and about life in general.

I also want to thank my supervisory committee, Dr. Roseline Godbout and Dr. Shelagh Campbell, for their insightful and helpful comments on my work and for keeping me focussed when I wanted to take my project in too many directions.

Thank you to David Primrose for technical assistance and pleasant conversation, and for reliably being a friendly smiling face, which is especially nice early in the morning!

Thank you to Namal Abeysundara, for mentoring me and showing me the ropes as an undergraduate student, for being someone I can look up to and go to for advice with experiments, and especially for being a great friend. It has meant a lot to me to have someone to talk to and to encourage me to do things outside the lab, especially when experiments weren't going so well!

Thanks to Dr. Andrew Simmonds for all the advice, both science-related and general, and for persistence in trying to get me to balance out seriousness with silliness – I'll keep working on it. I have really appreciated all of our conversations, silly and serious alike, and even (especially?) the ones that were just plain strange.

I want to also extend my gratitude to past members of the Hughes lab and to the Simmonds lab for making the work environment a pleasant one and for valuable lab meeting discussions.

Finally, thanks to my family for being patient with me when I came home late and frustrated and for listening to stories about my day even though much of what I talked about made no sense to them.

Table of Contents

List of Tables

List of Figures

Chapter 1 Introduction

1.1 | Neurofibromatosis Type 2

1.1.1 Genetics of Neurofibromatosis Type 2

Neurofibromatosis type 2 (NF2) is a tumour syndrome that is inherited in an autosomal dominant fashion (Asthagiri et al. 2009). It is caused by mutation in the gene *Neurofibromin 2* (*NF2*), which is located at chromosome 22q12 and encodes the tumour suppressor protein merlin (Rouleau et al. 1993; Trofatter et al. 1993). Tumour manifestations follow the two-hit model (Knudson 1971): one mutated copy of *NF2* is inherited and tumours arise from cells in which the second allele is mutated somatically. Loss or inactivation of both *NF2* alleles is also the most common genetic driver of sporadic meningiomas, and is associated with sporadic schwannomas and ependymomas (Riemenschneider, Perry, and Reifenberger 2006; Dumanski et al. 1987; Gonzalez-Gomez et al. 2003; Gutmann et al. 1997; Lomas et al. 2005) as well as a variety of malignant non-nervous system cancers, including mesothelioma (Bianchi et al. 1995; Sekido et al. 1995), melanoma (Bianchi et al. 1994; Murray, Lau, and Yu 2012), breast cancer (Yaegashi et al. 1995; Sjöblom et al. 2006), and colorectal cancer (Cačev et al. 2014). Severity of NF2 can vary in terms of disease features present, age of onset, tumour burden, and early mortality, and *NF2* mutation type is often correlated with disease severity – mutations causing frameshift, truncation, or altering a splice site within the first five exons are linked to more severe presentation, whereas missense mutations, in-frame deletions, and other splice site mutations correspond with milder disease (Ruttledge et al. 1996; Parry et al. 1996; Evans et al. 1998; Baser et al. 2002; Baser et al. 2004; Baser et al. 2005). Mosaicism is also frequent in NF2, leading to disease heterogeneity; it is estimated that at least 33% of people diagnosed with NF2 without a family history of the disease and having bilateral schwannomas of the auditory nerve are genetically mosaic for *NF2* (Evans et al. 2007; Evans, Wallace, et al. 1998; Kluwe et al. 2003). Generally, disease features are similar within affected families, supporting the genotype-phenotype correlation, but variation is sometimes seen within families (Kluwe

and Mautner 1996; Mautner, Baser, and Kluwe 1996; Bruder et al. 1999) and among individual tumours (Asthagiri et al. 2009). It has been suggested that some variability in manifestations and progression of NF2 may be owing to modifier loci (Bruder et al. 1999).

1.1.2 Disease manifestations

NF2 is estimated to occur in 1/25 000 live births and show complete penetrance by age 60 (Evans et al. 2005). It is heterogeneous in appearance, with manifestations in the nervous system, eyes, and skin; however, the hallmark of the syndrome is the development of bilateral schwannomas on the eighth cranial (auditory) nerves. These tumours almost never progress to metastasis, but can cause significant problems including hearing loss and tinnitus, loss of balance, dizziness, compression of the facial nerve, and compression of the brainstem (Blakeley et al. 2012; Slattery 2015). Schwannomas may also form on other cranial nerves, most commonly the trigeminal or oculomotor nerves (Slattery 2015), or on spinal or peripheral nerves, or in the skin (Asthagiri et al. 2009; Parry et al. 1994; Mautner et al. 1997). In addition, other nervous system tumour types are seen at higher incidence in people with NF2 compared with the general population, such as meningiomas, ependymomas, astrocytomas, and neurofibromas (McClatchey 2007; Asthagiri et al. 2009). These tumours can arise in the brain, spinal cord, or peripheral nerves; although generally benign, they can cause morbidity by exerting pressure on the nervous system. Tumours in the brain may cause headaches or migraines, loss of vision, speech, or memory, or lead to seizures (McClatchey 2007; Slattery 2015), while nerve compression from spinal or peripheral nerve tumours can lead to numbness, loss of motion, and potentially paralysis (Slattery 2015). Polyneuropathy can also be observed without tumours compressing the nerve, demonstrating a non-tumour related disease manifestation (Hanemann, Diebold, and Kaufmann 2007; Schulz et al. 2013). Other non-tumour presentations include the formation of juvenile cataracts and epiretinal membranes (Bouzas et al. 1993; Parry et al. 1994; Bosch et al. 2006).

1.1.3 Treatments for NF2

As the tumours that arise as a result of NF2 are nearly exclusively benign, they are generally not immediately acted upon, but monitored (McClatchey 2007). Tumours that cause morbidity are most often treated by surgical removal, although proximity of the tumours to nerve structures renders a high risk of nerve damage during surgery and makes it likely that not all of the tumour will be removed, allowing it to regrow (McClatchey 2007; Blakeley et al. 2012). Chemotherapeutic agents are largely ineffective as a treatment for NF2, potentially due to the slow growth rate of the tumours (Blakeley et al. 2012). Alternatively, radiotherapy may be effective in managing some NF2 tumours; however, it adds the risk of development of malignant tumours resulting from radiation (Baser et al. 2000; Balasubramaniam et al. 2007), and would not be useful in patients with a large tumour burden. Therefore, it is important to understand at a molecular level how tumours arise and progress in people with NF2 in order to consider targeted therapeutic interventions.

1.2 | Merlin

1.2.1 Merlin structure and relationship to ERM proteins

The *NF2* gene product merlin (**m**oesin-**e**zrin-**r**adixin-**l**ike protein) is so named for its structural similarity to the ezrin, radixin, and moesin (ERM) cytoskeleton-associated proteins (Trofatter et al. 1993; Rouleau et al. 1993). ERM proteins provide a link between the actin cytoskeleton and transmembrane or membrane-associated proteins (Tsukita et al. 1994; Reczek, Berryman, and Bretscher 1997; Yonemura et al. 1998; Jankovics et al. 2002), and function as membrane domain organisers, important for epithelial integrity, polarity, and structures such as microvilli (Fehon, McClatchey, and Bretscher 2010; Louvet et al. 1996; Polesello et al. 2002; Speck et al. 2003; Saotome, Curto, and McClatchey 2004). Merlin shares some binding partners with the ERM proteins, including F-actin (James et al. 2001), the cell adhesion protein CD44 (Morrison et al. 2001), and Rho-GDI (Maeda et al. 1999), which inhibits activation of Rho, a regulator of actin cytoskeleton organisation. However, merlin clearly also has a unique function from

the ERM proteins as it functions as a tumour suppressor, negatively regulating growth (Tikoo et al. 1994; Lutchman and Rouleau 1995). Merlin and the ERM proteins have similar domain structures, with an N-terminal FERM (band **f**our-point-one, **e**zrin, **r**adixin, **m**oesin) domain, an α-helical coiled-coil domain, and a short C-terminal domain (Rouleau et al. 1993; Bretscher, Edwards, and Fehon 2002). ERM proteins link the cytoskeleton to membrane associated proteins by binding actin via a conserved domain in the C-terminus (Algrain et al. 1993; Turunen, Wahlström, and Vaheri 1994; Pestonjamasp et al. 1995), but the C-terminal actin-binding region is not conserved in merlin (Turunen, Wahlström, and Vaheri 1994; Gary and Bretscher 1995). Instead, merlin binds actin via a region in the N-terminal FERM domain (Xu and Gutmann 1998; James et al. 2001). The C-terminal domain of merlin can also interact with the FERM domain of the same protein to form a closed conformation, or the FERM domain of ERM-merlin family members ezrin and moesin (Gary and Bretscher 1995; Gonzalez-Agosti et al. 1999; Grönholm et al. 1999; Pearson et al. 2000). Intramolecular interaction in ERM proteins is inactivating as it inhibits both the FERM and C-terminal domains from interacting with other partners (Gary and Bretscher 1995; Pearson et al. 2000), but while this conformational state also prevents merlin interaction with F-actin and membrane proteins, intramolecular binding is required for the tumour suppressive activity of merlin (Sherman et al. 1997; Gonzalez-Agosti et al. 1999; James et al. 2001; Shaw et al. 2001). The FERM domain of merlin, while structurally very similar to that of the ERM proteins, contains a series of residues known as the 'blue box' that differ from the ERM proteins, but are conserved in *Drosophila* and human merlin (LaJeunesse, McCartney, and Fehon 1998) and are located on the surface of the protein (Kang et al. 2002), suggesting that this region may be necessary for binding interactions and differentiate the function of merlin from ezrin, radixin, and moesin. In fact, deletion or mutation of these residues to a stretch of alanine results in a dominant-negative phenotype, causing over-proliferation when expressed in the *Drosophila* wing (LaJeunesse, McCartney, and

Fehon 1998), as well as disrupting adherens junctions and leading to malignant transformation in mammalian cells (Johnson et al. 2002; Lallemand et al. 2003).

1.2.2 Function of merlin in organisation of the actin cytoskeleton

Part of merlin function involves influencing the arrangement of the actin cytoskeleton, which may be achieved through multiple mechanisms. Merlin-deficient schwannoma cells have abnormal organisation of actin causing disorganised stress fibres and membrane ruffling (Pelton et al. 1998). These cytoskeletal phenotypes are rescued by expression of merlin (Bashour et al. 2002) or by dominant negative forms of Rho and Rac GTPases (Pelton et al. 1998), indicating that merlin normally functions to inhibit activation of Rho and Rac, members of the Rho family of small GTPases which function, in part, to promote actin remodeling (Hall 1998). In Schwann cells, negative regulation of the Rho GTPases RhoA, Rac1, and Cdc42 by merlin has been confirmed by numerous studies and linked to activities that are related to tumour formation and progression, including cytoskeleton organisation as well as inhibition of growth, migration, angiogenesis, and formation of focal adhesions (Shaw et al. 2001; Morrison et al. 2007; Flaiz et al. 2007; Flaiz et al. 2009; Zhan et al. 2011; Wong et al. 2012). Rac, in turn, phosphorylates merlin leading to merlin inactivation, thus forming a negative regulatory loop (Shaw et al. 2001). Conversely, merlin can bind RhoGDI in epithelial cells (Maeda et al. 1999), and in peripheral nerve axons, merlin isoform-2 binds RhoGDI and p190RhoGAP, promoting activation of Rho and subsequent phosphorylation of neurofilaments which is required for the maintenance of axonal integrity (Schulz et al. 2013). The ability of merlin to both upregulate and downregulate activity of the Rho GTPases suggests that merlin function may differ among cell types, perhaps depending on the availability of interacting partners. However, the Rho GTPase family is not the only mechanism by which merlin can modify actin structures; another modulator of actin cytoskeleton organisation, N-WASP is also negatively regulated by merlin (Manchanda et al. 2005). Furthermore, although regulation of Rho GTPases or N-WASP does not necessitate direct association of merlin with actin, binding of merlin to F-actin

has been found to be necessary for re-organisation of the cytoskeleton and formation of actin-based cell membrane protrusions, although this activity is not linked to its ability to suppress Schwann cell growth (Lallemand, Saint-Amaux, and Giovannini 2009). Merlin's activity in regulating organisation of the actin cytoskeleton is one of several currently identified ways merlin inhibits growth and tumour progression in NF2 and in other tumours.

1.2.3 Merlin activity in adhesion and contact-dependent inhibition of growth

Merlin has a role in sensing intercellular contact and inhibiting proliferation when this contact is established. Merlin localises to sites of cell-cell contact in *Drosophila* (McCartney and Fehon 1996). Similarly, merlin is present at adherens junctions of mammalian cells and interacts with adherens junction components, potentially linking these structures to the actin cytoskeleton (Lallemand et al. 2003; Gladden et al. 2010), and is also a component of a complex with angiomotin associated with the tight junction (Yi et al. 2011). Specifically in schwannoma primary cell culture, loss of merlin leads to a lack of mature adherens junctions, disrupting cell-cell adhesion (Flaiz et al. 2008). Loss of intercellular adhesion likely contributes to the ability of merlin-deficient cells to overcome contact-dependent inhibition of proliferation, promoting both tumour formation and metastasis. In contrast to decreasing cell-cell adhesion, loss of merlin appears to increase adhesion to the extracellular matrix. Using cultured Schwann cells, merlin has been shown to bind β1 integrin, paxillin, and CD44 transmembrane receptor (Obremski, Hall, and Fernandez-Valle 1998; Fernandez-Valle et al. 2002; Morrison et al. 2001), which are all linked to the extracellular matrix, and overexpression of merlin decreases cell attachment (Gutmann et al. 1999). Additionally, merlin-deficient schwannoma cells were found to form more focal contacts, leading to increased adhesion to the extracellular matrix (Flaiz et al. 2009). Merlin association with extracellular matrix-contacting proteins is also likely important in its role in inhibiting proliferation dependent on contact with the extracellular matrix and places it in a position to respond to signals from the extracellular matrix.

1.2.4 Merlin regulates signalling pathways to inhibit proliferation

Merlin can disrupt signalling by directly binding signalling pathway components. For example, merlin binding to PI3-kinase activator PIKE-L inhibits activation of PI3-kinase by preventing its interaction with PIKE-L (Rong et al. 2004). PI3-kinase signalling is important for Schwann cell survival (Li et al. 2001), and phosphorylated PI3-kinase and downstream targets including AKT and mTOR have been shown to be elevated in schwannomas (Jacob et al. 2008; Hilton, Ristic, and Hanemann 2009). Merlin also inhibits activation of mTORC1 through an unknown mechanism which appears to depend on extracellular matrix anchorage via integrins (James et al. 2009; Lopez-Lago et al. 2009). Recently, merlin has been shown to affect gene expression through microRNA regulation by binding Lin28, an inhibitor of the *let-7* microRNA (Hikasa, Sekido, and Suzuki 2016). *let-7* represses translation of growth-promoting factors, so merlin binding and sequestration of Lin28 negatively regulates proliferation by permitting *let-7* activity.

In mammalian cells, interaction of merlin with the actin cytoskeleton prevents downstream EGFR signalling by inhibiting its internalisation (Curto et al. 2007; Cole et al. 2008). Recently, roles of merlin in cytoskeleton organisation, cellular adhesion formation, interaction with ERM proteins, and inhibition of proliferation were found to be integrated: loss of merlin in mouse liver-derived epithelial cells leads to increased ezrin at the apical domain of cells, alterations in cytoskeleton dynamics, mechanical tension on cell-cell junctions, and inability to hold EGFR at the membrane in a contact-dependent context (Chiasson-MacKenzie et al. 2015).

Hippo pathway signalling has been linked to merlin function. The Hippo pathway, originally discovered in flies but with orthologues in mammals, effects control of proliferation and organ size, and is therefore highly relevant to tumour formation. It functions as a kinase cascade and ultimately phosphorylates a co-transcriptional activator, YAP in mammals or the *Drosophila* orthologue Yki, to inhibit its activity by preventing nuclear translocation (Yu, Zhao, and Guan 2015). It was also in flies that Merlin, together with Expanded, another FERM domain-containing tumour suppressor,

was discovered to participate in Hippo pathway regulation (McCartney et al. 2000; Hamaratoglu et al. 2006; Maitra et al. 2006; Pellock et al. 2007). Intriguingly, the Merlin associated branch of the Hippo pathway is required for regulation of proliferation of glia in *Drosophila* (Reddy and Irvine 2011). Merlin was confirmed as a regulator of Hippo signalling in mammalian cells, where overgrowth phenotypes caused by loss of merlin were rescued when the downstream effector, YAP, was reduced to a single functional allele (Zhang et al. 2010). Merlin has been shown to act on the Hippo pathway by recruiting the kinase Wts (*Drosophila*) or Lats (mammals) to the plasma membrane to enable its phosphorylation by Hippo/Mst (Yin et al. 2013), and this association is regulated by binding to angiomotin (Li et al. 2015). Alternatively, merlin may have a role in the nucleus affecting the Hippo pathway. Merlin can translocate to the nucleus where it binds and inhibits $CRL4^{DCAF1}$, an E3 ubiquitin ligase, preventing it from promoting degradation of the Hippo pathway Lats 1 and 2 kinases; therefore, functional merlin permits Hippo signalling (Li et al. 2010; Li et al. 2014).

1.2.5 Merlin interacting proteins

As *NF2* mutation type does not completely predict phenotype and NF2 disease severity, and since merlin appears to be widely expressed (Trofatter et al. 1993; Rouleau et al. 1993), but disease manifestations occur only in certain cell types, there is a strong indication that proteins that interact with merlin contribute to its efficacy as a tumour suppressor. A number of such proteins have been identified (Scoles 2008), including the ERM proteins, members of signalling pathways described above, cytoskeleton components and organisation regulators, as well as others which regulate merlin phosphorylation and conformation, or whose activity in conjunction with merlin is not well defined. Studying proteins that interact with merlin physically or genetically is valuable for gaining new insights into its tumour suppressor activity. For example, in addition to functioning in pathways that regulate expression of specific proliferation-promoting factors, merlin may affect proliferative capacity by regulating overall levels of translation through its interactions with transactivation-response RNA-binding protein

(TRBP) and eIF3c. TRBP inhibits PKR, preventing inactivating phosphorylation of eIF2α and therefore promoting translation, but merlin binding to TRBP inhibits its activity thereby downregulating translation and growth (Lee et al. 2004; Lee et al. 2006). A direct interaction with eIF3c has also been demonstrated, indicating merlin may be able to affect translation by direct binding to translation factors, although this effect has not been demonstrated (Scoles et al. 2006).

1.3 | Initial observations of Merlin and eIF4E-3 interaction and hypothesis

eIF4E-3 was identified in a genetic screen in *Drosophila* as an enhancer of dominant-negative Merlin phenotype, which results in over-proliferation when expressed in the fly wing (LaJeunesse, McCartney, and Fehon 2001). In addition to this genetic interaction, work in the Hughes lab has demonstrated that eIF4E-3 and Merlin interact biochemically as immunoprecipitation of Merlin from lysates of pupae pulls down eIF4E-3, and, reciprocally, Merlin is present when eIF4E-3 is immunoprecipitated. Their association is likely direct, as interaction can be observed by an *in vitro* GST binding assay. Additionally, RNA immunoprecipitation followed by microarray analysis (RIP-Chip) with pupal lysates demonstrates that eIF4E-3 and Merlin bind specific mRNAs, including transcripts implicated in nervous system development and function, and transcripts related to male fertility. As the expression of eIF4E-3 appears restricted to the male germline and the nervous system (Hernández et al. 2012, this study), it is a candidate for modifying the role of Merlin in the nervous system and linking nervous system specific NF2 features to loss of Merlin. We hypothesise that a complex including Merlin and eIF4E-3 executes at least one function of Merlin tumour suppressor activity by regulating translation of targeted mRNAs in specific cell types.

1.4 | eIF4E

1.4.1 Role of canonical eIF4E

Initiation of translation in eukaryotes is a multi-step process involving a number of proteins known as eukaryotic initiation factors (eIFs). The eIF4F group of proteins is

required for cap-dependent translation initiation (Grifo et al. 1983) and consists of the cap binding factor eIF4E, an RNA helicase eIF4A, and an adaptor protein eIF4G. eIF4G, linked to the cap by eIF4E, recruits the 43S pre-initiation complex to the 5' end of the transcript, which includes the 40S ribosomal subunit along with eIFs 1, 1A, 2, 3, 5a, and the initiator methionine tRNA. Coupled with unwinding of 5' UTR structure by eIF4A, this complex scans for an AUG start codon and, upon reaching it, is joined by other eIFs and the large ribosomal subunit and translation begins (Dever 2002; Richter and Sonenberg 2005).

Nearly all messenger RNA molecules (mRNAs) in eukaryotes are capped at the 5' end by 7-methyl-guanosine-triphosphate (m^7GTP), which facilitates translation initiation (Shatkin 1976; Both, Banerjee, and Shatkin 1975; Rose 1975). eIF4E was identified as a protein that binds the eukaryotic 5' cap (Sonenberg et al. 1978). The folded protein has an inner, cupped hydrophobic surface that binds the 5' cap, with the outer surface available for binding interacting proteins including eIF4G (Marcotrigiano et al. 1997; Matsuo et al. 1997) (see Figure 1 for an overview of the role of eIF4E in translation initiation). There is evidence that eIF4E may also interact with nucleotides adjacent to the cap (Matsuo et al. 2000; Tomoo et al. 2003) and that the neighbouring nucleotides can modify the affinity for eIF4E (Carberry et al. 1992; Niedzwiecka et al. 2002). Furthermore, one or two nucleotides following the m^7GTP cap may also be methylated in select transcripts (Shatkin 1976). It has been suggested that these circumstances which modify the affinity of eIF4E for the cap may permit control of translation efficiency in a transcript-specific manner (von der Haar et al. 2004).

Over-expression of eIF4E causes cells to become malignant and promotes development of tumours in mice (Lazaris-Karatzas, Montine, and Sonenberg 1990; Ruggero et al. 2004). Accordingly, increased expression of eIF4E is observed in many cancer cell lines (Miyagi et al. 1995) and in a broad array of human tumours including breast carcinoma, head and neck cancer, non-Hodgkin's lymphoma, adenocarcinoma, clear cell renal carcinoma, colorectal cancer, and multiple myeloma (Kerekatte et al.

1995; Nathan et al. 1997; Wang et al. 1999; Seki et al. 2002; Campbell et al. 2015; Xu et al. 2016; Li et al. 2016). However, it appears that the effect on translation is not equal among transcripts, rather translation of proto-oncogenes and growth factors appears to be especially upregulated (De Benedetti and Graff 2004; Lazaris-Karatzas et al. 1992; Rosenwald et al. 1993; Bommer et al. 1994; Kevil et al. 1996). This is thought to be due to a combination of the eIF4F complex, and eIF4E in particular, as a limiting factor for translation initiation and a more complex secondary structure in the 5' untranslated region (UTR) of these mRNAs (Koromilas, Lazaris-Karatzas, and Sonenberg 1992; De Benedetti and Graff 2004). In this model under normal conditions, transcripts with less 5' secondary structure are rapidly translated upon association with eIF4E, whereas those with greater secondary structure are not efficiently translated as there is a lag in scanning for the initiation codon due to the need to unwind the secondary structure. When eIF4E is more readily available, although there is still a delay in initiation codon scanning, more transcripts can be associated with eIF4F, therefore increasing translation more dramatically compared with transcripts lacking extensive secondary structure which will more quickly reach a saturation of translation initiation upon over-expression of eIF4E (De Benedetti and Graff 2004). In addition to its contribution to cancer development and progression, deregulation of eIF4E has been linked to autism spectrum disorder (Neves-Pereira et al. 2009; Gkogkas et al. 2013).

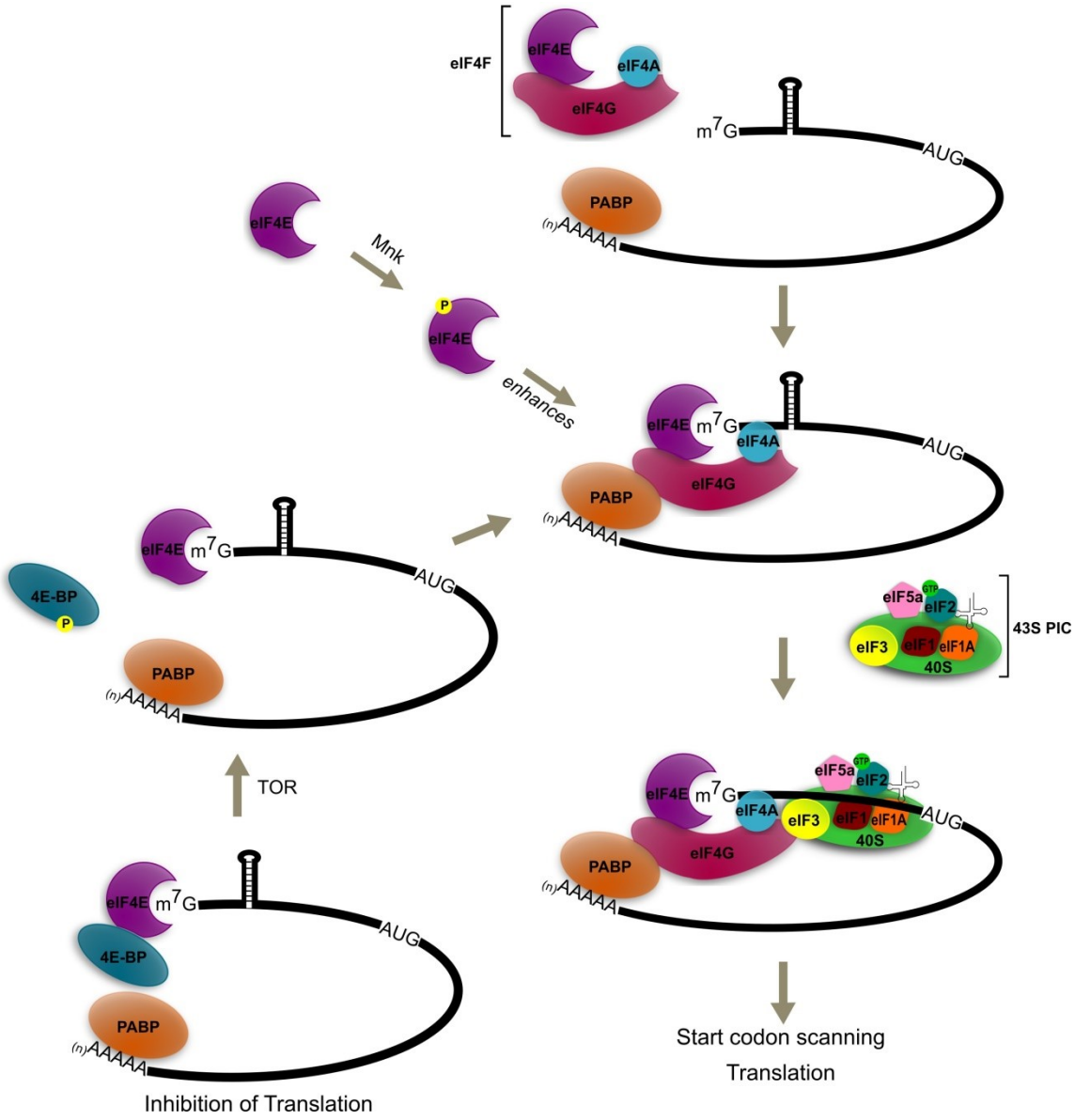
eIF4F
eIF4E
eIF4A
eIF4G
m7G
AUG
PABP
(n)AAAAA
Mnk
P
enhances
4E-BP
43S PIC
eIF5a
eIF2
eIF3
eIF1
eIF1A
40S
TOR
Start codon scanning
Translation
Inhibition of Translation

Figure 1 | The role of eIF4E in eukaryotic cap-dependent initiation of translation. eIF4G binding to eIF4E and eIF4A forms the eIF4F complex, which is recruited to mRNA by eIF4E binding of the 5' m^7G cap. The ability of eIF4E to promote translation is augmented by its phosphorylation mediated by the Mnk kinases. Increased function may be effected by enhanced binding to the cap and/or eIF4G. eIF4G also binds to poly-A binding protein (PABP), promoting circularisation of the mRNA which primes it for multiple rounds of translation, and to eIF3, which is associated with the 43S pre-initiation complex (PIC). Also included in this complex are the 40S small ribosomal subunit and initiation factors eIF1, eIF1A, eIF5a, and eIF2-GTP, as well as methionine initiator tRNA. Following association of the 43S PIC with eIF4F at the 5' end of the mRNA, the complex scans for an AUG start codon, aided by unwinding of the 5' UTR secondary structure by eIF4A helicase activity. Once the start codon is reached, other initiation factors and the large ribosomal subunit are recruited, and polypeptide synthesis commences. As eIF4E connection between the cap and eIF4G is a critical step in translation initiation, it is also highly regulated. 4E binding proteins (4E-BP) bind eIF4E at the same site as eIF4E, so when a 4E-BP is associated, recruitment of eIF4G and subsequent initiation factors is inhibited and the mRNA is not translated. 4E-BP mediated inhibition of translation can be reversed when 4E-BP is phosphorylated via TOR, causing it to release eIF4E which is then free to join eIF4G to promote translation.

1.4.2 Alternative eIF4Es in vertebrates and in Drosophila

Four isoforms of eIF4E have been identified in mammals – eIF4E, or eIF4E-1a, is the canonical protein which primarily promotes translation as described above. eIF4E-2, or 4E-HP (4E-homologous protein), is broadly expressed and is able to bind the m^7GTP cap and 4E-binding proteins (4E-BPs), but cannot interact with eIF4G, nor can it restore growth of yeast lacking eIF4E (Rom et al. 1998; Joshi, Cameron, and Jagus 2004). 4E-HP was therefore predicted to function as an inhibitor of translation, and was confirmed to function in this capacity, which is required for mouse embryonic development (Morita et al. 2012) and together with Prep1 to specifically repress translation of *Hoxb4* in mouse oocytes (Villaescusa et al. 2009). The expression of eIF4E-3, on the other hand, is restricted to muscle, spleen, and lung in mice; it binds the m^7GTP cap, but with lower specificity as binding of a cap analogue can be competed with non-methylated GTP, and it binds eIF4G but not 4E-BPs, however it does not rescue eIF4E-deficient yeast (Joshi, Cameron, and Jagus 2004). Recent studies have shown that mammalian eIF4E-3, in contrast to the canonical and proto-oncogenic eIF4E, acts as a tumour suppressor by competing with eIF4E for cap binding of transformation promoting transcripts, and this appears to be relevant to cancer progression as eIF4E-3 was found to be decreased in acute myeloid leukemia (Osborne et al. 2013; Landon et al. 2014). eIF4E-1b also shows restricted expression, to oocytes of vertebrate species including mice, zebrafish, and *Xenopus*, and has reduced affinity for the m^7GTP cap compared with eIF4E (Evsikov and de Evsikova 2009; Kubacka et al. 2015). It has been shown to have a role in a translationally repressive complex in *Xenopus* oocytes (Minshall et al. 2007), but its function has not otherwise been studied.

In *Drosophila* there are eight isoforms of eIF4E encoded by seven genes; isoforms eIF4E-1 and eIF4E-2 result from alternative splicing (Hernández et al. 2005). As in the mammalian system, eIF4E-1 is the canonical factor which functions to promote translation and can rescue growth of yeast lacking eIF4E (Hernandez and Sierra 1995; Hernández et al. 2005). The *Drosophila* eIF4E isoforms are all very similar in the

C-terminal region of the protein, but differ at the N-terminus (Hernández et al. 2005). eIF4E-8, or 4E-HP, in *Drosophila* is homologous to 4E-HP in mammals and functions as a repressor of translation (Hernández et al. 2005; Cho et al. 2005). By complexing with different proteins during embryogenesis, maternally contributed 4E-HP inhibits translation specifically of *caudal* and *hunchback* mRNAs in order to establish protein gradients necessary for anterior-posterior patterning (Cho et al. 2005; Cho et al. 2006). 4E-HP also represses translation of *belle*, encoding an RNA helicase, in the oocyte, although whether this is specified by additional binding proteins has not been determined (Yarunin et al. 2011). An additional requirement for 4E-HP later in development was recently elucidated. Loss of 4E-HP was found to prevent the transition from the larval to pupal life stage by loss of expression of enzymes required for synthesis of the steroid hormone ecdysone via an unknown mechanism (Valzania et al. 2016). A third eIF4E family member, eIF4E-3, is highly expressed in testes and is required during spermatogenesis (Hernández et al. 2012; Ghosh and Lasko 2015). This isoform, along with eIF4E-6 but unlike the remaining family members, does not have the serine residue equivalent to mammalian S209 which is phosphorylated to promote its cap binding activity (Hernández et al. 2005; Joshi et al. 1995). Furthermore, these two isoforms in addition to 4E-HP are unable to rescue eIF4E-deficient yeast, correspondent with a lack of binding to eIF4G in the case of eIF4E-6 and 4E-HP and weak eIF4G binding in the case of eIF4E-3 (Hernández et al. 2005). However, loss of eIF4E-3 reduces translation during spermatogenesis, indicating it is likely required to promote translation (Hernández et al. 2012). eIF4E-3 can also bind an alternative eIF4G, eIF4G2 or off-schedule, which is required for spermatogenesis and has strong testes expression (Hernández et al. 2012; Baker and Fuller 2007; Franklin-Dumont et al. 2007). Binding is also observed between eIF4E-3 and a translation activating 4E-BP Mextli (Hernández et al. 2013). Potentially, there is a preferential interaction between eIF4E-3 and either eIF4G2 or Mextli to initiate translation rather than the canonical eIF4G and this is perhaps why it is incapable of rescuing loss of eIF4E in yeast. The ability of eIF4E-3 to

bind Thor, the canonical 4E-BP that inhibits translation, is unclear as it was shown to have a weak interaction by a yeast two-hybrid method (Hernández et al. 2005), but did not co-immunoprecipitate with eIF4E-3 in testes lysates (Hernández et al. 2012). Additionally, eIF4E-3 has the greatest affinity for the m^7GTP cap among *Drosophila* eIF4E isoforms and interacts with the adjacent nucleotide (Zuberek et al. 2016), suggesting a potential role for eIF4E-3 in recognising altered cap structures. The remaining *Drosophila* eIF4Es – eIF4E-2, eIF4E-4, eIF4E-5, eIF4E-6, and eIF4E-7 – have not been characterised for their biological function, but, excepting eIF4E-6, are capable of binding eIF4G and the 4E-BP Thor as well as rescuing eIF4E-deficient yeast (Hernández et al. 2005) indicating they likely promote translation initiation.

1.4.3 Cap binding proteins as regulators of translation

eIF4E activity is regulated by phosphorylation at mammalian residue S209 (Joshi et al. 1995) via the MAPK-interacting kinases Mnk1 and Mnk2 (Waskiewicz et al. 1997). Phosphorylation of eIF4E promotes translation, potentially by enhancing its ability to interact with both the cap and eIF4G (Lamphear and Panniers 1990; Minich et al. 1994). Similarly, phosphorylation of eIF4E S209 augments its ability to promote malignant transformation (Topisirovic, Ruiz-Gutierrez, and Borden 2004). eIF4E is also regulated by binding 4E-BPs (Figure 2A), which prevent eIF4E binding to eIF4G by binding the same site, and thereby inhibiting translation initiation (Mader et al. 1995; Marcotrigiano et al. 1999; Ptushkina et al. 1999). There are three identified homologues of 4E-BP in mammals (Pause et al. 1994; Lin et al. 1994; Poulin et al. 1998) and two in *Drosophila* (Bernal and Kimbrell 2000; Hernández et al. 2013), although the *Drosophila* 4E-BP Mextli has been found to activate rather than repress translation (Hernández et al. 2013). Mammalian 4E-BPs are regulated by phosphorylation by mTOR; phosphorylation prevents association of the 4E-BPs with eIF4E, thus permitting translation initiation (Gingras, Raught, and Sonenberg 2001; Pause et al. 1994). *Drosophila* Thor is similarly regulated, with phosphorylation as a result of signalling to TOR causing release from eIF4E (Miron et al. 2001; Miron, Lasko, and Sonenberg 2003). Increased activity of the

mTOR signalling pathway and phosphorylated 4E-BPs, in particular 4E-BP1, are associated with disease progression in various human malignancies (Rojo et al. 2007; Petricoin et al. 2007; Qu et al. 2016). Thus, phosphorylation of inhibitory 4E-BPs and of eIF4E itself upregulates global translation.

Translational regulation mediated by eIF4E can also be transcript specific (Figure 2B). In *Xenopus* oocytes and developing embryonic nervous system, translation of a group of mRNAs with a cytoplasmic polyadenylation element (CPE) is inhibited by binding to this sequence of cytoplasmic polyadenylation element binding protein (CPEB), and bridging of CPEB to eIF4E via Maskin or Neuroguidin (Stebbins-Boaz et al. 1999; Jung, Lorenz, and Richter 2006). Similarly, patterning in *Drosophila* embryos requires repression of translation of the *oskar* transcript in the oocyte, which is achieved by binding of Bruno to Bruno response elements (BREs) in the 3' UTR of the *oskar* mRNA, and binding of both Bruno and eIF4E by Cup (Kim-Ha, Kerr, and Macdonald 1995; Nakamura, Sato, and Hanyu-Nakamura 2004). Translational regulation by Cup binding to eIF4E is also important in dorsoventral axis determination, where it interacts with Squid to repress translation of *gurken* in the oocyte (Clouse, Ferguson, and Schüpbach 2008). Cup also takes a position as an adaptor between eIF4E and Smaug, which binds Smaug recognition elements in the 3' UTR of *nanos* mRNA to repress its translation in the anterior portion of the embryo (Smibert et al. 1996; Smibert et al. 1999; Dahanukar, Walker, and Wharton 1999; Nelson, Leidal, and Smibert 2004). The RNA helicase Belle has also been shown to bind eIF4E and is predicted to negatively regulate translation of the *bruno* transcript in *Drosophila* oocytes, although a direct link between Belle and *bruno* mRNA has not been confirmed (Yarunin et al. 2011). In mammals, CYFIP was shown to bind both eIF4E and FMRP, effecting translational silencing of FMRP-bound transcripts in neurons (Napoli et al. 2008). Also, 4E-T (4E transporter), another eIF4E binding protein, represses a group of mRNAs including transcription factors promoting neuronal differentiation by sequestration in P-bodies, sites of translation repression and mRNA decay (Yang et al. 2014). Each of these interactions

inhibits translation of the bound mRNA by occupying the same eIF4E binding site that is recognised by eIF4G, so association with the translation initiation complex is prevented.

Alternatively, translation may be inhibited by competition for the cap with different eIF4Es (Figure 2C). During early *Drosophila* embryogenesis the protein Bicoid provides both sequence recognition, to a Bicoid binding region (BBR) in the 3' UTR of *caudal* mRNA, and binding to the cap binding isoform 4E-HP in order to repress translation of *caudal* in the anterior portion of the embryo (Rivera-Pomar et al. 1996; Cho et al. 2005). 4E-HP also participates in negative regulation of translation of *hunchback* at the embryo posterior by binding a complex of Nanos, Pumilio, and Brain tumour, which recognise Nanos response elements (NRE) in the *hunchback* 3' UTR (Wharton and Struhl 1991; Sonoda and Wharton 2001; Chagnovich and Lehmann 2001; Cho et al. 2006). Transcript-specific repression of translation has also been shown in mammalian oocytes, in which Prep1 recognises the 3' UTR of the transcript of the patterning gene *Hoxb4* as well as 4E-HP (Villaescusa et al. 2009).

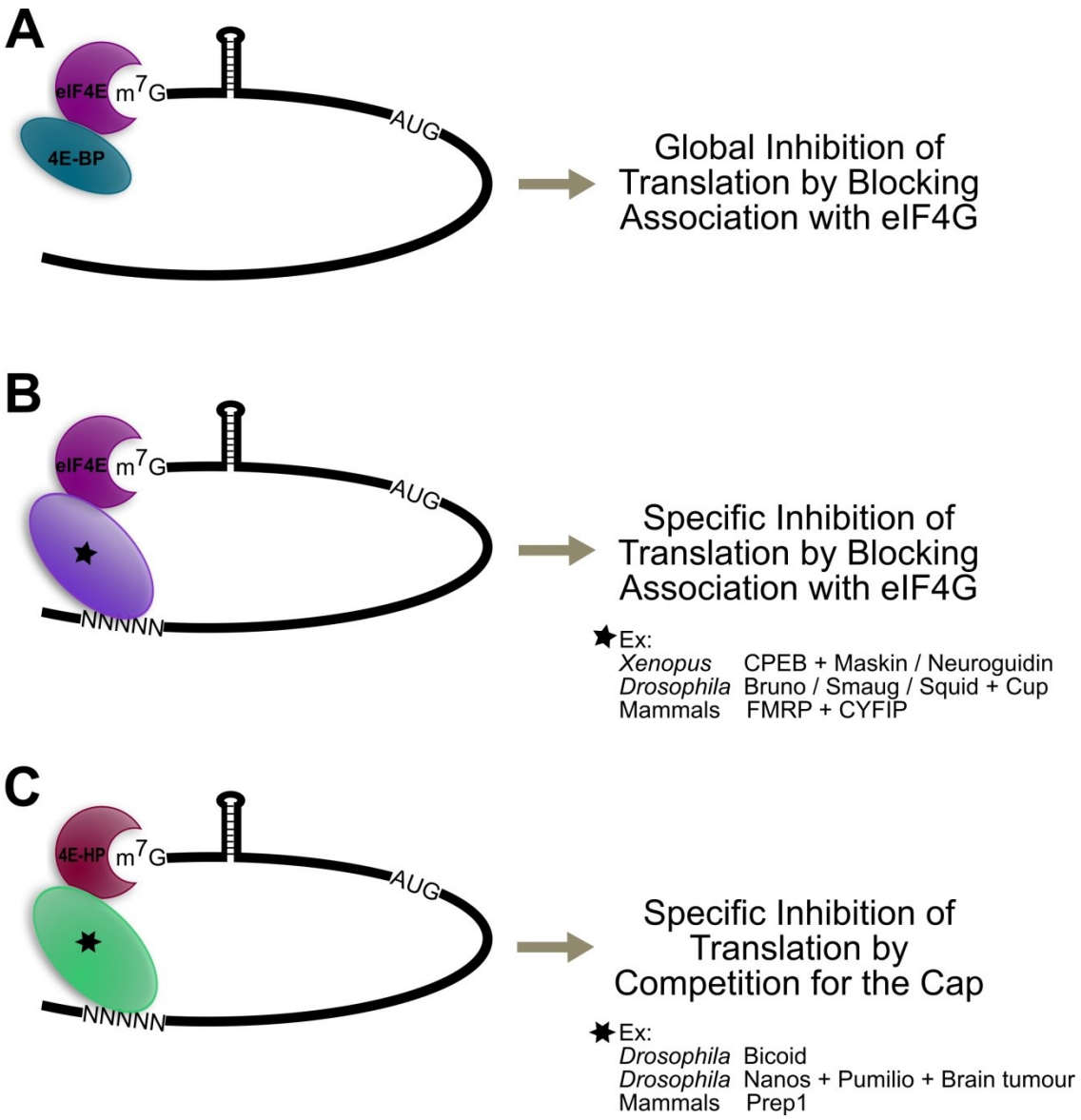
A
eIF4E
m7G
4E-BP
AUG
Global Inhibition of Translation by Blocking Association with eIF4G
B
eIF4E
m7G
AUG
NNNNN
Specific Inhibition of Translation by Blocking Association with eIF4G
★Ex:
Xenopus CPEB + Maskin / Neuroguidin
Drosophila Bruno / Smaug / Squid + Cup
Mammals FMRP + CYFIP
C
4E-HP
m7G
AUG
NNNNN
Specific Inhibition of Translation by Competition for the Cap
★Ex:
Drosophila Bicoid
Drosophila Nanos + Pumilio + Brain tumour
Mammals Prep1

Figure 2 | Modes of cap binding protein mediated inhibition of translation initiation. (A) Interacting proteins such as the 4E-BP family (4E-BP1-3 in mammals, Thor in *Drosophila*) bind eIF4E at the same site that eIF4G binds, so interaction between eIF4E and a 4E-BP prevents eIF4E association with eIF4G and therefore precludes translation initiation. Since 4E-BPs do not interact with RNA sequences, translation of all transcripts is inhibited. (B) Prevention of translation of only specific mRNAs can also be achieved via eIF4E interacting proteins. In this case, a protein or group of proteins binds eIF4E as well as a specific sequence in the 3' UTR of the targeted transcript. The mechanism of preventing translation initiation is similar to that of the 4E-BPs in that eIF4E is disallowed from interacting with eIF4G to promote translation. (C) An alternative method of inhibiting translation of certain transcripts through cap binding regulation involves recognition of the cap by a non-canonical eIF4E, such as 4E-HP, that also interacts with another protein partner or complex recognising specific 3' UTR sequences. Initiation of translation is prevented because eIF4E cannot bind the cap when it is occupied by 4E-HP, and 4E-HP cannot bind eIF4G to initiate translation.

1.5 | Regulation of translation is an important mechanism for controlling gene expression

Regulation of a gene at the level of translation allows for precise control of the level, location, and timing of protein expression. The importance of localised translation has been well studied in the nervous system. Translation is cued at precise locations within neuronal growth cones in response to extracellular ligands, permitting growth only in a certain direction (Campbell and Holt 2001), and re-sensitising the growth cone to a stimulus by on-site translation of receptors (Piper et al. 2005). Translational regulation keeps neurons primed for restricted and rapid response both pre- and post-synapse (Wang et al. 2009; Taylor et al. 2013). Spatial or temporal restriction of protein expression is also vital during oocyte maturation and early embryogenesis of *Xenopus* and *Drosophila*, as evidenced by the requirement of multiple known mechanisms for restricting translation of particular transcripts via blocking of eIF4F complex formation (Stebbins-Boaz et al. 1999; Jung, Lorenz, and Richter 2006; Nelson, Leidal, and Smibert 2004; Nakamura, Sato, and Hanyu-Nakamura 2004; Cho et al. 2005; Cho et al. 2006).

The finding of distinct preferred codon usage between mRNAs highly expressed in proliferating versus differentiated cells, concomitant with expression of corresponding tRNAs, implies an important role for translation in regulating the switch from proliferating to differentiating cell types (Gingold et al. 2014). In neuronal stem cells a translation repression program involving 4E-T binding to eIF4E inhibits expression of differentiation promoting transcription factors, demonstrating that there is more than one level of transcriptional regulation separating proliferating and differentiating cells (Yang et al. 2014). During *Drosophila* spermatogenesis, Mei-P26 is required for accumulation of bam, promoting proliferation, but increasing levels of bam inhibit translation of *mei-P26* so bam accumulation is no longer promoted, and a switch is made from a transit amplifying to differentiating cell type (Insco et al. 2012).

There is evidence that global translation dysregulation can contribute to disease. For example, decreased translation resulting from phosphorylation of eIF2 in response to

misfolded proteins that accumulate in Parkinson's, Alzheimer's and prion diseases has been determined to contribute to death of those neurons, as promoting dephosphorylation of eIF2 increases neuronal survival (Moreno et al. 2012). It has also been proposed that aggregation of RNA binding proteins mutated in amyotrophic lateral sclerosis leads to neuronal death by preventing translation of proteins required to promote neuron survival (Jung et al. 2014). Dysregulated translation is also linked to disorders of nervous system development including Fragile X syndrome, Down's syndrome, Rett's syndrome, and autism spectrum disorders (Napoli et al. 2008; Darnell et al. 2011; Gkogkas et al. 2013; Troca-Marín, Alves-Sampaio, and Montesinos 2012).

1.6 | Using *Drosophila* to investigate Merlin and eIF4E-3 function

1.6.1 Drosophila as a model to study Merlin function

Although *Drosophila* do not have Schwann cells, the primary cell type affected in NF2, they are a good model to study Merlin function in the context of a whole organism. Animal models (both mouse and *Drosophila*) have demonstrated that Merlin function is developmentally required, as null mutations exhibit lethality during development (McClatchey et al. 1997; Fehon et al. 1997). There are some differences between *Drosophila* and mammalian Merlin proteins, for example two isoforms of the merlin protein are present in humans and mice which differ at the C-terminus and result from alternative splicing (Huynh, Nechiporuk, and Pulst 1994) but in *Drosophila* there is a single expressed isoform. Nevertheless, *Drosophila* Merlin, like its mammalian orthologue, is involved in regulating proliferation and adhesion (LaJeunesse, McCartney, and Fehon 1998; McCartney et al. 2000; Hughes and Fehon 2006; Yang et al. 2012; Abeysundara et al. 2014). *Drosophila* Merlin is 55% identical to human merlin (McCartney and Fehon 1996), and expression of human *NF2* is sufficient to rescue *Merlin* null flies (LaJeunesse, McCartney, and Fehon 1998; Gavilan et al. 2014), indicating they are functionally identical. Additionally, some functions of Merlin, such as involvement in the Hippo pathway, were first identified in flies and later found to hold true in

mammalian systems (Hamaratoglu et al. 2006; Zhang et al. 2010), proving utility of *Drosophila* for uncovering the mechanisms of Merlin tumour suppressor activity. The profusion of technologies and techniques available for studying gene function in *Drosophila* contribute to its utility as an excellent model system for functional and genetic analysis of Merlin.

Since Merlin has a role in the nervous system and both Merlin and eIF4E-3 have been shown to function in spermatogenesis (Dorogova et al. 2008; Hernández et al. 2012), Merlin and eIF4E-3 interaction was examined in the nervous system and testes tissues in this study.

1.6.2 The central nervous system of Drosophila

The central nervous system of *Drosophila* is formed throughout the developmental stages of the fly, and consists of two brain lobes and a ventral nerve cord (see Figure 3 for an overview of the structure and some major cell types of the central nervous system in third instar larvae). Each brain lobe can be subdivided into an optic lobe and a central brain region. Stem cells that give rise to the central brain and ventral nerve cord of the fly are specified from the neurectoderm in the embryo (Campos-Ortega 1993). Division and differentiation of the embryonic neuroblasts form the brain and ventral nerve cord of the larva, whereupon the majority of the neuroblasts in the abdominal region undergo apoptosis (White et al. 1994) while the remainder enter a quiescent state. Late in the first instar larval stage, neuroblasts exit quiescence and continue to divide through the larval stages, producing the majority of adult CNS neurons, including 90% of the neurons in the thoracic region (Truman and Bate 1988; Prokop and Technau 1991; Ito and Hotta 1992). Neuroblasts continue to divide into the pupal stage until they either undergo apoptosis or a final non-self-renewing division (Cenci and Gould 2005; Maurange, Cheng, and Gould 2008). Most neuroblasts in the central brain and all ventral nerve cord neuroblasts are designated type I: these cells divide to self-renew and produce a ganglion mother cell which in turn divides to generate two differentiated neurons or glia (Homem and Knoblich 2012). In each brain lobe, eight neuroblasts are of the type II

lineage: division of a type II neuroblast results in self-renewal and generation of an intermediate neural progenitor that multiplies through transit amplifying divisions before asymmetrically dividing to renew itself and produce a ganglion mother cell that will produce two post-mitotic cells (Bello et al. 2008; Bowman et al. 2008; Boone and Doe 2008). The portion of the brain dedicated to the visual system, the optic lobe, is derived very differently. Precursors are specified during embryogenesis, but are an epithelial rather than a neuroblast cell type (Green, Hartenstein, and Hartenstein 1993; Egger et al. 2007). In larvae, the neuroepithelial cells divide symmetrically, then neuroblasts are derived from the expanded neuroepithelial pool (Egger et al. 2007). The optic lobe neuroblasts function in a similar manner to those of the central brain and ventral nerve cord, dividing asymmetrically to self-renew and produce a ganglion mother cell that subsequently divides into two differentiated cells. The proliferating cells of the larval optic lobe are present in two distinct regions: the outer proliferation centre from which neurons of the lamina and outer medulla are derived, and the inner proliferation centre which produces neurons of the inner medulla, lobula, and lobula plate (Meinertzhagen and Hanson 1993). The optic lobe is innervated by the cells of the retina during the third instar larval stage. Each ommatidium of the *Drosophila* compound eye consists of eight different photoreceptor cells (R1-R8). The axons from these cells innervate the lamina and medulla neuropils of the optic lobe (Fischbach and Hiesinger 2008). Following differentiation of the photoreceptor cells in the eye disc of the larva, the axons project to the brain neuropils by growing through the optic stalk, a structure created by a surrounding layer of surface glia. R1-R6 axons responsible for spatial vision terminate in the lamina, while colour vision-associated R7 and R8 axons progress through the lamina to the medulla (Fischbach and Hiesinger 2008). Growth of photoreceptor axons into the optic lobe influences the architecture of the optic lobe by promoting division and organisation of neuronal precursor cells in the lamina (Selleck and Steller 1991; Selleck et al. 1992; Huang and Kunes 1998; Huang, Shilo, and Kunes 1998), and differentiation of laminar glia (Winberg, Perez, and Steller 1992).

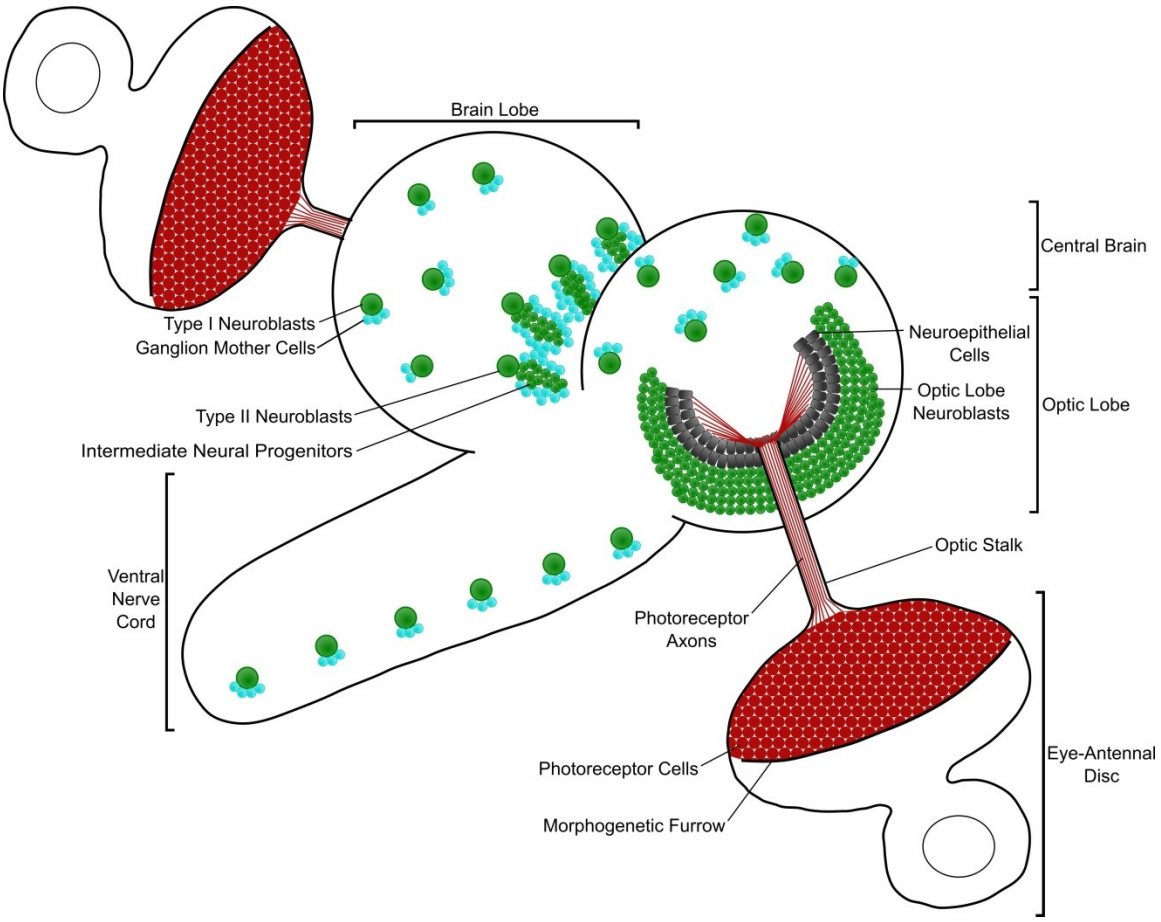
Brain Lobe
Central Brain
Type I Neuroblasts
Ganglion Mother Cells
Neuroepithelial
Cells
Optic Lobe
Neuroblasts
Optic Lobe
Type II Neuroblasts
Intermediate Neural Progenitors
Ventral
Nerve
Cord
Optic Stalk
Photoreceptor
Axons
Photoreceptor Cells
Morphogenetic Furrow
Eye-Antennal
Disc

Figure 3 | Third instar larval central nervous system and visual precursors. The central nervous system of a larva is comprised of two brain lobes and a ventral nerve cord. Within each brain lobe, there is an optic lobe region and a central brain region. Neuroblasts (green) in the optic lobe are specified from the neuroepithelium (grey) and divide to form the glia and neurons of the visual centre of the brain. These neurons are innervated by the axons of photoreceptor cells (red), which reach the brain by travelling through the optic stalk from the eye disc where the cell bodies are located posterior to the morphogenenetic furrow that separates differentiated from undifferentiated cells. In the central brain region, type I neuroblasts self-renew and produce a ganglion mother cell (blue) that will divide once more to generate two differentiated cells, neurons or glia. Division of type II neuroblasts results in self-renewal and generation of an intermediate neural progenitor that expands by transit amplifying division. The intermediate neural progenitors self-renew alongside generation of a ganglion mother cell, which divides into two differentiated cells. In the ventral nerve cord, all neuroblasts follow the type I lineage.

1.6.3 Spermatogenesis in Drosophila

The testes of adult *Drosophila melanogaster* are coiled tubes containing germline cells and somatic support cells, surrounded by a sheath of muscle and pigment cells (Fuller 1993). The final structure of the adult testes is derived from two larval precursor tissues: germline cells, somatic support cells, and muscle cells originate in the gonad, and pigment cells in the genital disc (Kozopas, Samos, and Nusse 1998). During metamorphosis these two tissues contact each other, inducing migration of muscle cells over the genital disc-derived seminal vesicle and of pigment cells to the gonad, concomitant with a morphological change of the gonad to its elongated and coiled adult structure (Stern 1941a; Kozopas, Samos, and Nusse 1998).

The *Drosophila* testis has a stem cell population at the closed end (tip), permitting continued gamete production through the lifespan of the fly (Fuller 1993) (see Figure 4 for an overview of spermatogenesis). At the testis tip is a cluster of somatic cells called the hub, surrounded by both germline stem cells and somatic cyst stem cells (Hardy et al. 1979). The hub provides structural and signalling support for both stem cell types (Tulina and Matunis 2001; Yamashita, Jones, and Fuller 2003). Asymmetric division of the germline stem cell results in self-renewal and production of a gonialblast, which is enveloped by two daughter cells of somatic cyst stem cell division (Fuller 1993). Throughout the process of spermatogenesis, the somatic cyst cells that surround the gonialblast remain associated with the germline cyst and grow as the cyst grows to accommodate it. Transit amplifying mitotic divisions of the gonialblast produce a cyst of 16 spermatogonia, which then differentiate to spermatocytes. Following meiotic division, the cyst is composed of 64 haploid spermatids which are characterised by their mitochondrial structure: the mitochondria aggregate and fuse to form two large mitochondrial structures that wrap around each other in such a way that their appearance by transmission electron microscopy resembles a cut onion (Tokuyasu 1975). Subsequently, the cyst polarises to orient all nuclei toward one end of the cyst and to orient the nuclear end toward the testis base, then the spermatids elongate as their

flagella grow and the nuclei become needle-shaped. To this point, all spermatids in a cyst remain connected by intercellular bridges; once elongation is complete, the process of individualisation begins with the formation of the individualisation complex. Each spermatid forms around its nucleus an investment cone from filamentous actin that progresses down the length of the spermatid toward the testis tip, containing each spermatid within its own membrane and extruding much of the cytoplasmic contents into a 'waste bag' which is degraded (Tokuyasu, Peacock, and Hardy 1972a; Fabrizio et al. 1998). Finally, the mature sperm is coiled before release into the seminal vesicle (Tokuyasu, Peacock, and Hardy 1972b).

Regulation of translation is important in spermatogenesis. Radioactive nucleotide incorporation studies did not detect transcription past the primary spermatocyte stage, although protein synthesis continues during the spermatid stages (Olivieri and Olivieri 1965; Gould-Somero and Holland 1974). Therefore, a mechanism of repression is required to maintain mRNAs transcribed in spermatocytes in a translationally silent state until they are needed later during spermiogenesis (Schäfer et al. 1993). *Drosophila* eIF4E family members eIF4E-3, eIF4E-4, eIF4E-5, and eIF4E-7 are highly expressed in testes compared with other tissues (Graveley et al. 2011), so potentially they have a role in regulating translation of specific mRNAs.

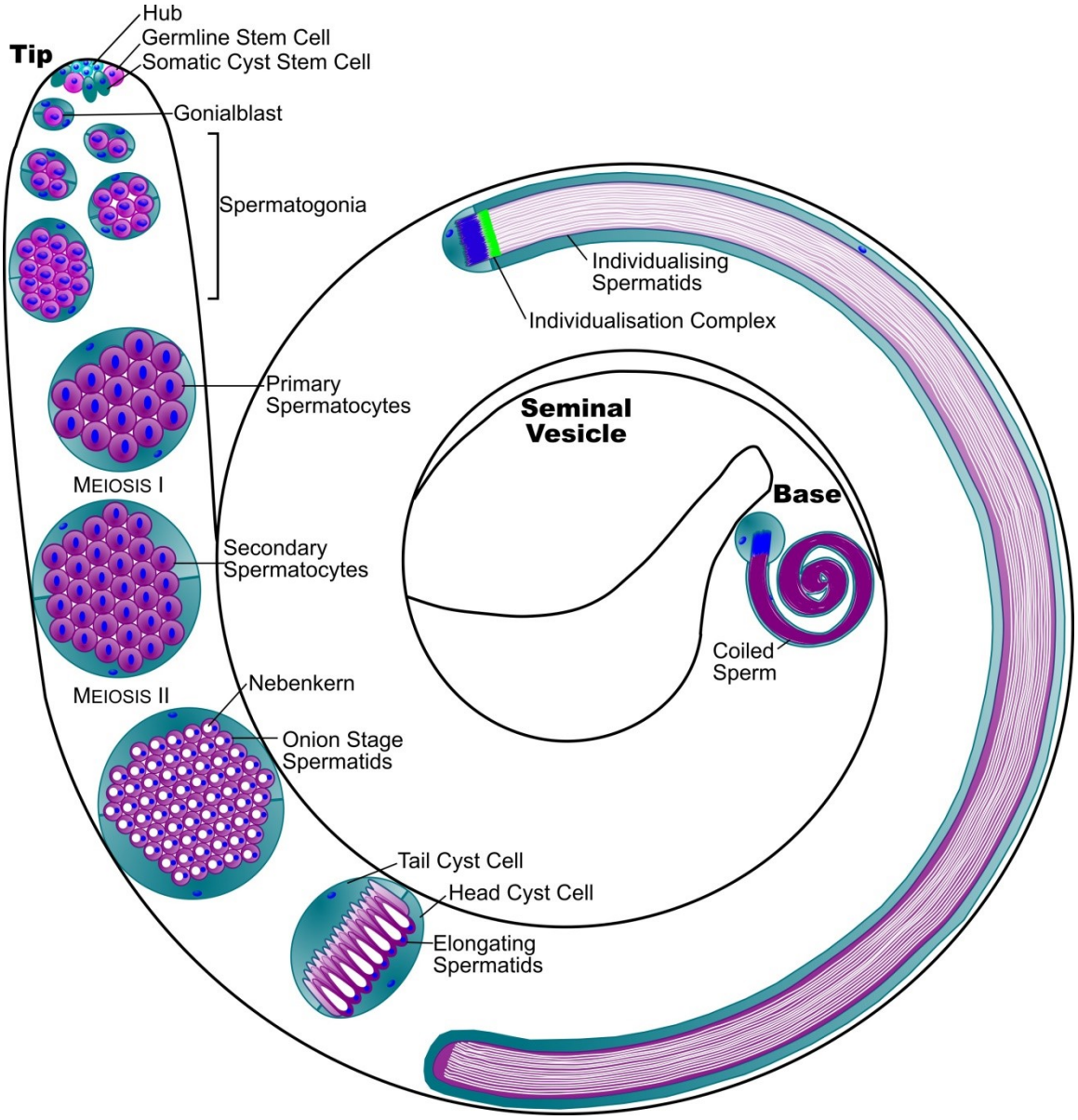
Hub
Germline Stem Cell
Somatic Cyst Stem Cell
Tip
Gonialblast
Spermatogonia
Individualising Spermatids
Individualisation Complex
Primary Spermatocytes
Seminal Vesicle
MEIOSIS I
Base
Secondary Spermatocytes
Coiled Sperm
MEIOSIS II
Nebenkern
Onion Stage Spermatids
Tail Cyst Cell
Head Cyst Cell
Elongating Spermatids

Figure 4 | Testis structure and spermatogenesis in *Drosophila melanogaster*. Spermatogenesis begins at the testis tip, where both somatic cyst stem cells and germline stem cells are in contact with somatic hub cells. Asymmetric division of the germline stem cell results in self-renewal and production of a gonialblast. Somatic cyst stem cells also divide asymmetrically to self-renew and produce daughter cells that associate with the gonialblast, with two somatic cyst cells surrounding each gonialblast. Mitotic division with incomplete cytokinesis of the gonialblast creates a two-cell spermatogonial cyst, which undergoes three more rounds of mitosis resulting in sixteen connected spermatogonia. The two somatic cyst cells associated with the gonialblast remain and grow to accommodate the expanding cyst. The sixteen spermatogonial cells increase in volume substantially as primary spermatocytes before undergoing two rounds of meiotic division to form a cyst of sixty-four round, haploid spermatids. At this stage the mitochondria aggregate and fuse to form the Nebenkern (represented by white structures) which has an 'onion-like' appearance, and these cells are known as onion stage spermatids. The spermatid cyst becomes polarised, with all nuclei directed toward the head somatic cyst cell at side of the cyst relatively nearer to the testis base than the tip, and the spermatids elongate with their tails growing toward the tip. The tail cyst cell must expand greatly to accommodate the growth of the spermatid tails. During elongation, chromatin is also compacted and the nuclei (blue) become needle-like in morphology. Completely elongated spermatids then undergo individualisation, in which an actin-rich individualisation complex is formed (green) that travels down the length of the spermatid, encasing each in its own membrane and removing excess cytoplasm. Finally, at the base of the testis, the sperm are coiled before release into the seminal vesicle.

1.7 | Project Overview

Merlin and eIF4E-3 are hypothesised to form a complex that regulates translation of a set of target mRNAs in specific cell types as one mechanism of Merlin tumour suppressor activity. To investigate this, the expression pattern of eIF4E-3 was examined by immunofluorescence, RNA fluorescence *in situ* hybridisation, and reporter expression. Two new null alleles of *eIF4E-3* were created in order to investigate the function of eIF4E-3 and its genetic interaction with Merlin in the nervous system and testes of *Drosophila*, and the effect these proteins have on translation of the transcripts they bind.

Chapter 2 Materials and Methods

2.1 | Drosophila culture

Flies were raised on media described by Schwarz et al. (2014), modified to 5 g/L agar and 2.5 g/L methyl 4-hydroxybenzoate, at 25°C.

To facilitate survival of mutant animals to appropriate stages, vials of each mutant and control genotype (15 females:7 males) were transferred daily, and approximately 24 hours after adults were transferred out of a vial, non-GFP balancer larvae were transferred to a new vial in which the food had been stirred with additional water. Animals in which *Merlin* mutations were rescued with a Myc-tagged transgene were also collected in this manner.

Fertility assays were performed as described by Hernández et al. (2012).

Table 1 | Drosophila stocks

Genotype	Stock Number/Reference
w^{1118}	
Actin5C-GAL4 / CyO Act-GFP	
en-GAL4	
w, Mer^{3}*, P{neoFRT}19A / FM7 Act-GFP*	(Fehon et al. 1997)
y,w, Mer^{4}*, P{neoFRT}19A / FM7 Act-GFP*	(Fehon et al. 1997)
w; UAS-Mer$^{\Delta BB}$ *24c / CyO*	(LaJeunesse, McCartney, and Fehon 1998)
w;; UAS-Myc-Mer	SCH0627 6232-1-4 M chr 3
y,w;; P{lacW}eIF4E-3^{L0139} */ TM3 Ser, Act-GFP*	BL10169 (Bier et al. 1989)
w;; e, eIF4E-3^{IIIa239} */ TM3 Ser, Act-GFP*	(LaJeunesse, McCartney, and Fehon 2001)
w;; e, eIF4E-3^{IIIa278} */ TM3 Ser, Act-GFP*	(LaJeunesse, McCartney, and Fehon 2001)
w;; eIF4E-3^{excision6} */ TM3 Ser, Act-GFP*	This study
w;; eIF4E-3^{null,mCherry} */ TM3 Ser, Act-GFP*	This study 18738-1-1M-Ch3
w;; Df(3L)BSC732 / TM3 Ser, Act-GFP	BL26830
w;; UAS-FLAG-eIF4E-3	SCH0648 6232-4-2 M chr 3
w;; ry^{506}*, Dr, P{Δ2-3}99B / TM6C Sb*	BL5908
w; P{w^{+mC} *=UAS-myr-mRFP}*	BL7118

*BL indicates stock number at Bloomington Drosophila Stock Center, Indiana University
**SCH indicates Hughes lab stock number

2.2 | Generation and isolation of a new *eIF4E-3* allele by P-element excision

eIF4E-3 null flies were generated by imprecise excision of a P-element marked with w^{+} from *eIF4E-3*^{L0139}*/TM3 Ser Actin-GFP* stock. Virgin females of this stock were crossed to

w^{1118}/*Y;;ry*^{506} *Dr P{Δ2-3}99B/TM6C Sb* males. *w*$^{+}$ *Dr* male progeny were selected and crossed to *w;;TM6 Tb/MKRS* virgin females. Single male progeny that had lost the P-element (selected for by loss of *w*$^{+}$) and did not have the chromosome with transposase to prevent further mutation (selected for by absence of *Dr* phenotype) were crossed to *w;;TM6 Tb/MKRS* virgin females. Both male and female progeny from these crosses were selected to start new stocks with the potentially mutant chromosomes balanced with *MKRS*.

Loss of all or a portion of the *eIF4E-3* gene was screened for by PCR, using the KAPA Mouse Genotyping Kit (KAPA Biosystems KK7352) for both DNA extraction and PCR genotyping. DNA extractions were performed as half-reactions according to the manufacturer's protocol, with one adult fly per reaction. PCR genotyping was also set up in half-reactions according to manufacturer's protocol, using 1 µl of adult fly DNA extract as template, and primers published by Hernandez et al. (2012) for the eIF4E-3 locus and the upstream P-element. PCR cycles were as follows: 94°C—3 min, 94°C—45 sec, 56°C—45 sec, 68°C—2 min, repeat steps 2-4 34 times, 68°C—5 min. PCR products were resolved on 0.8% agarose gels at 95 V for 45 min, which were subsequently stained with RedSafe Nucleic Acid Staining Solution (iNtRON Biotechnology 21141) at 1:20 000 in TAE overnight and visualised using a blue light plate. One fly stock that did not produce a PCR product with either the endogenous eIF4E-3 primers or those specific to the *L0139* P-element was further analysed with primers further out from the eIF4E-3 locus. The sequences of these primers (synthesised by Integrated DNA Technologies) were (5'-3'): fwd, ACGTAGCGACTCACATATTTTATTATCTGCAC; rev, CATATCAATTCACATTACGGTCCGAATAACTGC. Subsequently, males from this stock, hypothesised to have a deletion at the *eIF4E-3* locus, were crossed to *w;Df(3L)BSC732/TM3 Ser Actin-GFP* virgin females. Thirty adult flies from this cross (*w;;eIF4E-3*/Df(3L)BSC732*) were collected, and genomic DNA was extracted as described by Huang et al. (2009). The primers described above were used to amplify the region surrounding the *eIF4E-3* locus, and the product was sequenced using the same

primers at The Applied Genomics Core, University of Alberta. The resulting sequence was compared to that of the *eIF4E*-3 extended gene region, available at FlyBase (flybase.org, version FB2014_03).

The deletion allele resulting from this screen was isogenised by outcrossing to w^{1118}/Y flies for four generations. For each cross, virgin female progeny from the previous cross were individually genotyped by extracting DNA using a non-lethal PCR genotyping technique described by Carvalho et al. (2009), in which wings were cut from adults for DNA extraction and individual flies were distinguished by maintaining them in separate vials. Reaction and cycle conditions were modified from the original protocol as follows, and primers used are defined above. Final concentrations per reaction: 1xHF Buffer, 0.5 μM each forward and reverse primers, 0.25 mM dNTPs, 3 μL wing DNA extract, 3% DMSO, 0.02 U/μL Phusion DNA Polymerase (Thermo Scientific F530S); PCR cycles: 95°C–3 min, 95°C–45 sec, 56°C–45 sec, 72°C–2 min, repeat steps 2-4 34 times, 72°C–5 min. PCR products were resolved as described above. Individual females determined to carry the deletion allele were then pooled and crossed to w^{1118}/Y males. Following the last outcross, single males carrying the deletion allele were crossed to virgin female *w;;Df(3L)BSC732/TM3 Ser actin-GFP* flies. Progeny from these crosses were also individually genotyped by the non-lethal method and both male and female progeny of a single male were pooled to initiate a stock. Five fly stocks resulted from this selection: *eIF4E-3*^{excision4}*/TM3 Ser Actin-GFP* , *eIF4E-3*^{excision5}*/TM3 Ser Actin-GFP* , *eIF4E-3*^{excision6}*/TM3 Ser Actin-GFP* , *eIF4E-3*^{excision7}*/TM3 Ser Actin-GFP* , *eIF4E-3*^{excision10}*/TM3 Ser Actin-GFP*.

2.3 | Immunofluorescence (IF)

2.3.1 Tissue dissection

Testes were dissected from adult flies 0-24 hours post-eclosion, or from pharate adults about 24 hours after pigmentation for $y,w,Mer^{4}/Y$ and $y,w,Mer^{4}/Y;;eIF4E\text{-}3^{excision6}$ genotypes. Larval tissues were dissected from wandering third instar larvae. To dissect

pupal wings, white pre-pupae were selected and aged in a Petri dish with wet Whatman paper in the bottom.

2.3.2 Fixation and IF of larval tissues and adult testes

For IF analysis of adult or pharate testes and brains or wing discs from third instar larvae, tissue was dissected in PBS and fixed in freshly prepared 4% paraformaldehyde (Sigma P6148) in PBS for 20 minutes at room temperature. After several PBS washes, tissue was blocked with PTN (PBS, 0.1% Triton X-100, 1% normal donkey serum) at room temperature for a minimum of 1 hour. Tissue was then incubated with primary antibodies (Table 2) diluted in PTN at 4°C overnight, washed with PTN at room temperature 30 minutes, incubated with secondary antibodies (Table 2) diluted in PTN at room temperature 2 hours, and washed again with PTN at room temperature 30 minutes. DAPI (5 mg/ml) diluted 1:10 000 in PTN was used to stain nuclei at room temperature for 10 minutes. Tissue was washed with PBS and then mounted in ProLong Gold Antifade Mountant (Molecular Probes P36934). Larval brains were mounted on the coverslip with the dorsal side facing the coverslip.

2.3.3 Fixation and IF procedure for α-eIF4E-3 Ab#53

For larval brains labelled with α-eIF4E-3 Ab#53, a periodate-lysine-paraformaldehyde (PLP) fixing procedure was used. Dissections were performed in 0.072 M sodium phosphate dibasic, 0.028 M sodium phosphate monobasic. Brains were fixed with PLP (0.01 M sodium periodate, 0.075 M lysine, 2% paraformaldehyde, 0.038 M sodium phosphate dibasic, 0.011 M sodium phosphate monobasic) at room temperature for 45 minutes, then washed (0.072 M sodium phosphate dibasic, 0.028 M sodium phosphate monobasic, 0.1% Triton X-100) at room temperature for 45 minutes. Brains were blocked with wash buffer + 10% normal donkey serum at room temperature for 1 hour, incubated with primary antibody (Table 2) diluted in wash solution at 4°C overnight, washed 3 times, 10 minutes per wash, and incubated with secondary antibody (Table 2) diluted in wash buffer at room temperature for 2 hours. Brains were then washed again

3 times, 10 minutes per wash, with DAPI (5 mg/ml) diluted to 1:10 000 added to the second wash, and mounted, dorsal side facing the coverslip, in ProLong Gold Antifade Mountant (Molecular Probes).

2.3.4 Fixation and IF of pupal wings

Once pupae had reached the desired age (indicated in figure legends) post-puparium formation, pupae were removed from the pupal case using sharp forceps and fixed in fresh 4% paraformaldehyde in PBS for 1 hour at room temperature. Paraformaldehyde was removed and wings were dissected off the pupa and out of the covering membrane in PBS, then fixed in 4% paraformaldehyde for 20 minutes at room temperature. After washing several times with PBS, wings were blocked with PTN (PBS, 0.1% Triton X-100, 1% normal donkey serum) at room temperature for a minimum of 1 hour, then incubated with primary antibodies (Table 2) diluted in PTN at 4°C overnight. The wings were then washed with PTN at room temperature for 30 minutes, incubated with secondary antibodies (Table 2) diluted in PTN at room temperature for 2 hours, then washed again with PTN at room temperature for a minimum of 30 minutes. DAPI (5 mg/ml) was diluted 1:10 000 in PTN and wings were incubated at room temperature for 10 minutes, after which they were washed briefly with PBS and mounted in ProLong Gold Antifade Mountant (Molecular Probes).

2.3.5 Fixation and IF of embryos

Embryos were collected in small fly cages on apple juice agar plates. Embryos were dechorionated in 50% bleach for 90 seconds and rinsed thoroughly with water, then with embryo wash solution (0.7% NaCl, 0.03% Triton X-100). The embryos were then transferred to a scintillation vial with 8 ml heptane, 2.5 ml PBS, and 250 µl 40% paraformaldehyde, and agitated for 20 minutes at room temperature. Embryos were then transferred to a 1.5 ml tube for removal of the vitelline membrane using 1:1 heptane:methanol and shaken vigorously for 30 seconds. The solution was replaced with methanol and shaken again, then methanol was removed as well as any embryos that

had not settled to the bottom of the tube, and embryos were rinsed twice more with methanol. Embryos were then rinsed twice with PBTBB (PBS, 0.1% Tween-20, 0.5% skim milk powder, 0.05% BSA) and blocked with PBTBB for a minimum of 2 hours at room temperature. Primary antibodies (Table 2) were diluted in PBTBB and embryos incubated at 4°C overnight, then washed with PBTBB at room temperature 30 minutes, incubated with secondary antibodies (Table 2) diluted in PBTBB at room temperature for 2 hours, washed with PBTBB at room temperature for 30 minutes, and incubated with 1:10 000 DAPI (from 5 mg/ml stock solution) in PBTBB at room temperature for 10 minutes. After rinsing with PBS, embryos were mounted in ProLong Gold Antifade Mountant (Molecular Probes).

2.3.6 Image acquisition and analysis

Images were acquired with a Zeiss LSM 700 confocal microscope with a 20x / NA 0.8 lens or a 40x / NA 1.4 lens.

Measurements of the lamina plexus length for brains labelled with α-chaoptin were made using the line tool in ImageJ (National Institutes of Health). A two-tailed T-test was performed for statistical significance using Microsoft Excel.

To count central brain neuroblasts, z-stacks were taken of whole brain lobes, one lobe per mounted brain. Neuroblasts, identified as cells labelled with α-deadpan and including both type I and type II neuroblasts but not intermediate neural progenitor cells, were counted in each z-plane in Zeiss Zen software. Statistics were calculated using Mann-Whitney U-Tests.

2.4 | Western blot analysis

2.4.1 Preparation of testes lysates

Testes were dissected in PBS with protease and phosphatase inhibitors [Roche: complete mini EDTA-free tablet (cat. no. 04 693 159 001), PhosSTOP tablet (cat. no. 04 906 837 001)]. Up to 25 pairs testes were lysed in 10 µl of 2x SDS sample buffer (0.0625 M Tris-HCl pH6.8, 2% SDS, 0.04% bromophenol blue, 5% β-mercaptoethanol, 0.5x PBS) and

heated to 95°C for 10 minutes. A volume equivalent to approximately 3 testes pairs per lane was used to observe eIF4E-3 expression.

2.4.2 Preparation of lysates for target protein analysis

Wing discs from 10 wandering third instar larvae were dissected in Schneider's Insect Medium (Sigma S0146), then treated to inhibit proteasomal degradation as described by Lim and Kelly (2012), incubating at room temperature for 3 hours in Schneider's Medium with 10 μM MG132 (Sigma C2211) dissolved in DMSO, or with an equal volume of DMSO only. Media was removed and tissue lysed in 10 μl of 2x SDS sample buffer, then heated to 95°C for 10 minutes. The whole lysate volume was loaded on the gel.

2.4.3 SDS-PAGE and Western blotting

Lysates were separated on 12% polyacrylamide gels when probing for eIF4E-3, or 10% polyacrylamide gels for other antigens with Precision Plus Protein Standards (Bio-Rad 161-0374) as molecular weight markers, and transferred to nitrocellulose membranes (Bio-Rad electrophoresis and Western blotting systems), then blocked in LI-COR Odyssey Blocking Buffer (PBS) at room temperature for 2 hours. Membranes were incubated with primary antibody (Table 2) diluted in 1:1 PBT:Odyssey Blocking Buffer at 4°C overnight, then washed 4 times with PBT, minimum 5 minutes per wash, and incubated with secondary antibody (Table 2) diluted in PBT at room temperature for 45 minutes. After washing three times each with PBT and PBS, minimum 5 minutes per wash, blots were scanned using an Odyssey Infrared Imager (LI-COR).

2.5 | Wing measurements

The *UAS-Mer*$^{\Delta BB}$ transgene was recombined with the *en-GAL4* driver, and recombinant flies were crossed to each mutant allele of *eIF4E-3*. Wings were prepared for measuring as described previously (LaJeunesse, McCartney, and Fehon 2001): adult male flies of appropriate genotype were submerged in 70% ethanol for a minimum of 24 hours, then wings were removed and mounted in Aquamount (Thermo-Fisher 14-390-5).

Images were obtained using Zeiss Axioskop with Zeiss CP-Achromat 5x / NA 0.12 lens and a Coolsnap HQ (Photometrics) camera. The area measurements from vein IV to the posterior margin were made using the polygon tool in ImageJ (National Institutes of Health). Between 18 and 24 wings were measured per genotype, and statistics were calculated by two-tailed T-test in Microsoft Excel.

2.6 | RNA Fluorescence *in situ* hybridisation (RNA FISH)

2.6.1 eIF4E-3 probe synthesis

An antisense *eIF4E-3* run-off probe was generated using as a template a vector containing the sequence encoding the N-terminal region of *eIF4E-3*, as this portion of the sequence is unique compared with other eIF4Es (Hernández et al. 2005). The probe was labelled with digoxigenin (DIG) by synthesising using a DIG RNA Labeling Kit (Roche cat. no. 11 175 025 910).

2.6.2 RNA FISH in adult testes

Adult testes were dissected from 0-24 hour post-eclosion w^{1118}/Y males. FISH was carried out as previously described (Toledano et al. 2012). Signal was detected using peroxidase (POD)-conjugated α-DIG (Roche cat. no. 11 207 733 910) at 1:500 and a TSA Plus Cyanine 3 kit at 1/50 (PerkinElmer NEL744001KT).

2.6.3 RNA FISH in larval tissues

w^{1118} wandering third instar larvae were dissected in PBS and fixed as described in (Pattatucci and Kaufman 1991). Post-fixation FISH steps were then carried out as previously described for dissected tissue (Wilk et al. 2010). POD-α-DIG (Roche) at 1:400 and TSA Plus Cyanine 3 at 1/50 (PerkinElmer) were used for probe detection.

2.7 | Generation of a new *eIF4E-3* allele using CRISPR-Cas9 and homologous recombination

A targeted mutation in *eIF4E-3* was carried out with a modified version of the protocol described in Baena-Lopez et al. (2013). Two kilobases immediately upstream of

the transcription start site of *eIF4E-3* (5′ homology arm) and two kilobases immediately downstream of the polyadenylation site (3′ homology arm) were amplified from w^{1118} genomic DNA and inserted into the pTV^{Cherry} targeting vector (Baena-Lopez et al. 2013). An injection mix consisting of $pTV^{Cherry\text{-}eIF4E\text{-}3}$ (600 ng/µl), synthetic CRISPR targeting RNA (crRNA) targeting the first exon of eIF4E-3 (Dharmacon; sequence 5′-CAACGGAUUGCAGAAUGCUGGUUUUAGAGCUAUGCUGUUUUG-3′ 50 ng/µl), and synthetic trans-activating crRNA (tracrRNA, Dharmacon U-002000-05; 50 ng/µl) in 10% glycerol, 0.5x PBS was prepared and sent to BestGene Inc for injection into *vas-Cas9* embryos and transformant selection.

Table 2 | Antibodies / stains used for immunofluorescence and Western blotting

Antigen	Species	Source	Concentration	
			IF	WB
β-galactosidase	Mouse	Promega Z378A	1:200	
β-tubulin	Mouse	Developmental Studies Hybridoma Bank (DSHB) E7		1:3000
Boule	Rabbit	S. Wasserman (Cheng, Maines, and Wasserman 1998)	1:1000	1:1000
Chaoptin	Mouse	DSHB 24B10	1:200	
Cleaved Caspase-3	Rabbit	Cell Signaling 5A1E	1:400	
Dachshund	Mouse	DSHB mAbdac2-3	1:1000	
Deadpan	Rabbit	Y. Jan (Bier et al. 1992)	1:1000	
Deadpan	Guinea Pig	J. Skeath	1:500	
DIG	Sheep	Roche 11207733910	1:400	
dsRed	Mouse	Santa Cruz Biotechnology E-8	1:75	
E-cadherin	Rat	DSHB DCAD2	1:200	
eIF4E-3	Mouse	N-term affinity purified	1:1000	1:2000
eIF4E-3	Rabbit	#23 – peptide Ab	1:1000	1:2000
eIF4E-3	Rabbit	#53 – N-term affinity purified	1:500	1:1000
eIF4E-3	Rabbit	#968 – peptide Ab, P. Lasko (Hernández et al. 2012)	1:1000	1:2500
ELAV	Rat	DSHB 7E8A10	1:500	
FLAG	Mouse	Sigma M2	1:20 000	
Futsch	Mouse	DSHB 22C10	1:500	
Held-out-wings	Rabbit	T. Volk (Nabel-Rosen et al. 1999)	1:100	1:3000
Merlin	Guinea Pig	#93	1:500	
Myc-Tag	Mouse	Cell Signaling 9B11	1:4000	
phospho-Histone H3	Mouse	Abcam ab5176	1:1000	
Prospero	Mouse	DSHB MR1A	1:500	
Repo	Mouse	DSHB 8D12	1:500	
Sip1	Guinea Pig	#1475	1:1000	
DAPI		Invitrogen D3571	1:10 000	
Phalloidin AF488		Invitrogen A12379	1:1000	
AF488/AF555/AF647 conjugated against various species	Donkey	Abcam Jackson ImmunoResearch	1:2000	
Mouse IgG AF680	Donkey	Abcam		1:20 000
Rabbit IgG AF790	Donkey	Abcam		1:10 000

Chapter 3 Results

3.1 | Generation and characterisation of a null *eIF4E-3* mutation by P-element excision

3.1.1 P-element mobilisation results in a deletion of eIF4E-3

A new *eIF4E-3* null allele was created in order to ensure that observed effects result only from loss of eIF4E-3, as the $eIF4E\text{-}3^{L0139}$ allele exhibits lethality due to background effects (Hernández et al. 2012). To create the new allele, a P-element mutagenesis method was used (Hummel and Klämbt 2008), wherein the P-element from the $eIF4E\text{-}3^{L0139}$ allele, which is inserted 14 nucleotides upstream of the *eIF4E-3* transcription start site (Hernández et al. 2012), was mobilised by crossing $eIF4E\text{-}3^{L0139}$ flies to flies carrying Δ2-3 transposase. Flies in which the P-element was excised, identified by loss of the positive eye colour marker, were screened by PCR for loss of flanking genomic DNA in addition to the P-element, resulting in one line which was further analysed. Sequencing of the genomic region surrounding *eIF4E-3* revealed that 1224 bp of genomic DNA were deleted, including the entire coding region of *eIF4E-3* (Figure 5A). This stock was subsequently isogenised by outcrossing to w^{1118} flies for four generations, resulting in three fly lines which were viable as homozygotes.

Each of these excision alleles was tested for loss of *eIF4E-3* transcript by quantitative RT-PCR, which showed greater than 99.5% loss of transcript for each allele in trans with the deficiency chromosome *Df(3L)BSC732* (analysis done by David Primrose). The $eIF4E\text{-}3^{excision6}$ allele was selected for further experimentation as it showed the greatest loss of transcript by qRT-PCR. Loss of eIF4E-3 protein was examined using α-eIF4E-3 Ab#968, an antibody previously used to characterise $eIF4E\text{-}3^{L0139}/Df(3L)BSC732$ in *Drosophila* testes (Hernández et al. 2012). By Western blot analysis, eIF4E-3 protein is absent in testes lysates from animals heterozygous for each excision allele and *Df(3L)BSC732* or homozygous for $eIF4E\text{-}3^{excision6}$ (Figure 5B). Similarly, no fluorescence signal is observed above background in whole mount $eIF4E\text{-}3^{excision6}/Df(3L)BSC732$ testes as in $eIF4E\text{-}3^{L0139}/Df(3L)BSC732$ testes (Figure 5C), indicating absence of protein.


A
P-element excision deletion

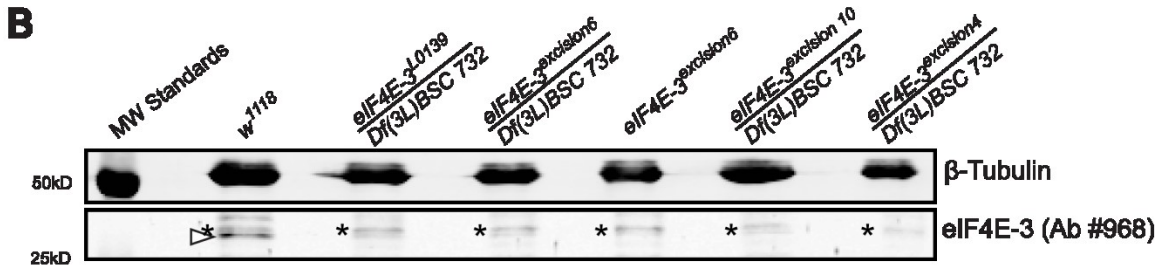
B
MW Standards
w1118
eIF4E-3L0139/Df(3L)BSC 732
eIF4E-3excision6/Df(3L)BSC 732
eIF4E-3excision6
eIF4E-3excision 10/Df(3L)BSC 732
eIF4E-3excision4/Df(3L)BSC 732
50kD
25kD
β-Tubulin
eIF4E-3 (Ab #968)

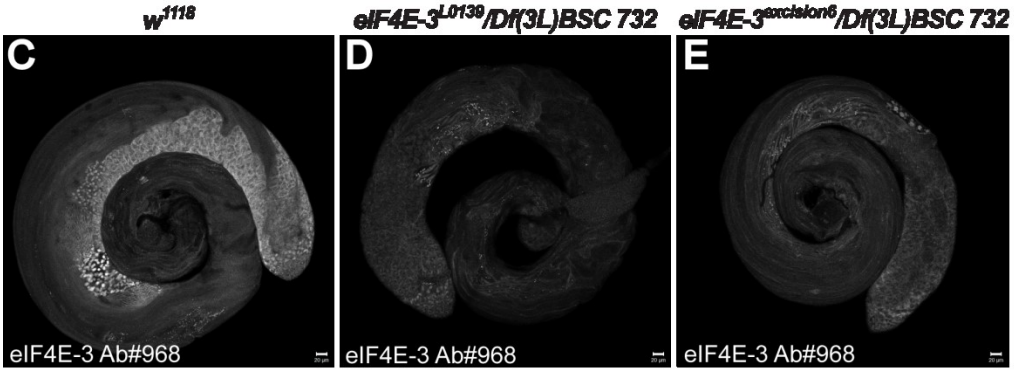
w1118
eIF4E-3L0139/Df(3L)BSC 732
eIF4E-3excision6/Df(3L)BSC 732
C
D
E
eIF4E-3 Ab#968
eIF4E-3 Ab#968
eIF4E-3 Ab#968

Figure 5 | A novel *eIF4E-3* mutation created by P-element imprecise excision is a null allele. (A) Schematic indicating the deleted portion of *eIF4E-3*. Shaded boxes represent exon coding regions, lines represent intron regions, and unshaded boxes represent untranslated regions. (B) Western blot analysis of testes lysates using a characterised antibody raised against an eIF4E-3 peptide (Hernández et al. 2012). A band at the approximate size predicted for eIF4E-3 (28.5 kDa, arrowhead) is present in w^{1118} lysates, but not in $eIF4E\text{-}3^{L0139}/Df(3L)BSC732$ (eIF4E-3 null) lysates. Likewise, there are no corresponding bands in lysates from any of the outcrossed P-element excision mutant alleles in trans with *Df(3L)BSC732* or homozygous $eIF4E\text{-}3^{excision6}$. Asterisks indicate non-specific bands. (C-E) IF analysis using the same antibody shows an absence of fluorescence above background levels in $eIF4E\text{-}3^{excision6}/Df(3L)BSC732$ testes as in $eIF4E\text{-}3^{L0139}/Df(3L)BSC732$ testes, which have been previously established as lacking eIF4E-3 expression (Hernández et al. 2012).
Scale bars: 20 μm

3.1.2 eIF4E-3^{excision6} exhibits previously reported eIF4E-3 mutant phenotypes

The *eIF4E-3^{excision6}* allele was further characterised by comparing the mutant phenotype to previously identified effects of loss of eIF4E-3. Loss of eIF4E-3 causes complete sterility in male flies (Hernández et al. 2012). Male flies heterozygous for *eIF4E-3^{L0139}* or *eIF4E-3^{excision6}* with *Df(3L)BSC732* produced no progeny in a fertility test (Figure 6A). Sterility caused by eIF4E-3 loss is a result of an inability to produce mature sperm, due at least in part to defective meiotic cytokinesis which leads to early spermatids with multiple nuclei and expanded Nebenkern structures (a mitochondrial derivative) (Hernández et al. 2012). Examination of the base of testes, where nearly fully mature spermatid bundles are normally found, showed a lack of spermatid bundles in *eIF4E-3^{excision6}/Df(3L)BSC732* testes as in *eIF4E-3^{L0139}/Df(3L)BSC732* testes (Figure 6B-D). It is common for antibodies to non-specifically bind to mitochondria in immunofluorescence analyses of testes (Julie Brill, personal communication). Using α-Merlin, which acts in this manner, large Nebenkern structures were observed in *eIF4E-3^{excision6}* early spermatids compared with early spermatids in *w^{1118}/Y* testes (Figure 6E,F). These data indicate that *eIF4E-3^{excision6}* replicates spermatogenesis defects previously observed for loss of eIF4E-3.

The excision mutant allele was also tested for its ability to modify dominant-negative Merlin phenotype. In the genetic screen that first identified *eIF4E*-3 as a *Merlin* interacting gene (LaJeunesse, McCartney, and Fehon 2001), EMS-induced mutations in complementation group IIIa, corresponding to *eIF4E-3* (Sarah Hughes, unpublished data), enhanced the dominant-negative Merlin overgrowth phenotype caused by expressing *Mer$^{\Delta BB}$* in the posterior region of the wing with *en-GAL4*. In order to replicate these findings and test the new allele, all available *eIF4E-3* mutations, including two from the screen (*eIF4E-3^{IIIa239}* and *eIF4E-3^{IIIa278}*), were crossed to flies with a recombined chromosome including *en-GAL4* and *UAS-Mer$^{\Delta BB}$*, a dominant-negative *Merlin* allele (LaJeunesse, McCartney, and Fehon 1998). The area of the posterior region of adult male wings was then measured, and was found to be significantly larger when any of the *eIF4E-3* mutant alleles is combined with *en>Mer$^{\Delta BB}$* as compared with *en>Mer$^{\Delta BB}$* alone

(Figure 7B). This confirms that *eIF4E-3*^{excision6} acts in a similar manner to previously described *eIF4E-3* alleles, and that it is eIF4E-3 and not a secondary mutation that modifies dominant-negative Merlin phenotype.

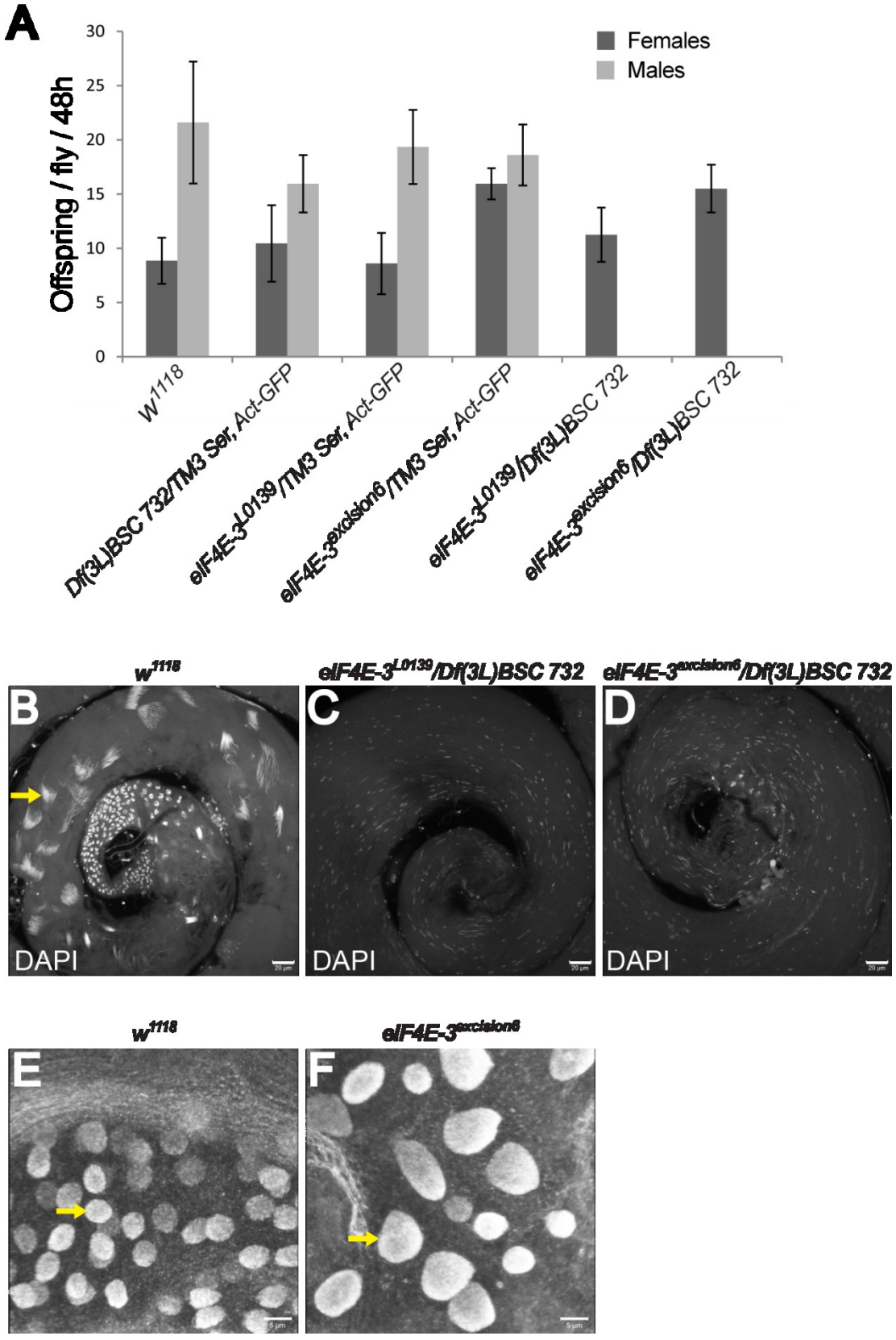
A
Offspring / fly / 48h
30
25
20
15
10
5
0
Females
Males
w1118
Df(3L)BSC 732/TM3 Ser, Act-GFP
eIF4E-3L0139/TM3 Ser, Act-GFP
eIF4E-3excision6/TM3 Ser, Act-GFP
eIF4E-3L0139/Df(3L)BSC 732
eIF4E-3excision6/Df(3L)BSC 732
w1118
eIF4E-3L0139/Df(3L)BSC 732
eIF4E-3excision6/Df(3L)BSC 732
B
C
D
DAPI
DAPI
DAPI
w1118
eIF4E-3excision6
E
F

Figure 6 | Infertility and spermatogenesis defects caused by the P-element excision allele *eIF4E-3^{excision6}* are consistent with those of previously reported *eIF4E-3* mutations. (A) As loss of eIF4E-3 is reported to lead to male sterility, male and female flies of each indicated genotype were assayed for ability to produce progeny when mated to *w^{1118}* flies. Complete sterility is seen in male *eIF4E-3^{L0139}/Df(3L)BSC732* flies as previously described (Hernández et al. 2012), and complete male sterility is also seen in *eIF4E-3^{excision6}/Df(3L)BSC732* flies, demonstrating consistency and specificity of the phenotype. (B-D) Maximum intensity projection images of the base region of testes. Bundles of needle-shaped spermatid nuclei are abundant in *w^{1118}* testes (arrow), and are absent in *eIF4E-3^{L0139}/Df(3L)BSC732* testes. Similarly, no spermatid bundles are seen in *eIF4E-3^{L0139}/Df(3L)BSC732* testes. In the mutant testes, scattered spermatid nuclei are observed, but they have not appropriately condensed to the needle-shaped form, nor are they bundled as in control testes. (E,F) Mitochondrial structures, non-specifically labelled by α-Merlin (arrows), are enlarged in *eIF4E-3^{excision6}* spermatids compared with *w^{1118}* control, which is consistent with a reported phenotype of *eIF4E-3^{L0139}/Df(3L)BSC732* (Hernández et al. 2012).

Scale bars in B-D: 20 μm; scale bars in E,F: 5 μm

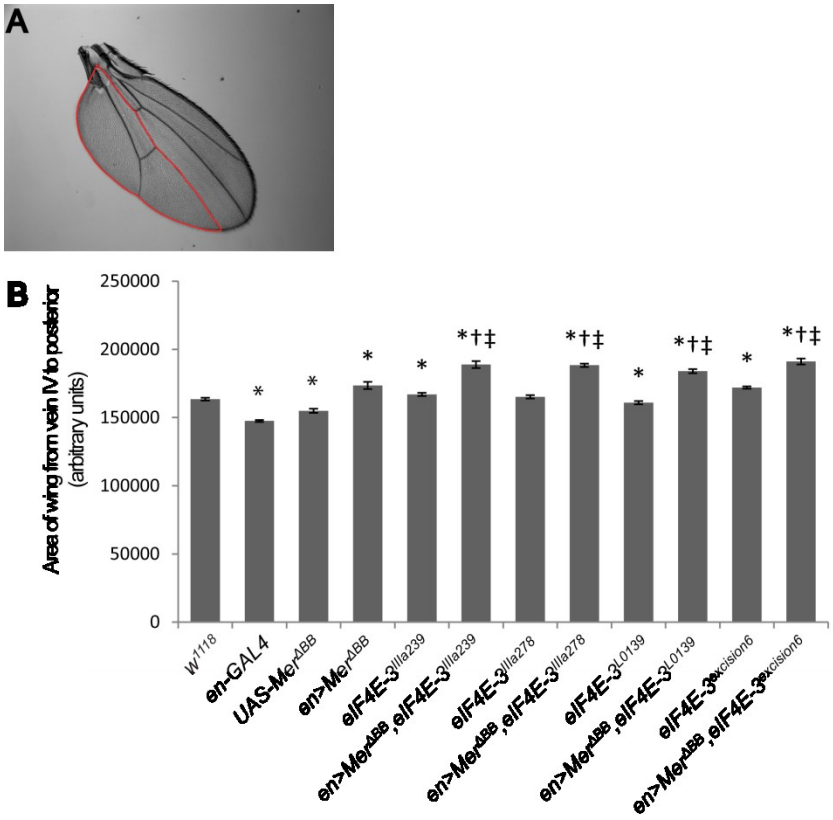

Figure 7 | The P-element excision allele *eIF4E-3^{excision6}* interacts with *Mer$^{\Delta BB}$* in a manner consistent with previously reported alleles. *eIF4E-3^{excision6}* was tested for ability to interact with *Mer$^{\Delta BB}$* (dominant negative Merlin) in the wing like *eIF4E-3^{IIIa239}* and *eIF4E-3^{IIIa278}*, which were identified as enhancers of *Mer$^{\Delta BB}$* phenotype in a genetic screen (LaJeunesse, McCartney, and Fehon 2001). Results from this screen indicated that when *eIF4E-3* mutant alleles are combined with over-expression of *Mer$^{\Delta BB}$* in the posterior of the wing using *en-GAL4*, there is greater over-proliferation, measured by wing area, than occurs with over-expression of *Mer$^{\Delta BB}$* on its own. (A) Representative image showing the area of adult male wings measured, from vein IV to the posterior margin, using ImageJ software. (B) Measured wing area replicated findings from the genetic screen with all *eIF4E-3* mutant alleles tested, including *eIF4E-3^{excision6}*, confirming specificity of the genetic interaction to *eIF4E-3*. Statistical differences were determined by two-tailed T-tests. *p<0.05 compared with *w^{1118}*, †p<0.05 compared with *en> Mer$^{\Delta BB}$*, ‡p<0.05 compared with respective *eIF4E-3* allele alone.

3.2 | Characterisation of eIF4E-3 antibodies

3.2.1 α-eIF4E-3 antibody #23 is valid for Western blotting and for IF in testes only

Antibody #23 (Ab#23) was produced in rabbit against an N-terminal peptide of eIF4E-3, amino acids 39-60 (ELMSGNEEELQPSLNRVMKNID; Hernández et al. 2005), the same peptide used to produce Ab#968 (Hernández et al. 2012). On Western blots of testes lysates, Ab#23 identifies a double band near the expected size of 28.5 kDa (Figure 8A). These bands are not apparent in lysates from *eIF4E-3^{L0139}/Df(3L)BSC732* flies or any of the excision mutants, indicating that Ab#23 is specifically recognising eIF4E-3 in testes lysates. Ab#23 also recognises eIF4E-3 in fixed tissue, as a fluorescent signal greater than background overlaps with α-FLAG when a *UAS-FLAG-eIF4E-3* transgene is expressed in the posterior compartment of the larval wing disc with *en-GAL4* (Figure 8B''',C'''). Spermatocytes and spermatids are shown to express eIF4E-3 when Ab#23 is used to label fixed testes (Figure 8F), as has been previously described (Hernández et al. 2012). eIF4E-3 null testes do not show any fluorescent signal above background (Figure 8G), indicating Ab#23 is suitable for IF with this tissue. When Ab#23 was tested on embryos 12-16 hours after egg laying (AEL), a repeating pattern of two cells per segment within the ventral nerve cord was observed (Figure 8D,D'); however this pattern was also seen in *eIF4E-3^{L0139}/Df(3L)BSC732* embryos of the same age (Figure 8E). A similar pattern was also seen in both control and mutant embryos using Ab#968. Likewise, a distinctive pattern which appeared to be a pair of cells and axonal projections was observed in third instar larval brains, but was also seen in *eIF4E-3^{excision6}* brains (Figure 8H,I); this same pattern is seen using Ab#968 in either control or mutant brains. Ab#23 also marks wing veins in pupal wings; a pattern that is also observed in *eIF4E-3^{excision6}* pupal wings 26 hours after puparium formation (APF) (Figure 8J,K). Therefore, while Ab#23 is reliable for use in Western blot analysis and IF in adult testes, it is not suitable for IF with other tissues.

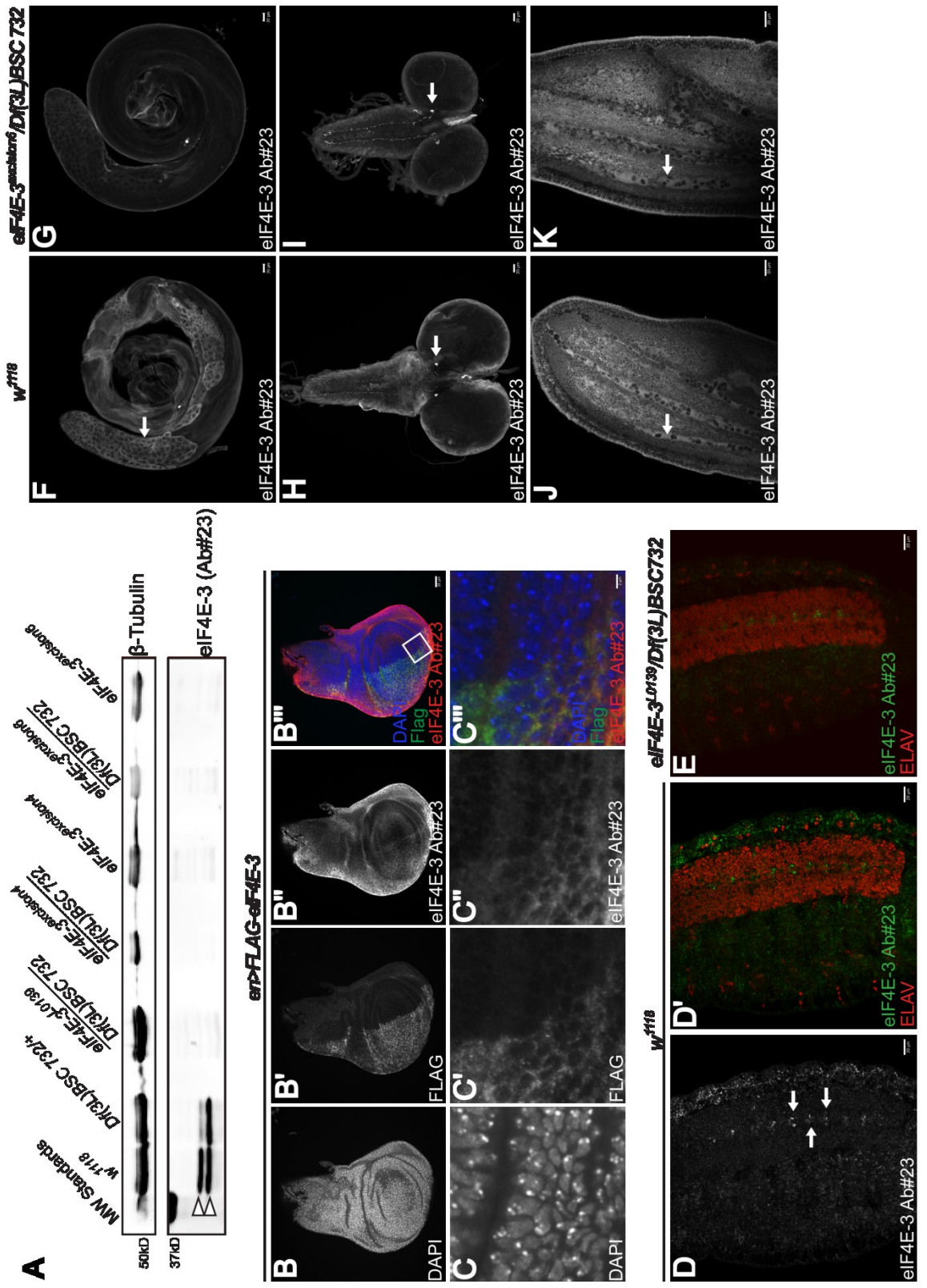
A
MW Standards
w1118
Df(3L)BSC 732/+
eIF4E-3 01939/ Df(3L)BSC 732
eIF4E-3 excision/ Df(3L)BSC 732
eIF4E-3 excision
eIF4E-3 excision/ Df(3L)BSC 732
50kD
37kD
β-Tubulin
eIF4E-3 (Ab#23)
ey>FLAG-eIF4E-3
B
B'
B''
B'''
C
C'
C''
C'''
DAPI
FLAG
eIF4E-3 Ab#23
Flag
w1118
eIF4E-3 01939/Df(3L)BSC732
D
D'
E
eIF4E-3 Ab#23
ELAV
eIF4E-3 excision/Df(3L)BSC 732
F
G
H
I
J
K

Figure 8 | Ab#23 is reliable for Western blots and for IF on testes only. (A) Western blot analysis of testes lysates using Ab#23. A double band near the expected size of 28.5 kDa is present in w^{1118} and *Df(3L)BSC732* lysates (arrowheads), but not in lysates of eIF4E-3 null testes. (B-B''') Wing disc from a third instar larva expressing the *UAS-FLAG-eIF4E-3* transgene with *en-GAL4*. The signal intensity of Ab#23 is greater in the *en* expressing area as indicated by FLAG expression. (C-C''') Higher magnification images of the area indicated in B'''. (D-E) IF using Ab#23 on embryos 12-16 hours AEL. In w^{1118} embryos, two cells per segment within the ventral nerve cord (marked by ELAV) are labelled. The same cells are labelled in eIF4E-3 null embryos, indicating the pattern is non-specific. (F,G) Ab#23 shows cytoplasmic eIF4E-3 expression in spermatocytes and spermatids, indicated by arrow, and no fluorescence above background is seen in eIF4E-3 null testes, suggesting Ab#23 is reliable for IF in testes. (H-K) Ab#23 labelling for endogenous eIF4E-3 is non-specific in tissue other than testes: (H,I) Ab#23 labels specific cells and apparent axonal projections in third instar larval brains, but the same pattern is seen in eIF4E-3 null brains (arrows). (J,K) Forming veins in 26h APF pupal wings are labelled with Ab#23 in both w^{1118} and $eIF4E\text{-}3^{excision6}$/*Df(3L)BSC732* animals (arrows). All scale bars 20 μm except in C''', 2 μm

3.2.2 α-eIF4E-3 antibody #53 is appropriate for Western blotting and for IF in testes only

Antibody #53 (Ab#53) was raised in rabbit and affinity purified using the N-terminal portion of eIF4E-3, which is unique compared with other *Drosophila* eIF4E proteins (Hernández et al. 2005). This antibody recognises a band at the appropriate molecular weight for eIF4E-3 when lysates of w^{1118}/Y testes are analysed by Western blotting, and this band does not appear in blots of $eIF4E\text{-}3^{L0139}/Df(3L)BSC732$ or excision mutant testes lysates (Figure 9A). Ab #53 recognises eIF4E-3 by immunofluorescence analysis of fixed tissue, as there is overlapping signal with α-FLAG in larval wing discs when FLAG-eIF4E-3 is expressed with the *en-GAL4* driver (Figure 9B''',C'''). IF with Ab#53 in adult testes shows eIF4E-3 expression in spermatocytes and spermatids, as has been described (Hernández et al. 2012), and no signal above background is seen with the loss of eIF4E-3 (Figure 9E). Ab#53 was also tested for use in IF analysis of third instar larval brains. When the standard paraformaldehyde fixation procedure was used, Ab#53 did not label anything, so a variety of alternative methods of tissue fixation were attempted. With a periodate-lysine-paraformaldehyde fix, fluorescence in a cluster of cells as well as apparent axonal projections was seen in w^{1118} larval brains (Figure 9F); however, the same labelling was seen in $eIF4E\text{-}3^{excision6}/Df(3L)BSC732$ brains (Figure 9G), indicating that Ab#53 is not suitable for IF in this tissue type.

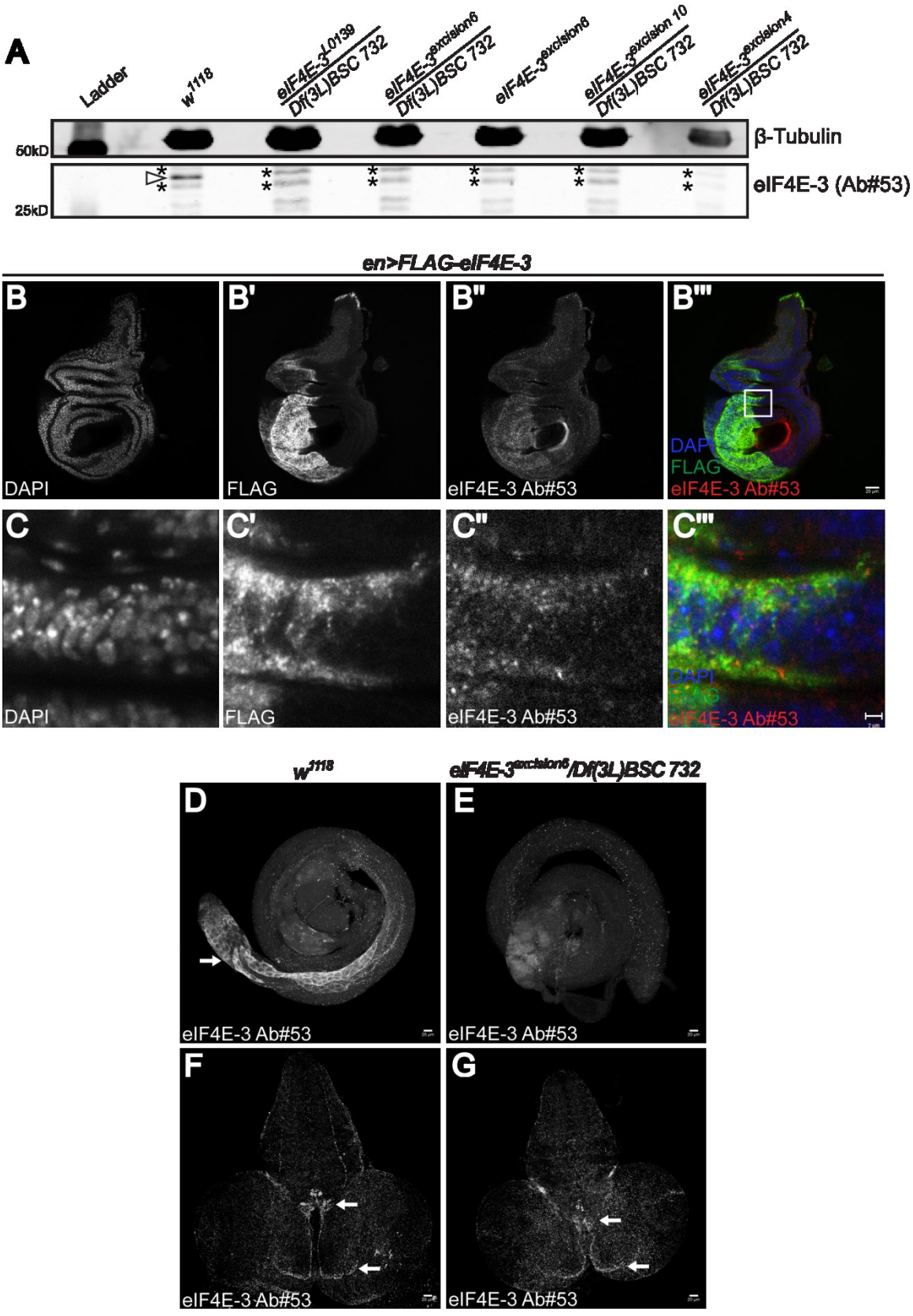
A
Ladder
w1118
eIF4E-3L0139/Df(3L)BSC 732
eIF4E-3excision6/Df(3L)BSC 732
eIF4E-3excision6
eIF4E-3excision 10/Df(3L)BSC 732
eIF4E-3excision4/Df(3L)BSC 732
60kD
25kD
β-Tubulin
eIF4E-3 (Ab#53)
en>FLAG-eIF4E-3
B
B'
B''
B'''
DAPI
FLAG
eIF4E-3 Ab#53
C
C'
C''
C'''
w1118
eIF4E-3excision6/Df(3L)BSC 732
D
E
F
G

Figure 9 | Ab#53 is reliable for Western blots and for IF in testes only. (A) Western blot analysis of testes lysates shows Ab#53 recognises a band near the expected size of eIF4E-3 (28.5 kDa, arrowhead) which is not present in lysates from animals with *eIF4E-3* null mutations. Asterisks indicate non-specific bands. (B-B''') In *en>FLAG-eIF4E-3* wing discs, greater intensity of signal with Ab#53 overlaps with α-FLAG in the *en* region, indicating the antibody recognises eIF4E-3 in fixed tissue. (C-C''') Higher magnification of the region indicated by the white square in B''', showing correspondence between Ab#53 and α-FLAG labelling. (D,E) Using Ab#53 to immunolabel adult testes shows eIF4E-3 in spermatocytes and spermatids as expected (arrow), and this signal is absent in eIF4E-3 null testes, showing specificity. (F,G) Third instar larval brains fixed with PLP and labelled with Ab#53 show fluorescence in a cluster of cells in each brain lobe near the ventral nerve cord as well as toward the anterior portion of each brain lobe (arrows). This pattern is seen in both w^{1118} and *eIF4E-3*^{excision6}/*Df(3L)BSC732* brains, indicating that it is non-specific and that Ab#53 is not appropriate for IF in this tissue.
All scale bars 20 μm except in C''', 2 μm

3.2.3 Mouse-α-eIF4E-3 is suitable for Western blotting and for IF in testes only

An antibody raised in mouse against eIF4E-3 (msAb) and purified against the unique N-terminal region of the protein was also tested for various applications. In Western blot analysis of testes lysates, the msAb shows a double band near the expected size for eIF4E-3 of 28.5 kDa, with fewer background bands than the antibodies produced in rabbit (Figure 10A). These bands were absent when testes lysates of *eIF4E-3* null animals were analysed. To test the ability of the msAb to recognise eIF4E-3 in fixed tissue, *en-GAL4* flies were crossed to flies carrying the transgenes *UAS-FLAG-eIF4E-3* and *UAS-Myr-RFP* so that cells expressing the *eIF4E-3* transgene would be positively labelled with membrane-targeted RFP. Signal from the msAb overlapped with RFP expression in wing discs of the resulting progeny (Figure 10B''',C'''), indicating that this antibody could be used for IF. The antibody was found to be reliable for IF in adult testes, as it recognised protein expression in spermatocytes and spermatids in w^{1118}/Y testes, but nothing above background in $eIF4E\text{-}3^{excision6}/Df(3L)BSC732$ testes (Figure 10D,E). While an expression pattern is seen in w^{1118} third instar larval brains with the msAb, this same pattern of fluorescence is seen in $eIF4E\text{-}3^{excision6}/Df(3L)BSC732$ brains, indicating the pattern is non-specific (Figure 10F,G). In IF analysis of pupal wings, the msAb labels large cells within the developing wing veins (Figure 10H). In $eIF4E\text{-}3^{excision6}/Df(3L)BSC732$ pupal wings, the fluorescent signal with the msAb is more diffuse in the wing vein, but a few of the large cells are recognised as well (Figure 10I), indicating that the antibody is not reliable for IF in this tissue.

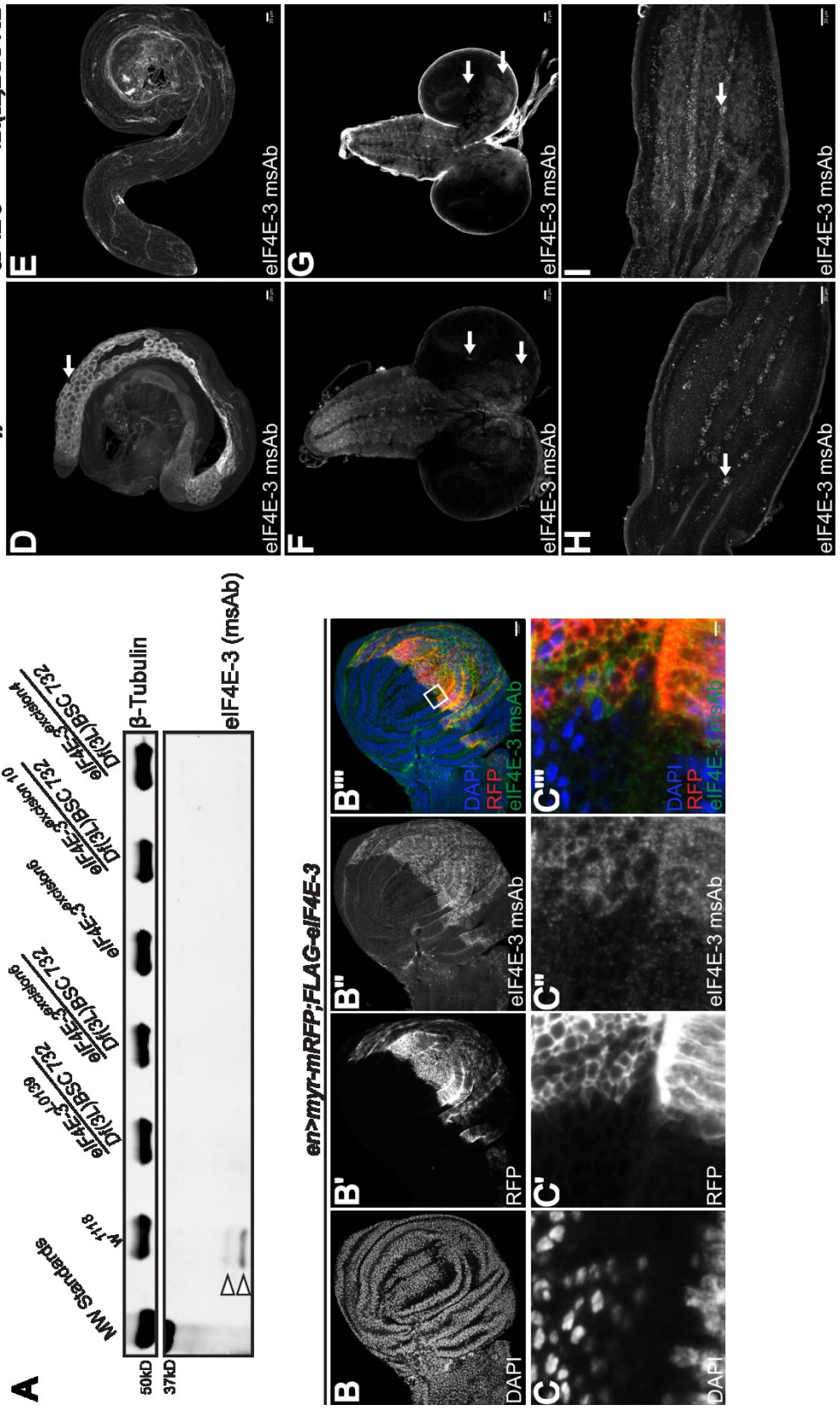
A
MW Standards
w 1118
Df(3L)BSC139 eIF4E-3
Df(3L)BSC732 eIF4E-3exckson
Df(3L)BSC732 eIF4E-3exckson
eIF4E-3exckson
Df(3L)BSC732 eIF4E-3exckson 10
Df(3L)BSC732 eIF4E-3exckson4
β-Tubulin
eIF4E-3 (msAb)
50kD
37kD
w1118
eIF4E-3exckson4/Df(3L)BSC732
D
E
F
G
H
I
eIF4E-3 msAb
en>myr-mRFP;FLAG-eIF4E-3
B
B'
B''
B'''
C
C'
C''
C'''
DAPI
RFP
eIF4E-3 msAb

Figure 10 | msAb is reliable for Western blots and for IF in testes only. (A) msAb is appropriate for Western blot analysis as it recognises a double band near the expected size of 28.5 kDa in w^{1118} testes lysates (arrowheads) and no bands in eIF4E-3 null testes lysates. (B-B''') msAb recognises eIF4E-3 in fixed tissue. Labelling with msAb is congruent with RFP expression in the *en* region of the wing disc when *en-GAL4* is used to drive expression of both *UAS-myr-RFP* and *UAS-FLAG-eIF4E-3*. (C-C''') Higher magnification of the region shown in B''', showing msAb recognition only where RFP is expressed. (D,E) msAb is appropriate for IF analysis of testes as it labels spermatocytes and spermatids in w^{1118} testes, but no signal above background is seen in eIF4E-3 null testes. (F-I) msAb is not appropriate for IF analysis of other tissues: (F,G) A few scattered cells in each third instar larval brain hemisphere and an area near the anterior portion of the brain lobe are labelled with msAb (arrows). However, the same pattern in w^{1118} brains is seen in *eIF4E-3*^{excision6}/*Df(3L)BSC732* brains. (H,I) msAb stains large cells along the w^{1118} developing wing vein at 26 hours APF, and although this pattern is slightly altered in eIF4E-3 null wings with more ubiquitous fluorescence in the vein, some large cells are still seen (arrow).
All scale bars 20 μm except in C''', 2 μm

3.3 | Generation of a null *eIF4E-3* mutation and expression reporter using CRISPR-Cas9 and homologous recombination

3.3.1 CRISPR-Cas9 targeted mutation of eIF4E-3 results in a null allele

As none of the antibodies tested reliably showed expression of eIF4E-3 in tissue other than testes, replacement of *eIF4E*-3 at the endogenous site with a fluorescent reporter was used as an alternative approach to investigate the expression pattern of eIF4E-3. Successful replacement would also result in a null allele of *eIF4E-3*. The method used to generate this allele involved using CRISPR-Cas9 to target *eIF4E-3*, and homologous recombination to replace the endogenous sequence with the reporter. CRISPR (**c**lustered **r**egularly **i**nterspaced **s**hort **p**alindromic **r**epeats) and CRISPR-associated (Cas) nucleases are a mechanism used by bacteria and archaea to defend against foreign plasmids and viruses (Barrangou et al. 2007). In the type II CRISPR-Cas9 systems, the Cas9 nuclease cleaves double-stranded DNA, sequence-specified by complementarity to a targeting CRISPR RNA (crRNA) and short protospacer adjacent motif (PAM), and in the presence of the structure formed by crRNA bound to trans-activating crRNA (tracrRNA) (Jinek et al. 2012). Jinek et al. (2012) demonstrated that double-stranded breaks could be induced at specific sites by engineering a chimeric crRNA:tracrRNA with sequence targeting the site of interest, and the CRISPR-Cas9 system has since been used for targeted genome alteration in a variety of cells and model organisms (reviewed in Doudna and Charpentier 2014) , including *Drosophila* (Gratz et al. 2013; Bassett et al. 2013; Baena-Lopez et al. 2013).

Double-stranded DNA breaks can be repaired either by non-homologous end joining, which, in the context of targeted genome alteration, would result in a deletion mutation, or by homology directed repair/homologous recombination (HR), allowing for sequence alterations and knock-ins. Baena-Lopez et al. (2013) devised a targeting plasmid for use in HR genome modification in *Drosophila*, which includes an *mCherry* reporter among other features. This pTV^{Cherry} plasmid was used to target *eIF4E-3* by cloning genomic regions 2kb upstream of the transcription start site and 2kb downstream of the

polyadenylation site of *eIF4E-3* into the respective multiple cloning sites of pTV^{Cherry}. The objectives of using this plasmid were to create a complete knock-out of *eIF4E-3* and to make a reporter of endogenous *eIF4E-3* expression. A modified version of the described direct injection protocol (Baena-Lopez et al. 2013) was used, in which embryos expressing Cas9 under control of the *vasa* promoter were injected with pTV$^{Cherry\text{-}eIF4E\text{-}3}$, synthetic tracrRNA, and a synthetic crRNA targeted to the first exon of *eIF4E-3*. The resulting allele was analysed for presence of the *mCherry* reporter and for insertion at the correct genomic location by PCR. A 776bp *mCherry* verification product indicated that *mCherry* was present in the genome, and downstream of the sequence used for *eIF4E-3* upstream homology (Figure 11B). A 659bp insert site verification product indicated that pTV^{Cherry} appropriately integrated into the genome at the *eIF4E-3* site, and did not integrate any part of the vector outside the homology regions (Figure 11B).

This allele, *eIF4E-3^{null,mCherry}*, was also examined for congruency with known phenotypes caused by loss of eIF4E-3. Western blot analysis of testes lysates showed that eIF4E-3 protein is absent in *eIF4E-3^{null,mCherry}* testes as in *eIF4E-3^{excision6}* testes (Figure 11C). IF analysis of *eIF4E-3^{null,mCherry}* testes also shows an absence of fluorescent signal, indicating that eIF4E-3 expression is lost (Figure 11F). Male flies homozygous for *eIF4E-3^{null,mCherry}* are completely sterile (Figure 11D), consistent with the *eIF4E-3^{excision6}* allele and with *eIF4E-3^{L0139}/Df(3L)BSC732* (Hernández et al. 2012). Defects in spermatogenesis initially reported for *eIF4E-3^{L0139}/Df(3L)BSC732* (Hernández et al. 2012) are also seen in *eIF4E-3^{null,mCherry}* testes: the testis base is completely void of sperm bundles (Figure 11H), and Nebenkern structures in spermatids as visualised by non-specific antibody labelling are enlarged as a result of a defect in meiosis (Figure 11J). *eIF4E-3^{null,mCherry}* therefore appears to be a functional null mutation with phenotypes consistent with previously described mutations.

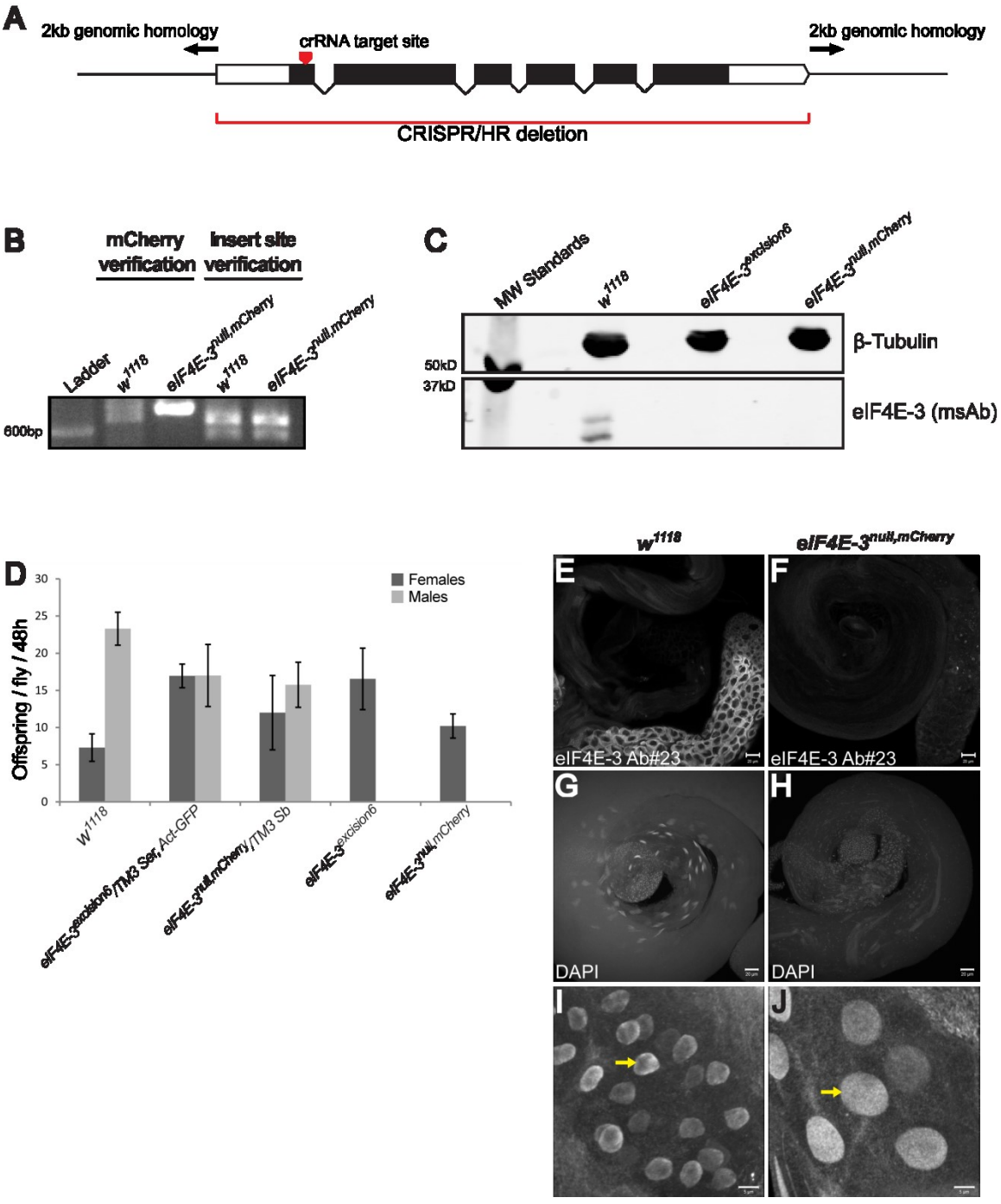
A
2kb genomic homology
crRNA target site
2kb genomic homology
CRISPR/HR deletion
B
mCherry verification
Insert site verification
Ladder
w1118
eIF4E-3null,mCherry
w1118
eIF4E-3null,mCherry
600bp
C
MW Standards
w1118
eIF4E-3excision6
eIF4E-3null,mCherry
50kD
37kD
β-Tubulin
eIF4E-3 (msAb)
D
Females
Males
Offspring / fly / 48h
0
5
10
15
20
25
30
w1118
eIF4E-3excision6/TM3 Ser, Act-GFP
eIF4E-3null,mCherry/TM3 Sb
eIF4E-3excision6
eIF4E-3null,mCherry
w1118
eIF4E-3null,mCherry
E
F
eIF4E-3 Ab#23
eIF4E-3 Ab#23
G
H
DAPI
DAPI
I
J

Figure 11 | *eIF4E-3*^{null,mCherry}, generated using CRISPR-Cas9 and homologous recombination, is a null allele. (A) Schematic of *eIF4E-3* gene region showing sites cloned for 5' and 3' homology into pTV^{Cherry}, site of *eIF4E-3* targeted crRNA complementarity, and region deleted in *eIF4E-3*^{null,mCherry}. Shaded boxes represent regions coding for exons, lines represent introns or genomic regions outside the transcribed *eIF4E-3* sequence, and unshaded boxes represent untranslated regions. (B) Confirmation of pTV^{Cherry} insertion by PCR from genomic extracts. Primers for mCherry verification were designed to amplify a 776 bp region from a site within the 5' homology region to a site within the *mCherry* sequence, in order to confirm integration of the vector. Primers for insert site verification were designed to amplify a 659 bp region from within the 3' homology region to a site further downstream, not included in the pTV$^{Cherry\text{-}eIF4E\text{-}3}$ vector, in order to show the vector was inserted at the appropriate site and that no regions outside the cloned genomic homology were integrated. (C) Western blot analysis of testes lysates shows absence of protein in *eIF4E-3*^{null,mCherry} animals as in *eIF4E-3*^{excision6} animals. (D) Males and females of the indicated genotypes were assessed for fertility when mated to w^{1118} females or males, respectively. As with *eIF4E-3*^{excision6}, *eIF4E-3*^{null,mCherry} males do not produce any offspring, while females remain fertile. (E,F) IF analysis of adult testes shows absence of protein in *eIF4E-3*^{null,mCherry} animals. (G,H) Maximum intensity projection images of the base of testes demonstrates loss of sperm bundles in *eIF4E-3*^{null,mCherry} testes, a known phenotype of eIF4E-3 null animals. (I,J) Nebenkern mitochondrial structures (arrows) in *eIF4E-3*^{null,mCherry} spermatids, visualized by non-specific α-Merlin signal, are larger than those in w^{1118} spermatids, a phenotype previously described for loss of eIF4E-3 (Hernández et al. 2012).
Scale bars in E-H: 20 μm; scale bars in I,J: 5 μm

3.3.2 mCherry reporter analysis shows nervous system expression of eIF4E-3

As the *eIF4E-3*^{null,mCherry} allele replaces all of the *eIF4E-3* sequence that would be transcribed with vector DNA including *mCherry*, it is predicted that mCherry would be expressed under endogenous *eIF4E-3* regulation. An antibody to dsRed was used to detect mCherry in fixed tissue. mCherry appears to be expressed in a semi-circular pattern in the brain lobe of third instar larvae apparently in the area of photoreceptor axon projections, similar to the expression pattern of chaoptin (Figure 12B,C). mCherry does not, however, appear to be expressed in spermatocytes (Figure 12A), a cell type in which eIF4E-3 is known to be expressed and function (Hernández et al. 2012; Ghosh and Lasko 2015). Potentially, the reporter is not capturing the whole expression of *eIF4E-3* due to deletion of regulatory elements when creating the *eIF4E-3*^{null,mCherry} allele. Nevertheless, mCherry reporter data indicate that eIF4E-3 is expressed in the central nervous system of *Drosophila*.

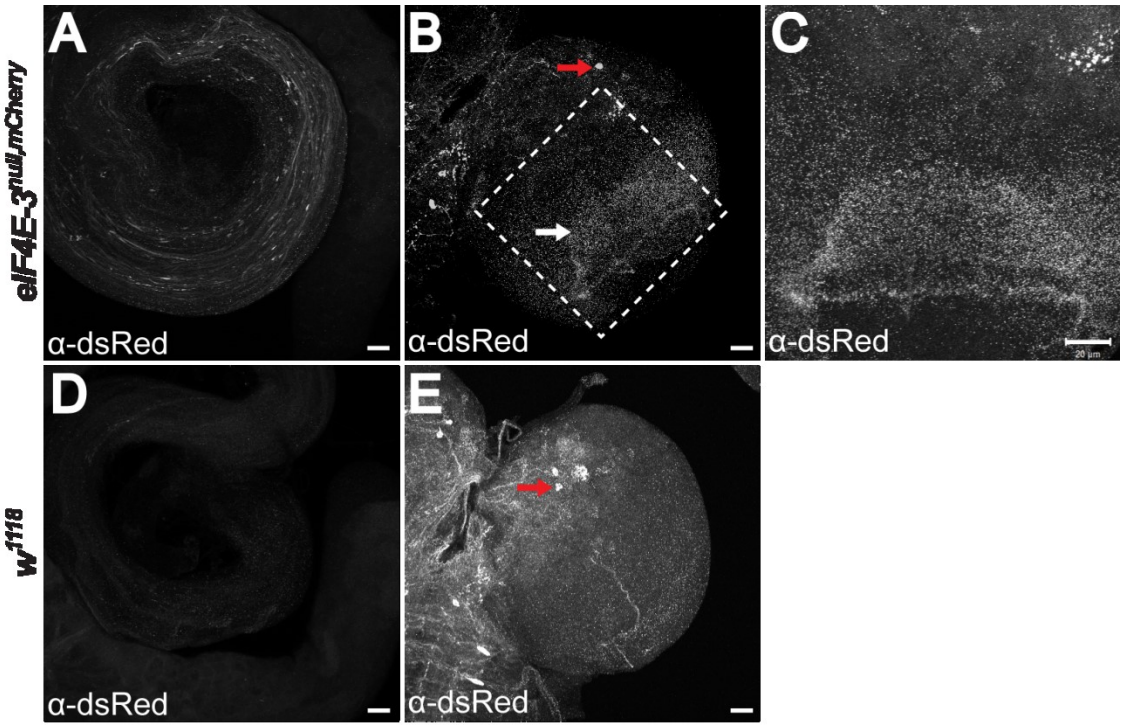

Figure 12 | mCherry reporter of eIF4E-3 expression is seen in the central nervous system of third instar larvae. (A,D) Although eIF4E-3 is known to be expressed in spermatocytes, mCherry expression visualised using α-dsRed is not observed in *eIF4E-3*^{null,mCherry} testes. (B) mCherry is specifically recognised in the brain lobe of third instar larvae, in a region which appears to correspond to innervation by photoreceptor axons in the lamina and medulla, noted by the white arrow (compare expression of chaoptin in Figure 16). (C) Higher magnification of the area indicated by dashed lines in B, maximum intensity projection. Fluorescence is seen in a semi-circular pattern with a more prominent line at the base, potentially corresponding to photoreceptor axons in the medulla and the lamina plexus. (E) Some of the sites recognised by α-dsRed are non-specific as they are seen in negative control w^{1118} brains as well (red arrows); however, the site that resembles chaoptin expression is not seen in w^{1118} brains.
Scale bars: 20μm

3.4 | eIF4E-3 is expressed in the nervous system

3.4.1 RNA fluorescence in situ hybridisation demonstrates eIF4E-3 expression in the larval brain and imaginal discs

As an alternative to determining eIF4E-3 expression pattern by protein localisation, expression of *eIF4E-3* mRNA was examined by RNA fluorescence in situ hybridisation (RNA FISH). Using an antisense probe to the sequence coding for the N-terminal region of eIF4E-3, which is unique compared with other *Drosophila eIF4E* isoforms (Hernández et al. 2005), *eIF4E-3* transcript was detected in spermatocytes in w^{1118}/Y adult testes (Figure 13A). This is consistent with protein expression seen with IF analysis (see Figure 8F, Figure 9D, Figure 10D) and with previously described protein expression data (Hernández et al. 2012). RNA FISH with the same probe in third instar larval tissues shows *eIF4E-3* transcripts in the brain toward the anterior part of the lobe (Figure 13C). This pattern is somewhat similar to what is seen with two of the α-eIF4E-3 antibodies tested, Ab#53 and msAb (Figure 9F, Figure 10F). *eIF4E-3* transcripts are also detected in the wing disc (Figure 13E), and in the eye-antennal disc apparently at the morphogenetic furrow, a boundary beyond which cells have differentiated into photoreceptors (Figure 13G). The RNA FISH data indicate that eIF4E-3 is expressed in the developing wing and nervous system of the fly.

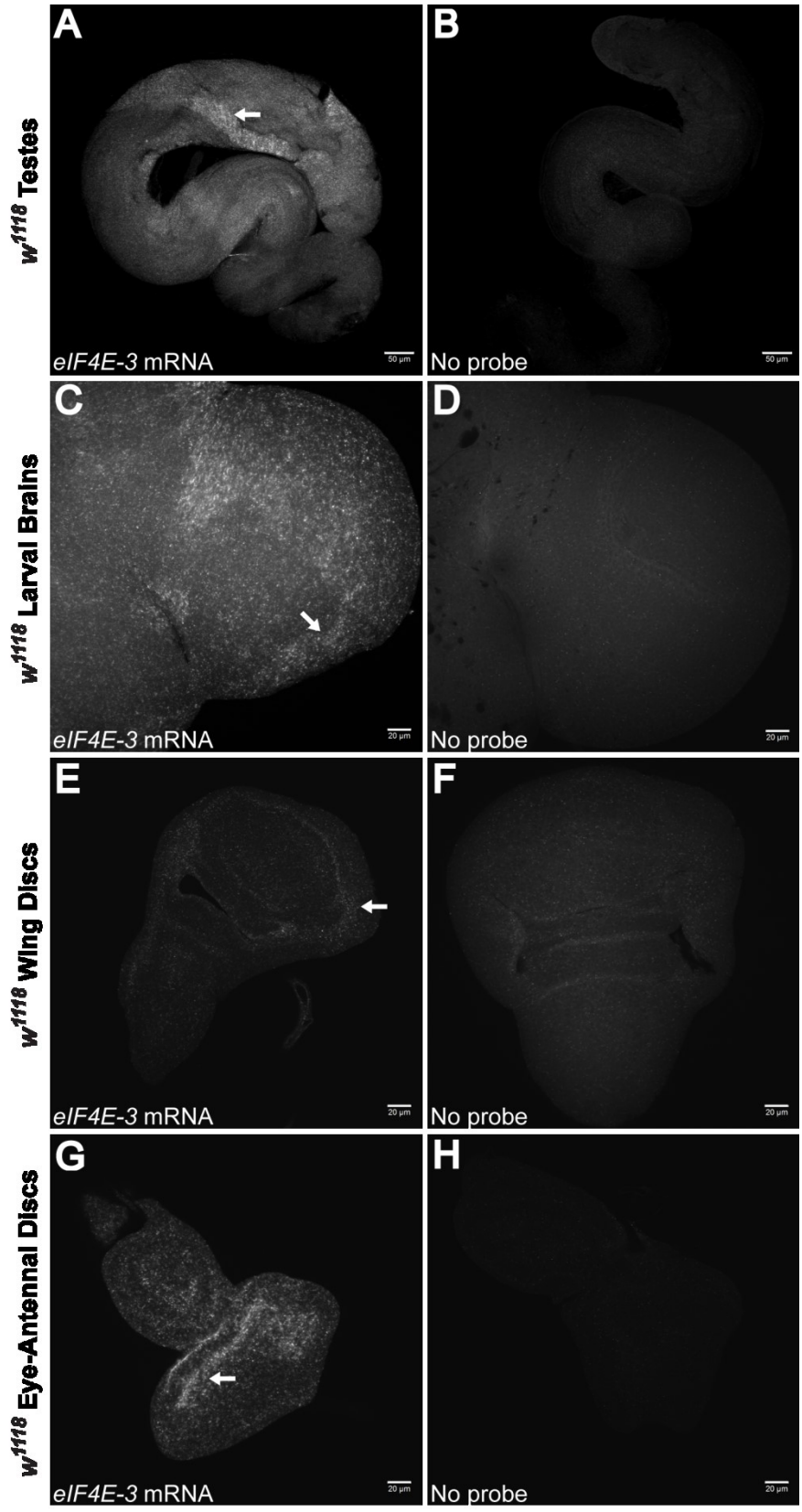
A
B
w1118 Testes
eIF4E-3 mRNA
No probe
C
D
w1118 Larval Brains
eIF4E-3 mRNA
No probe
E
F
w1118 Wing Discs
eIF4E-3 mRNA
No probe
G
H
w1118 Eye-Antennal Discs
eIF4E-3 mRNA
No probe

Figure 13 | *eIF4E-3* RNA FISH demonstrates transcript expression in testes, brains, and imaginal discs. (A) *eIF4E-3* transcripts are detected in primary spermatocytes, consistent with protein expression seen using antibodies to eIF4E-3. (C) *eIF4E-3* transcripts are seen in the anterior region of each brain lobe of third instar larvae, in an area similar to expression seen using Ab#53 or msAb (see Figure 9F, Figure 10F). (E) *eIF4E-3* transcripts in wing imaginal discs of third instar larvae, at the periphery of the wing pouch. (G) *eIF4E-3* transcripts are expressed in third instar larval eye-antennal discs, potentially at the morphogenetic furrow, which indicates the boundary between undifferentiated cells and cells differentiated to photoreceptors. (B,D,F,H) Fluorescent signal is not detected in these tissues when the RNA FISH procedure is carried out in the same way, but no DIG-labelled antisense probe is added.
Scale bars in A,B: 50 μm; scale bars in C-H: 20 μm

3.4.2 β-galactosidase expression from an eIF4E-3 enhancer trap indicates nervous system expression

In addition to acting as a null allele of *eIF4E-3*, the P-element insertion of the *eIF4E-3^{L0139}* allele also functions as an expression reporter as the P-element contains *lacW*, which encodes β-galactosidase (β-gal) (Bier et al. 1989). Therefore, β-gal expression should mimic the endogenous eIF4E-3 expression pattern, at least in part. IF using α-β-gal in *eIF4E-3^{L0139}/TM3 Ser, Act-GFP* testes shows expression in spermatocytes (Figure 14B), congruent with previously described eIF4E-3 expression (Hernández et al. 2012) and IF and RNA FISH observations. α-β-gal signal is observed in the Nebenkern in early spermatids, but this is also seen in testes from *w^{1118}/Y* negative control (see arrows in Figure 14A,B), supporting non-specific antibody binding. In *eIF4E-3^{L0139}/TM3 Ser*, *Act-GFP* third instar larval brains, specific β-gal expression is seen at several sites: a small cluster of cells at the antero-medial portion of the brain lobe (Figure 14D,H) as well as a few individual cells in the medial part of the lobe, a group of cells in the interior of the brain lobe (Figure 14D,G), another at each end of the arc of neuroepithelial cells of the optic lobe (Figure 14D,E), and cells in the optic stalk (Figure 14D,F). Wing and eye-antennal imaginal discs were also examined, but no signal specific to *eIF4E-3^{L0139}/TM3 Ser, Act-GFP* was observed.

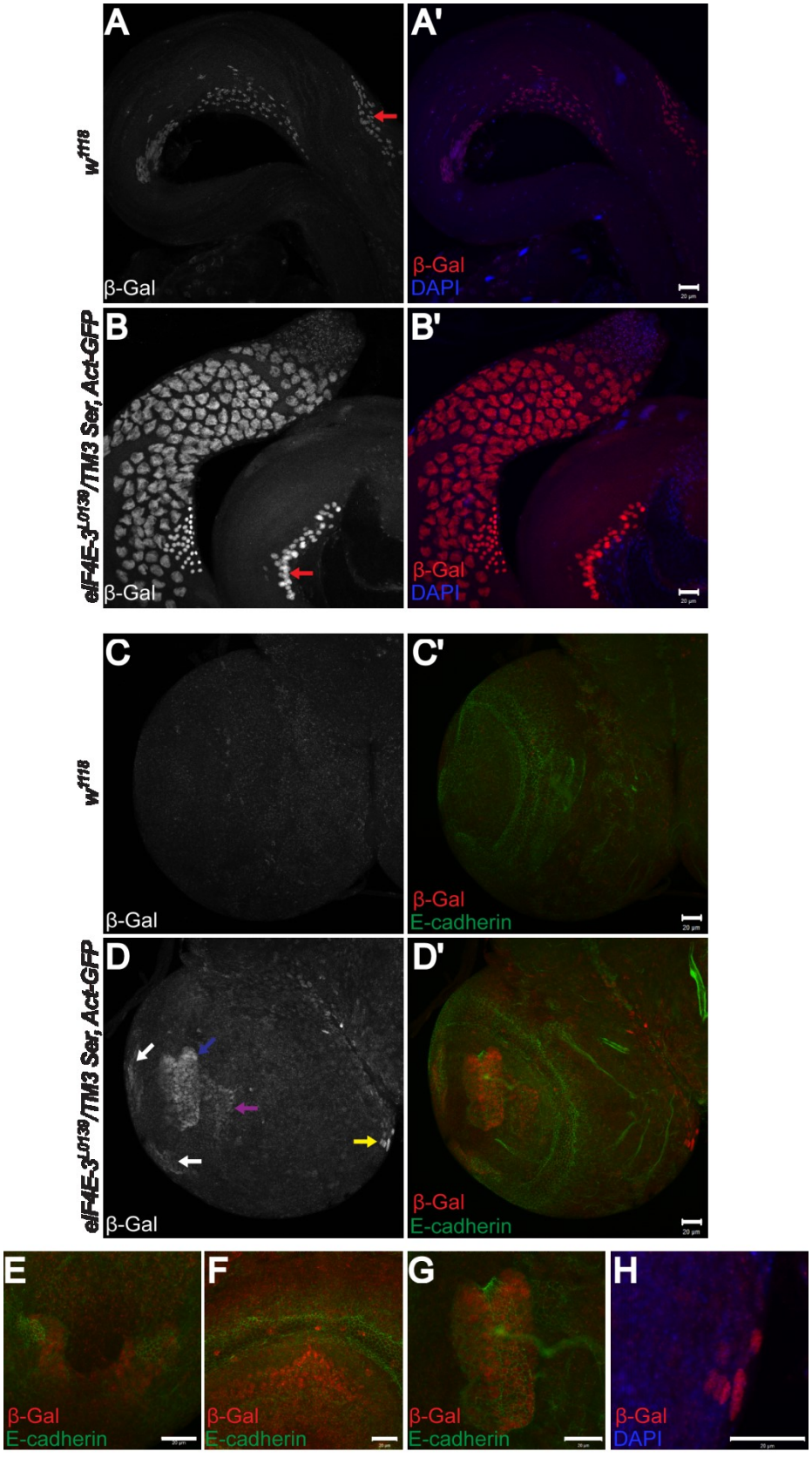
A
A'
w1118
β-Gal
β-Gal
DAPI
B
B'
eIF4E-3L0139/TM3 Ser,Act-GFP
β-Gal
β-Gal
DAPI
C
C'
w1118
β-Gal
β-Gal
E-cadherin
D
D'
eIF4E-3L0139/TM3 Ser,Act-GFP
β-Gal
β-Gal
E-cadherin
E
F
G
H
β-Gal
E-cadherin
β-Gal
E-cadherin
β-Gal
E-cadherin
β-Gal
DAPI

Figure 14 | *eIF4E-3^{L0139}* functions as an enhancer trap and shows β-galactosidase expression in testes and nervous system. (A-B') β-gal is expressed in spermatocytes of *eIF4E-3^{L0139}/TM3 Ser, Act-GFP* testes. This antibody recognition is specific as it is not observed in control *w^{1118}* testes, but Nebenkern labelling is seen in both genotypes (red arrows) and is therefore not indicative of *eIF4E-3* expression pattern. (C-D') α-β-gal is not seen in brain lobes of *w^{1118}* third instar larvae, but is apparent in multiple areas of *eIF4E-3^{L0139}/Df(3L)BSC732* brains, indicated by coloured arrows. (E-H) Maximum intensity projections of areas of the brain with β-gal expression: (E) β-gal is expressed in cells adjacent to the ends of the arc of neuroepithelial cells, indicated by white arrows in D. (F) β-gal expression in the optic stalk, purple arrow in D. (G) β-gal expression in a group of cells toward the interior of the brain lobe, blue arrow in D. (H) A cluster of cells in the anterior region of the brain lobe expresses β-gal, yellow arrow in D.
Scale bars: 20μm

Table 3 | Summary of eIF4E-3 expression observations

Method	Western Blot	Larval Brains	Larval Eye Discs	Larval Wing Discs	Pupal Wings	Adult Testes
Ab#968	Specific bands	2 cell bodies + projections	Not tested	Not tested	Not tested	Specific labelling of spermatocytes-early spermatids
Ab#23	Specific bands	2 cell bodies + projections	Photoreceptor cells + axons	Not tested	Wing veins (not specific)	Specific labelling of spermatocytes-early spermatids
Ab#53	Specific bands	Cluster of cells + projections in brain lobes and anterior part of VNC; anterior portion of brain lobe (with PLP fix; not specific) No labelling with 4%PF, heat, or heptane/DMSO/PF fixes	No labelling	Not tested	No labelling with 4%PF fix; other fixes not tested	Specific labelling of spermatocytes-early spermatids
msAb	Specific bands	Cell body in centre of each brain lobe; projections in VNC; anterior of brain lobes	No labelling	Not tested	Large cells in wing vein (not specific)	Specific labelling of spermatocytes-early spermatids
RNA FISH	N/A	Specific in anterior region of brain lobes	Near morphogenetic furrow	At wing pouch periphery	Not tested	Specific labelling of spermatocytes
β-gal reporter	Not tested	Specific near neuroepithelial cells, at anterior surface of brain lobes, in lobe interior, and in optic stalk	Not tested	No expression	Not tested	Specific expression in spermatocytes
mCherry reporter	Not tested	Specific in proximity to innervating photoreceptor axons	No expression	No expression	Not tested	No expression

3.5 | Mutations in *Merlin* and *eIF4E-3* lead to nervous system phenotypes

3.5.1 eIF4E-3 and Merlin may interact to affect photoreceptor axon distribution in brains of third instar larvae

Expression of eIF4E-3 in the central nervous system was examined by Western blot analysis, and impact of its loss or over-expression on nervous system development was investigated by IF to visualise proteins characteristic of particular nervous system cell populations in third instar larval brains. Bands corresponding to eIF4E-3 were not observed by Western blotting against lysates of up to 50 w^{1118} third instar brains (Figure 15), indicating that although eIF4E-3 is expressed in the nervous system (Figure 12, Figure 13, Figure 14), the level of expression in this tissue is low. Both loss and over-expression of eIF4E-3 were examined by IF, using the $eIF4E\text{-}3^{excision6}$ allele and *UAS-FLAG-eIF4E-3* expressed with *Actin5C-GAL4*, respectively. The majority of the markers analysed were not obviously changed with either loss or over-expression of eIF4E-3 (Table 4). However, chaoptin (chp), a protein expressed in photoreceptor axons, appeared to be expressed in a slightly larger area in $eIF4E\text{-}3^{excision6}$ larval brains compared with control w^{1118} brains. Initial experimental observations also indicated that this expression area was more similar to the control phenotype when *Merlin* mutation was introduced ($Mer^{4}/Y;;eIF4E\text{-}3^{excision6}$), suggesting a repressive genetic interaction. However, subsequent biological replicates did not clearly corroborate these initial observations, as the phenotypes were found to be fairly variable even within the control genotype, and accurate analysis is highly dependent on subtle orientation of the mounted brains. Maximum intensity projections of confocal z-stacks taken of the chp-expressing area of w^{1118} and $eIF4E\text{-}3^{excision6}$ brains at similar orientations (n=9 per genotype) were generated to quantify the domain of chp expression (Figure 16). Image J software was then used to measure the length of the lamina plexus (demarcates lamina from medulla, formed by a dense layer of expanded growth cones from R1-R6 cells [Garrity et al. 1999]). While a subtle trend toward greater lamina plexus length was observed for $eIF4E\text{-}3^{excision6}$ brains, the difference was not statistically significant (p=0.63, two-tailed T-test).

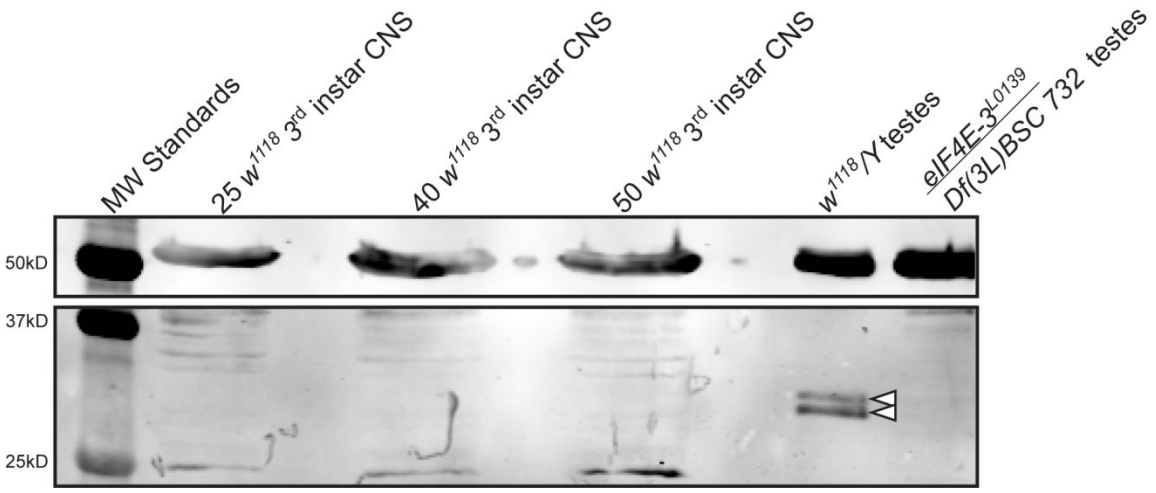

Figure 15 | eIF4E-3 expression in third instar larval CNS is not detectable by Western blot analysis. Increasing numbers of brains/ventral nerve cords were dissected from *w*^{1118} third instar larvae, lysed, and separated on a polyacrylamide gel. Adult testes from *w*^{1118}/*Y* and *eIF4E-3*^{L0139}/*Df(3L)BSC732* males were used as a positive and negative control, respectively. Blot was probed with α-eIF4E-3 Ab#23. Although a double band is seen in the positive control testes lysates, corresponding bands are not observed in CNS lysates.

Table 4 | Proteins marking specific cell populations examined for changes in expression or localisation in the larval nervous system with loss or general over-expression of eIF4E-3. Brains from third instar larvae *eIF4E-3^{excision6}/Df(3L)BSC732* and *Act5C>FLAG-eIF4E-3* were dissected and labelled by immunofluorescence for each protein alongside *w^{1118}* control brains.

NS = not significant

Protein	Structure/Cell Type	Loss or Over-expression of eIF4E-3
Chaoptin	Photoreceptor axons	Larger area covered with loss (NS)
Dachshund	Optic lobe lamina	No change
Deadpan	Neuroblasts	Increased number in central brain with loss (NS)
E-cadherin	Cell membranes	No change
ELAV	Neurons	No change
Futsch	Nervous system, axons	No change
Merlin	Ubiquitous	No change
Prospero	Ganglion mother cells	No change
Repo	Glia	No change
Sip1	Neuroblasts and progeny	Increased number of neuroblasts with loss (see deadpan)

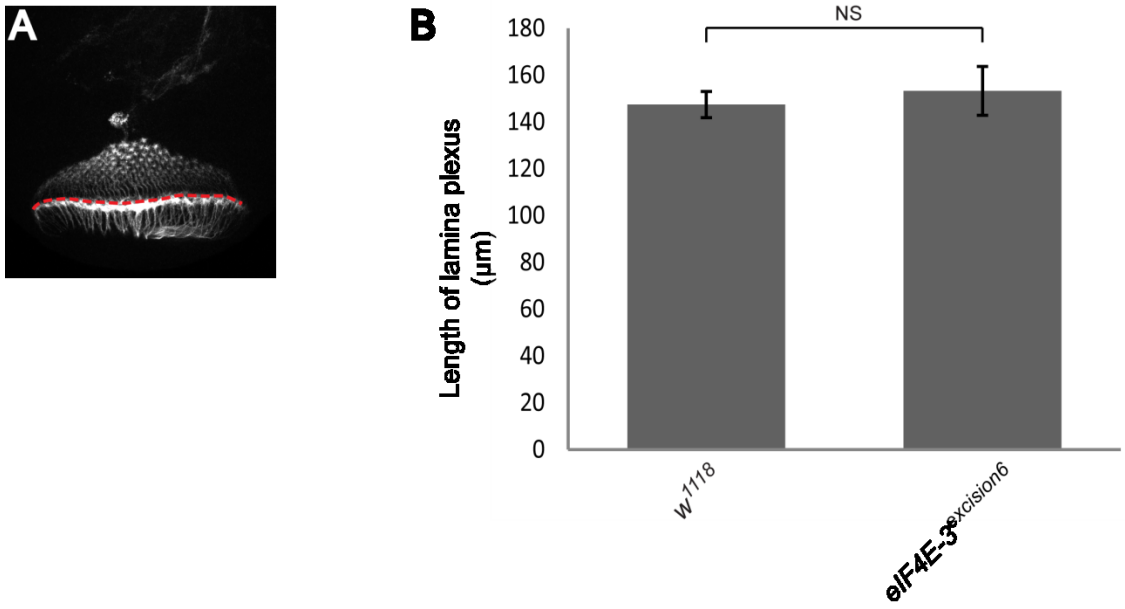

Figure 16 | The distribution of chp⁺ axon projections in third instar larval brains trends greater in *eIF4E-3*^{excision6} compared with *w*^{1118}. (A) Representative image of chp labelling in a third instar larval brain lobe. Maximum intensity projections taken at approximately the same angle were used to measure the length of the lamina plexus (red dashed line) using ImageJ software. (B) The difference in lamina plexus length is not statistically significant (two-tailed T-test, p=0.63, n=9 per genotype).

3.5.2 Merlin and eIF4E-3 genetically interact to influence central brain neuroblast abundance

In addition to the potentially expanded expression of chp, *eIF4E-3*^{excision6} brains also appeared to have fewer neuroblasts in the central brain compared with the *w*^{1118}/*Y* control, as initially observed with Sip1 expression. Central brain neuroblast count was further analysed including *Mer*^{4}/*Y* and *Mer*^{4}/*Y;;eIF4E-3*^{excision6} third instar larval brains in order to determine whether there is a genetic interaction with this phenotype, and using deadpan (Dpn) as a neuroblast marker, as it is more specific than Sip1 which is also expressed in ganglion mother cells. For each genotype, brains were analysed from male larvae only. Data pooled from two biological replicates indicate a trend toward a greater number of central brain neuroblasts in both *Mer*^{4}/*Y* and *eIF4E-3*^{excision6} larvae than *w*^{1118}/*Y*, and significantly fewer central brain neuroblasts in *Mer*^{4}/*Y;;eIF4E-3*^{excision6} brains compared with either mutant genotype alone (Figure 17B). To ascertain whether differences in neuroblast number may arise from changes in the mitotic neuroblast population, male third instar larval brains of each genotype were co-labelled for Dpn and phosphorylated histone H3 (pH3) to mark mitotic cells. More central brain neuroblasts marked with pH3 were observed in *Mer*^{4}/*Y;;eIF4E-3*^{excision6} animals versus both *w*^{1118}/*Y* and *Mer*^{4}/*Y* (Figure 17D), indicating that there are more mitotic neuroblasts although there are significantly fewer neuroblasts overall in this genotype than in *Mer*^{4}/*Y*. Neuroblasts were also analysed for co-expression of cleaved caspase-3 (casp-3) to determine if there are differences in apoptotic neuroblasts leading to altered overall counts between genotypes (Figure 17E). Casp-3 was not found in neuroblasts of any genotype, indicating that apoptosis is not a factor determining central brain neuroblast numbers in larvae with *Merlin* or *eIF4E-3* mutations.

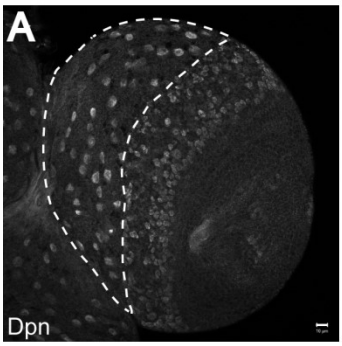
A
Dpn

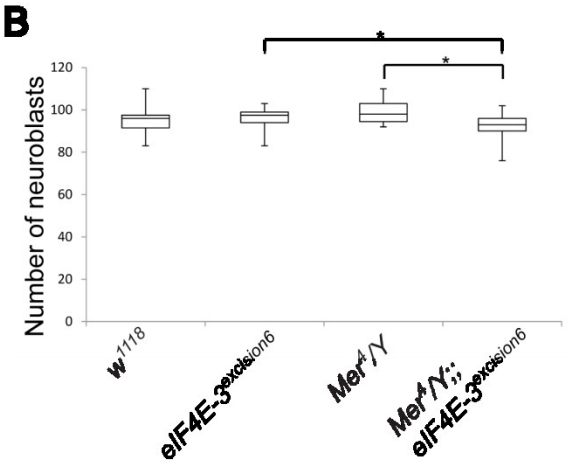
B
Number of neuroblasts
120
100
80
60
40
20
0
*
*
w1118
eIF4E-3excision6
Mer4/Y
Mer4/Y;;
eIF4E-3excision6

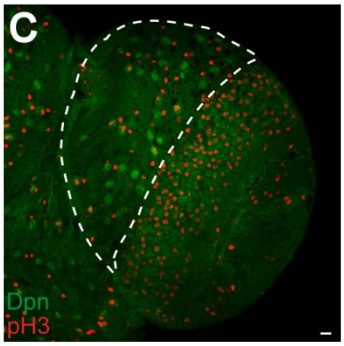
C
Dpn
pH3

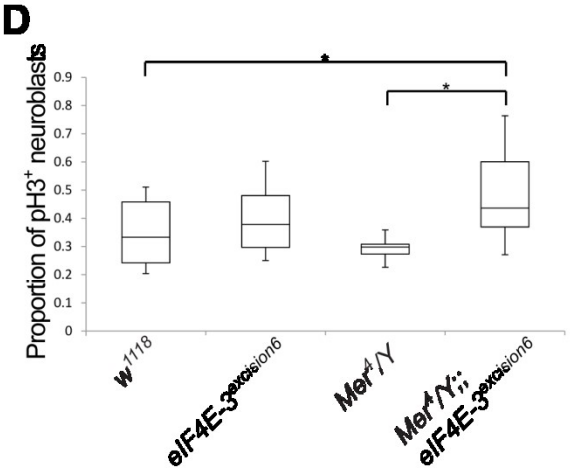
D
Proportion of pH3+ neuroblasts
0.9
0.8
0.7
0.6
0.5
0.4
0.3
0.2
0.1
0
*
*
w1118
eIF4E-3excision6
Mer4/Y
Mer4/Y;;
eIF4E-3excision6

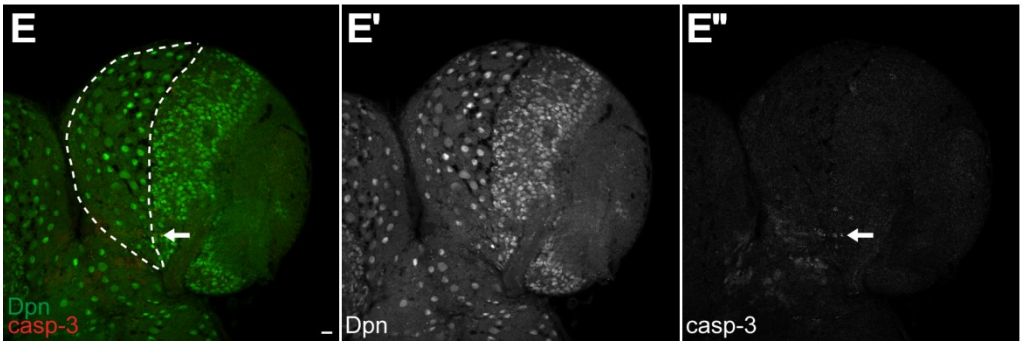
E
Dpn
casp-3
E'
Dpn
E''
casp-3

Figure 17 | Merlin and eIF4E-3 affect the number of neuroblasts present in the central brain of third instar larvae. (A) Single focal plane image showing the area in which neuroblasts (Dpn$^+$ cells) were counted. Z-stacks of the whole brain lobe were obtained to count cells. (B) There is a non-significant trend toward a greater number of central brain neuroblasts in both *eIF4E-3^{excision6}* and *Mer^4/Y* third instar larval brains, and significantly fewer neuroblasts in *Mer^4/Y;;eIF4E-3^{excision6}* compared with single mutant genotypes ($p<0.05$, Mann-Whitney U-test). (C) Neuroblasts labelled for both Dpn and pH3 in the central brain were counted as a ratio to the total number of Dpn$^+$ cells. (D) The proportion of mitotic neuroblasts is not changed in either *Mer^4/Y* or *eIF4E-3^{excision6}* brains, but is significantly greater in *Mer^4/Y;;eIF4E-3^{excision6}* brains compared with *w^{1118}/Y* and with *Mer^4/Y* ($p<0.05$, Mann-Whitney U-test). (E-E'') Neuroblasts were labelled with α-Dpn, and the central brain populations (indicated by the area enclosed by the dashed line) were examined for co-labelling with cleaved caspase-3. Some casp-3$^+$ cells were observed (arrow); however, no co-labelling neuroblasts were seen in any genotype. Scale bars: 20 μm

3.6 | Loss of Merlin or eIF4E-3 results in defects in the male germline

Both eIF4E-3 and Merlin are known to be involved in spermatogenesis and male fertility (Hernández et al. 2012; Ghosh and Lasko 2015; Dorogova et al. 2008), so spermatogenesis was used as a second system in which to investigate the interaction between Merlin and eIF4E-3. Both loss of eIF4E-3 and a hypomorphic allele of *Merlin* have been shown to cause abnormalities in spermatocyte meiosis and in shaping nuclei post-meiosis. Germ cells in *eIF4E-3^{L0139}/Df(3L)BSC732* (eIF4E-3 null) males fail to progress to the individualisation stage (Hernández et al. 2012); *Mer^{3}/Y* (Merlin hypomorph) and *Mer^{4}/Y* (Merlin null) flies are able to generate individualising sperm, albeit at a lower quantity compared with control males, and the sperm bundles at individualisation stage have scattered rather than neatly aligned nuclei (Dorogova et al. 2008). eIF4E-3 null adult males are completely sterile (Hernández et al. 2012), as are *Mer^{3}/Y* adults (LaJeunesse, McCartney, and Fehon 1998). *Mer^{4}/Y* animals do not survive to the adult stage (Fehon et al. 1997), so fertility cannot be assayed; all experiments subsequently described with *Mer^{4}/Y* or *Mer^{4}/Y;;eIF4E-3^{excision6}* testes were completed using animals at the pharate stage, approximately 24 hours after pigmentation of the pupae, and compared with testes from other genotypes 0-24 hours post-eclosion.

3.6.1 A Merlin–eIF4E-3 genetic interaction in testes morphology

Mutations in *Merlin* alter morphology of the testes. Control (*w^{1118}/Y*) testes are elongated and coiled, while *Mer^{3}/Y* testes are often smaller or sometimes absent, and testes from *Mer^{4}/Y* animals are approximately spherical (Figure 18C), more closely resembling the morphology of larval testes than that of adults. This is a specific effect of disruption of Merlin, as it is partly or fully rescued when *Act5C-GAL4* is used to drive expression of wild-type Merlin (Myc-Mer) (Figure 18E). The effect of loss of Merlin is partially rescued by loss of eIF4E-3: about 50% of *Mer^{4}/Y;;eIF4E-3^{excision6}* pharate adults have spherical testes, while the remainder have partially elongated testes (Figure 18D). Therefore, *eIF4E-3* acts as a genetic suppressor of *Merlin* mutant testes morphology phenotype.

The testis sheath, and in particular the muscular layer, is important for determining the outgrowth and final shape of the testis (Stern 1941a; Kozopas, Samos, and Nusse 1998). The pigment cells of the sheath did not appear to be affected in *Mer*^{4}/*Y* testes (Figure 19H); therefore, the testis muscle sheath was also examined in *Merlin* and *eIF4E-3* mutant animals to determine if the differences in morphology could be attributed to differences in the surrounding musculature. Muscle of *eIF4E-3*^{excision6} testes, as observed by phalloidin staining of F-actin, appeared the same as in *w*^{1118} testes, in a pattern similar to that of smooth muscle in vertebrates (Susic-Jung et al. 2012) (Figure 19A,B). *Mer*^{4}/*Y* testis sheath, on the other hand, appeared very disorganised, with bundles of fibres oriented in multiple directions and parts of the testis left uncovered by the muscle layer (Figure 19C). Muscle filament organisation is restored when the loss of Merlin is rescued by *Act5C>Myc-Mer* expression (Figure 19E), indicating that like testis morphology, muscle sheath arrangement defects are specific to loss of Merlin. *Mer*^{4}/*Y;;eIF4E-3*^{excision6} testes have a variable phenotype that falls in line with the variability observed in testis morphology. The testes that are partially rescued in terms of morphology have muscle sheaths which are similar to control sheaths (Figure 19F), while the testes that are spherical have muscle sheaths similar to those seen with *Mer*^{4}/*Y* testes (Figure 19D). Thus, testis muscle sheath architecture appears to be well correlated with final testis morphology in *Merlin* and *eIF4E-3* mutant flies.

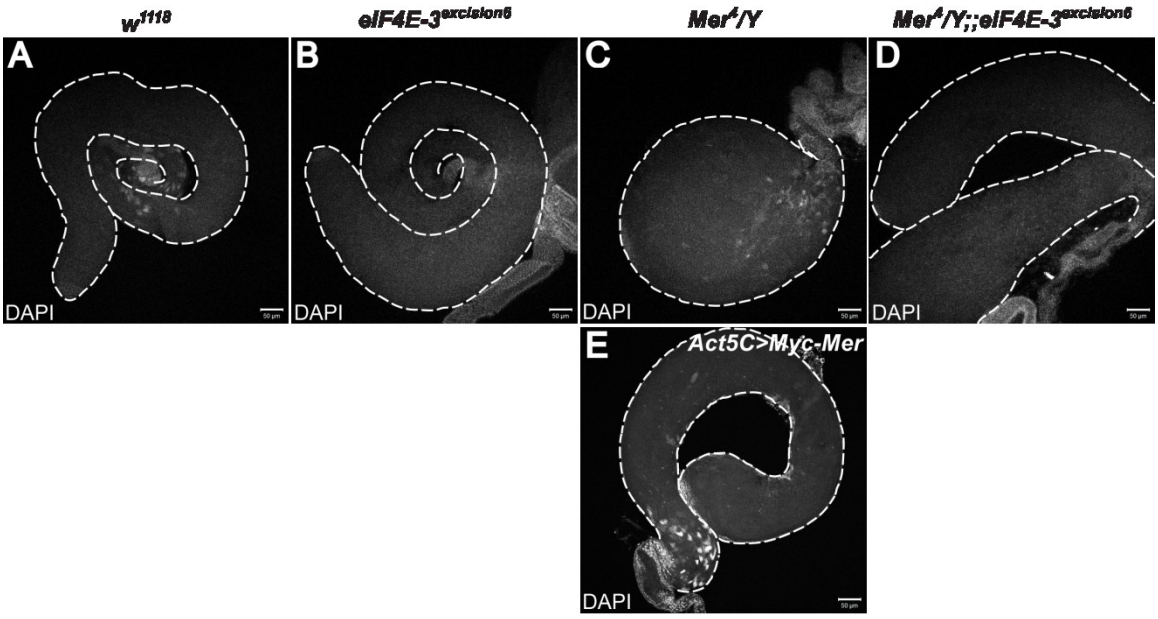

Figure 18 | *Mer*^{4}*/Y* testes have abnormal morphology that is partially rescued by addition of a null *eIF4E-3* mutation. (A) Control testes are elongated and coiled. (B) Morphology of *eIF4E-3*^{excision6} testes is not different from that of the control. (C) *Mer*^{4}*/Y* testes are relatively spherical, and this phenotype is specific to loss of Merlin, as it is rescued by expression of Myc-Mer with *Act5C-GAL4* (E). Testes from animals with null mutations in both *Merlin* and *eIF4E-3* may be partially elongated, as in (D), or spherical. Scale bars: 50 μm

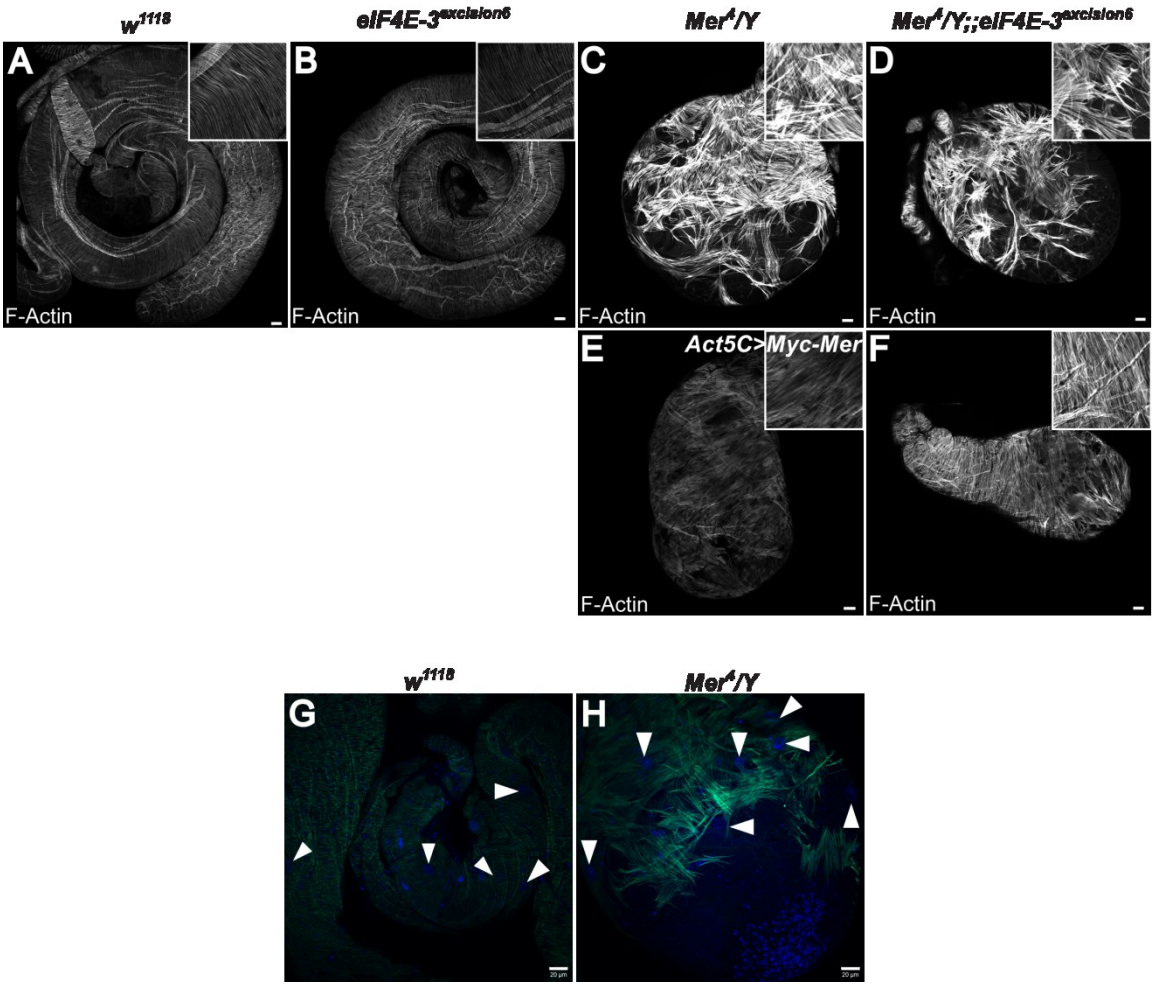
w1118
eIF4E-3excision6
Mer4/Y
Mer4/Y;;eIF4E-3excision6
A
B
C
D
F-Actin
F-Actin
F-Actin
F-Actin
E
Act5C>Myc-Mer
F
F-Actin
F-Actin
w1118
Mer4/Y
G
H

Figure 19 | Testis muscle sheath is disrupted by loss of Merlin, and is partially rescued by additional loss of eIF4E-3. (A) Muscle filaments, visualised with F-actin labelled by phalloidin, are arranged parallel to the circumference of the testis tube, and cover the whole testis in the w^{1118} control genotype. (B) The muscle sheath of *eIF4E-3*^{excision6} testes does not appear different from that of the control. (C) Muscle filaments surrounding Mer^4/Y testes are not regularly patterned and do not completely encompass the testis, an effect that is rescued by expression of Myc-Mer with the *Act5C-GAL4* driver (E). The appearance of the filaments of the muscle sheath in double mutant Mer^4/Y;;*eIF4E-3*^{excision6} testes is correlated with their morphological appearance: testes that remain spherical like Mer^4/Y testes also have a similar muscle appearance with filaments in disarray (D), whereas testes that elongate somewhat have more orderly muscle filaments (F). (G,H) The pigment cell population of the testis sheath, identified by large nuclei (arrowheads), does not appear to be altered in Mer^4/Y testes.
Scale bars: 20 μm

3.6.2 Merlin and eIF4E-3 have reciprocal effects on localisation in spermatocytes

Merlin and eIF4E-3 have both been reported to be expressed in primary spermatocytes, and loss of Merlin or eIF4E-3 to impact meiosis of these cells (Dorogova et al. 2008; Hernández et al. 2012). Using any of the eIF4E-3 antibodies described in (3.2), eIF4E-3 expression is seen in spermatocyte through spermatid stages as previously described (Hernández et al. 2012). In w^{1118}/Y spermatocytes, eIF4E-3 is cytoplasmic but also appears very distinct at the plasma membrane (Figure 20A). Mer^{4}/Y spermatocytes exhibit a range of eIF4E-3 localisation phenotypes: about 20% of spermatocyte cysts in late prophase show eIF4E-3 membrane localisation that approximates that observed in the control, 30% have much reduced membrane localisation (Figure 20B), and the remainder display a mid-range phenotype in which membrane localisation is still distinguishable, but is less distinct than in the control spermatocytes (Figure 20C). This phenotype is observed when either the msAb or Ab#23 is used to detect eIF4E-3 expression. Additionally, the reduction of eIF4E-3 membrane localisation is specific to loss of Merlin, as expression of Myc-tagged wild-type Merlin with *Act5C-GAL4* restores eIF4E-3 localisation (Figure 20D).

A polyclonal antibody raised against Merlin is detected by IF in a similar pattern to what has been previously described (Dorogova et al. 2008); however, this antibody labelling is mostly retained in Mer^{4}/Y testes, indicating that the signal is non-specific (Figure 21B). To better understand where Merlin is expressed and localised in the testes, Myc-Mer was expressed with *Act5C-GAL4* in a Mer^{4}/Y background and Merlin was visualised by IF using α-Myc (Figure 21C-E). Mitochondrial labelling observed with α-Merlin is not observed with α-Myc (red arrows in Figure 21). However, the labelling at the outside edge of the cysts, potentially corresponding to the tail somatic cyst cell, and at the anterior end of elongated spermatid bundles is observed with both antibodies, suggesting these are real sites of Merlin localisation (Figure 21C-C'',D-D''''). In primary spermatocytes, faint cortical fluorescence with α-Myc is observed only as spermatocytes approach meiosis (Figure 21E'). Nevertheless, a subtle difference in pattern was

observed with α-Merlin in eIF4E-3 null spermatocytes. While in w^{1118}/Y spermatocytes Merlin appears ubiquitous and non-distinct at the cortex (Figure 22A), its appearance in $eIF4E\text{-}3^{excision6}$ spermatocytes is much more distinctive, displaying a somewhat striated pattern (Figure 22B). The change in localisation is also seen in $eIF4E\text{-}3^{null,mCherry}$ testes (Figure 22C). This suggests that eIF4E-3 may affect Merlin function in spermatocytes by directing its subcellular localisation, either directly or indirectly.

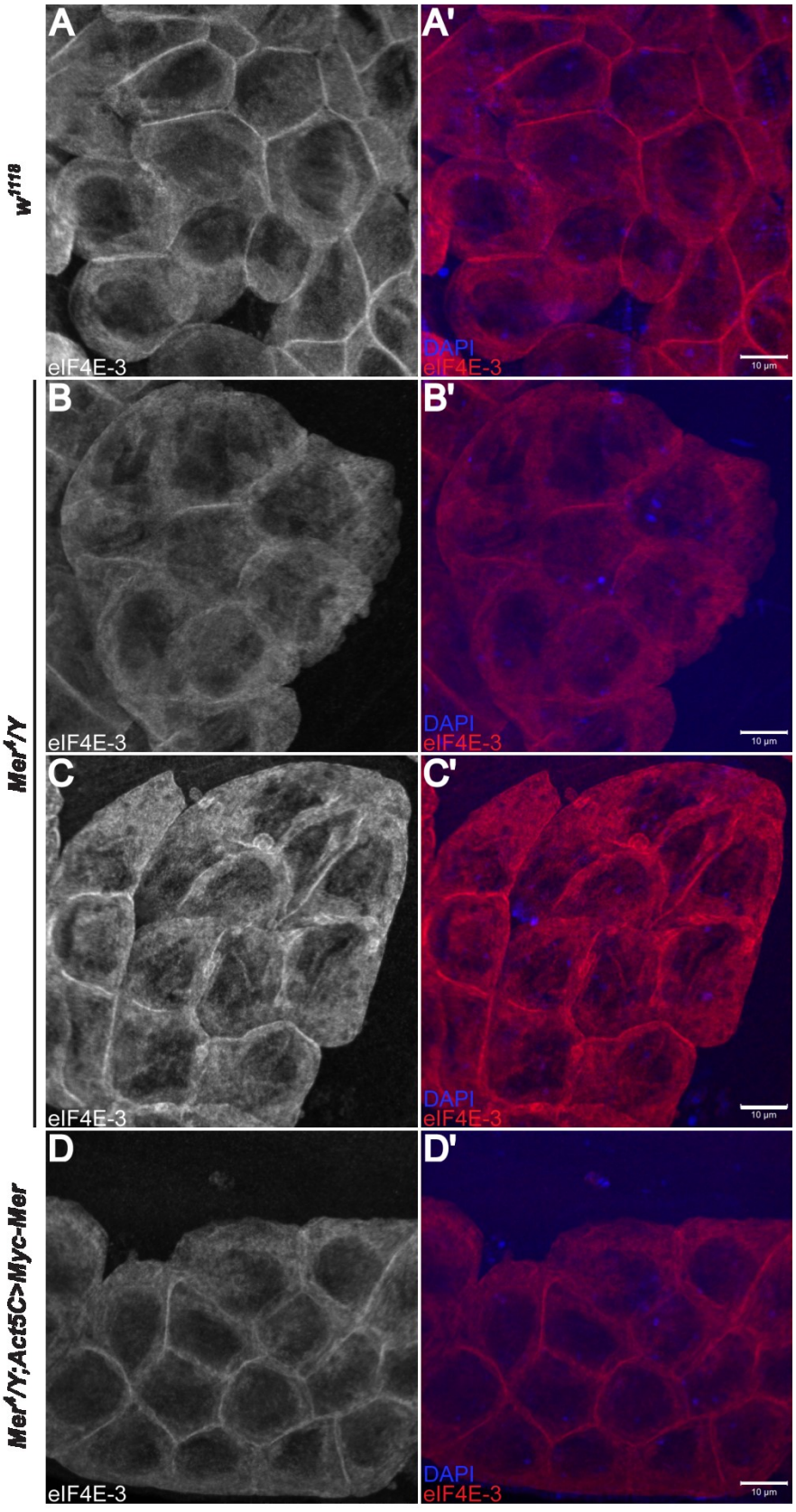
A
A'
w1118
eIF4E-3
DAPI
eIF4E-3
10 µm
B
B'
MerΔ/Y
eIF4E-3
DAPI
eIF4E-3
10 µm
C
C'
eIF4E-3
DAPI
eIF4E-3
10 µm
D
D'
MerΔ/Y;Act5C>Myc-Mer
eIF4E-3
DAPI
eIF4E-3
10 µm

Figure 20 | Loss of Merlin alters localisation of eIF4E-3 in late prophase spermatocytes. (A-A') In control w^{1118} spermatocytes in late prophase (staged by appearance of chromatin according to [Cenci et al. 1994]), eIF4E-3 is localised to the cytoplasm of spermatocytes and also appears distinct at the plasma membrane. (B-B') Approximately 30% of cysts of late prophase spermatocytes observed in Mer^4/Y testes have greatly reduced membrane localisation of eIF4E-3, although there is a phenotypic range with about 20% of cysts appearing similar to control, and 50% of cysts with somewhat reduced membrane localisation compared with the control (C-C'). (D-D') Membrane localisation of eIF4E-3 in late prophase spermatocytes is rescued when Myc-Mer is expressed using the *Act5C-GAL4* driver in a Mer^4/Y genetic background. Scale bars: 10 μm

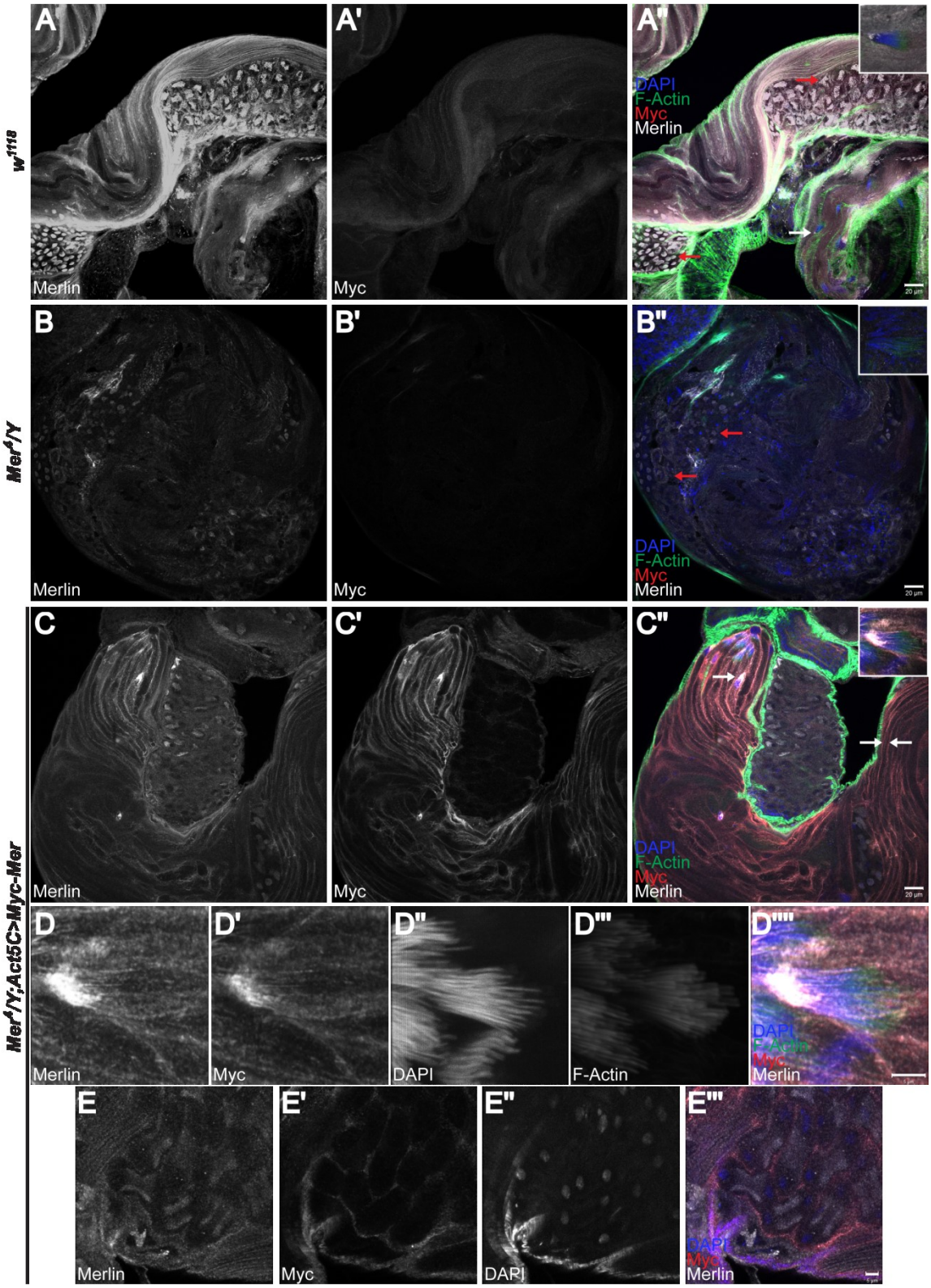
w1118
Merf/Y
Merf/Y;Act5C>Myc-Mer
A
A'
A''
B
B'
B''
C
C'
C''
D
D'
D''
D'''
D''''
E
E'
E''
E'''
Merlin
Myc
DAPI
F-Actin
Myc
Merlin

Figure 21 | Expression and localisation of Merlin during spermatogenesis.
(A-A'') In control w^{1118}/Y testes, α-Merlin labels germ cells beginning with primary spermatocytes, especially the mitochondrial derivatives (red arrows). Particularly strong localisation is also seen anterior to the needle-shaped nuclei of elongated spermatid bundles (white arrow in A'', also in inset). α-Myc does not show any fluorescence above background. (B-B'') The majority of the α-Merlin labelling seen in w^{1118}/Y testes is also observed in Mer^{4}/Y testes, including the mitochondria (red arrows). However, no fluorescence is seen near elongated spermatid nuclei (inset in B''). α-Myc does not show any fluorescence above background in Mer^{4}/Y testes. (C-C'') Testes in which Myc-Merlin is expressed in a Merlin null background reveal Merlin localisation by α-Myc, which is seen at the outside edge of cysts and anterior to needle-shaped nuclei of spermatid bundles (arrows in C'', spermatid bundle also in inset). (D-D'''') Both α-Merlin and α-Myc are observed at the anterior end of the nuclei in individualising spermatid bundles, identified by the presence of actin cones of the individualisation complexes posterior to the nuclei. (E-E''') α-Myc labelling is observed at the cell cortex in spermatocytes undergoing meiosis I.
Scale bars in A'',B'',C'': 20 μm; scale bars in D'''',E''': 5 μm

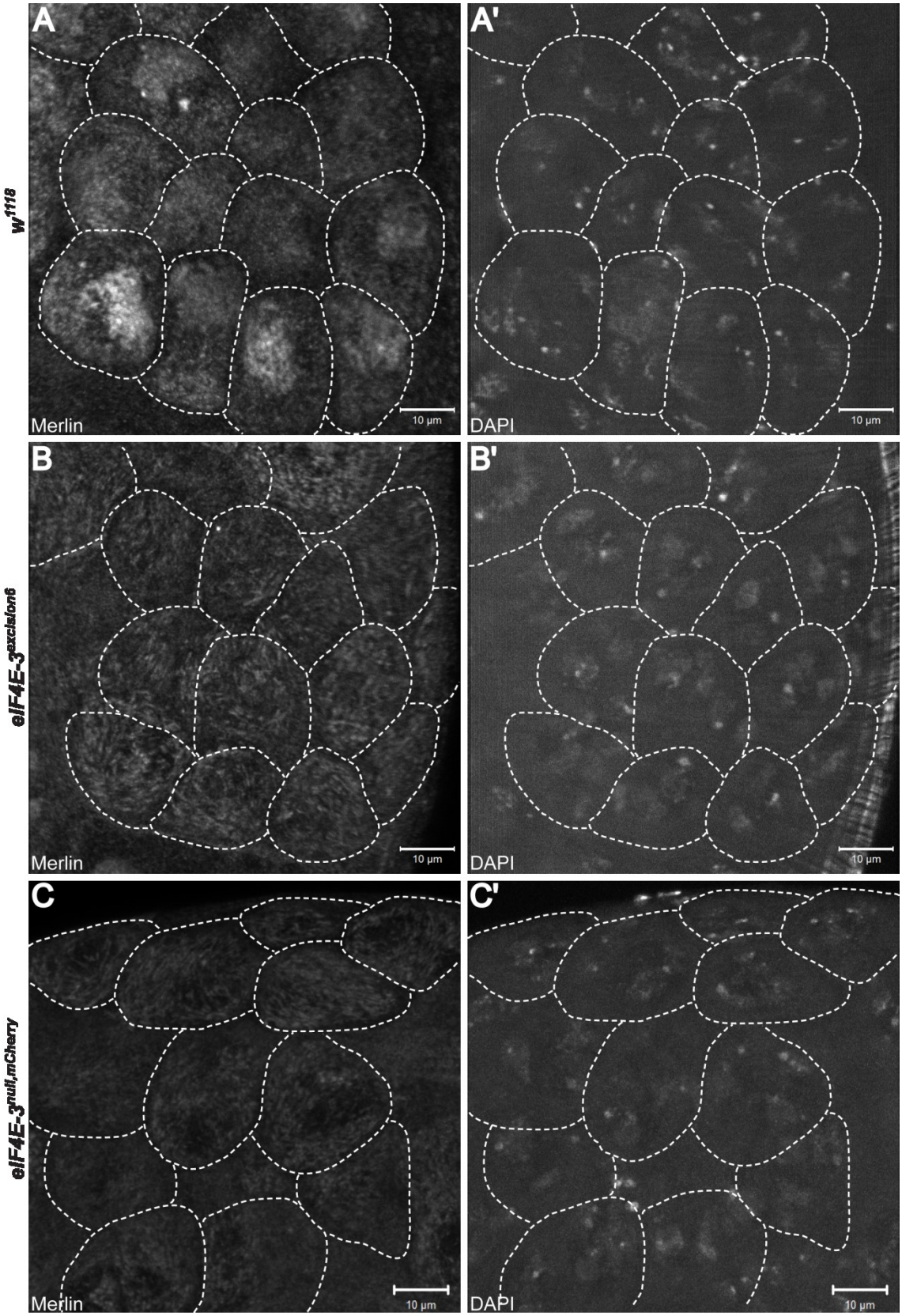
A
A'
w1118
Merlin
DAPI
10 µm
B
B'
eIF4E-3exclusion6
Merlin
DAPI
10 µm
C
C'
eIF4E-3null,mCherry
Merlin
DAPI
10 µm

Figure 22 | Cortical Merlin localisation is altered in late prophase spermatocytes of *eIF4E-3* null mutant testes. (A) Merlin, as visualised with α-Merlin, appears ubiquitous and lacking a distinctive pattern in control w^{1118} spermatocytes in late prophase (A', staged according to chromatin appearance described by Cenci et al. [1994]).
(B) Spermatocytes from the same stage (B') in $eIF4E\text{-}3^{excision6}$ testes show Merlin localisation as a more definitive, striated pattern. (C) A similar striated Merlin localisation is also observed in $eIF4E\text{-}3^{null,mCherry}$ late prophase spermatocytes, indicating this appearance of Merlin is specific to loss of eIF4E-3.
Scale bars: 10 μm

3.6.3 Loss of Merlin affects spermatid bundle integrity

Mer^{3}/*Y* animals are known to have spermatid bundle defects: cysts that progress to the individualisation stage have scattered nuclei and actin cones of the individualisation complex (IC), and fewer than 64 nuclei (Dorogova et al. 2008). Mutations in *Merlin* also affect the orientation of the bundles with respect to the tip-base axis of the testes (Figure 23). This phenotype has been observed mainly in *Mer*^{3}/*Y* animals, as the spherical nature of the *Mer*^{4}/*Y* testes prevents axis definition. Normally, sperm nuclei are oriented toward the testis base, with tails and individualisation cones toward the tip relative to the nuclei, as observed in *w*^{1118}/*Y* control testes (Figure 23A-A''). In *Mer*^{3}/*Y* testes, the sperm bundles appear to be randomly oriented (Figure 23B-B''). Additionally, in *Mer*^{3}/*Y* animals, bundles are found throughout the length of the testis, whereas in *w*^{1118}/*Y* testes they are exclusively located near the base. These phenotypes are direct effects of loss of Merlin function, as sperm bundle orientation and location within the testis, as well as organisation of the nuclei and actin cones, can be rescued by expression of Myc-Mer driven by *Act5C-GAL4* in a *Mer*^{3}/*Y* background (Figure 23C-C''). Similarly, *Act5C>Myc-Mer* in a *Mer*^{4}/*Y* background restores bundle organisation, and restores morphology fully or in part such that a tip-base axis can be defined, with sperm bundles appropriately aligned, oriented, and localised with respect to the axis (Figure 23E-E''). Furthermore, male fertility is rescued when Myc-Merlin is expressed in the *Mer*^{3}/*Y* background, demonstrating the functional requirement of Merlin in sperm maturation (Figure 23F).

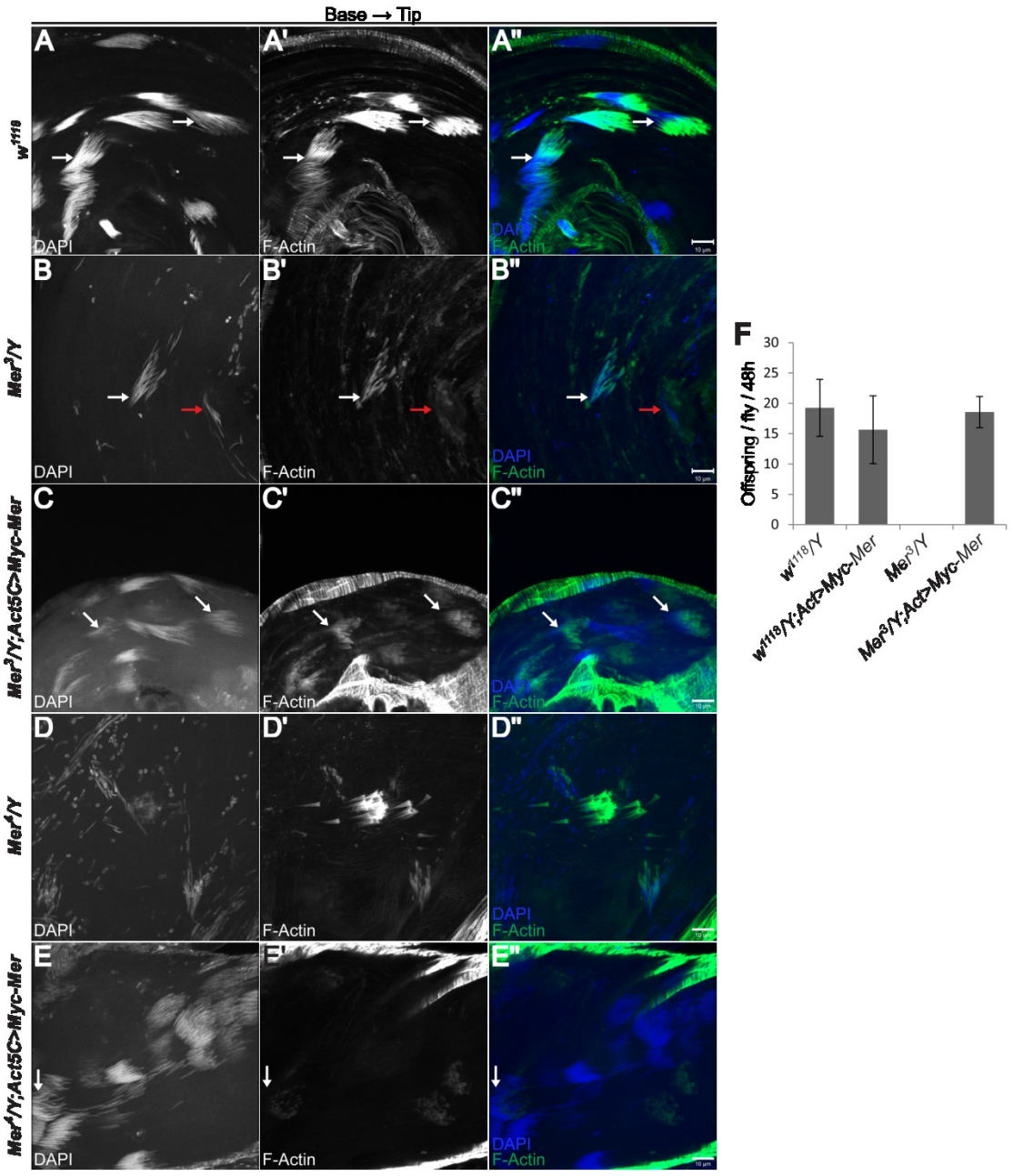
Base → Tip
A
A'
A"
B
B'
B"
C
C'
C"
D
D'
D"
E
E'
E"
DAPI
F-Actin
w1118
Mer3/Y
Mer3/Y;Act5C>Myc-Mer
Mer4/Y
Mer4/Y;Act5C>Myc-Mer
F
Offspring / fly / 48h
0
5
10
15
20
25
30
w1118/Y
w1118/Y;Act>Myc-Mer
Mer3/Y
Mer3/Y;Act>Myc-Mer

Figure 23 | Bundles of individualising spermatids are disorganised and randomly oriented relative to the testis axis in *Merlin* mutant testes. (A-A') Control w^{1118} spermatid cysts with needle-shaped nuclei have neatly aligned nuclei and are oriented with nuclei near the testis base and tails toward the tip, such that the ICs (indicated by F-actin staining) move toward the testis tip. In these and subsequent panels, white arrows point to the nuclei of spermatid bundles correctly oriented within the testis, with nuclei toward the base relative to the IC. (B-B') As previously reported (Dorogova et al. 2008), elongated spermatid bundles in Mer^3/Y testes have fewer nuclei than control bundles, and both nuclei and actin cones are scattered. Additionally, the individualising spermatid bundles appear to be randomly oriented within the testis as some have nuclei toward the base and tails toward the tip (white arrow) and others are in the reverse orientation (red arrow). (C-C') Addition of Myc-Mer expressed with *Act5C-GAL4* in the Mer^3/Y genetic background rescues both the scattering and the orientation defects observed in Mer^3/Y testes. (D-D') In Mer^4/Y testes, nuclei and actin cones are scattered as in Mer^3/Y testes, and appear randomly oriented, although there is no clear testis axis as these testes are relatively spherical (see Figure 18C). (E-E') Using *Act5C-GAL4* to drive expression of Myc-Mer in the Mer^4/Y genetic background rescues morphology of the testes (see Figure 18E), so an axis can be defined, and spermatid bundle orientation relative to this axis is normal (white arrow). Alignment of nuclei and ICs is also rescued. (F) Expression of Myc-Merlin in a Mer^3/Y background restores male fertility in addition to spermatid bundle integrity and orientation.
Scale bars: 10 μm

3.7 | Effect of Merlin and eIF4E-3 on translation

To investigate how the association between Merlin and eIF4E-3 affects the translation of their target mRNAs identified by RIP-Chip, two target transcripts – *boule* (*bol*) and *held out wings* (*how*) – were chosen based on their expression patterns to analyse protein levels among animals lacking Merlin, eIF4E-3, or both by Western blotting and IF. Bol is an RNA binding protein that is highly expressed in the male germline and is required for meiosis by promoting translation of the Cdc25/Twine phosphatase in late spermatocytes (Cheng, Maines, and Wasserman 1998; Maines and Wasserman 1999). Bol also functions in the nervous system, in part by inhibiting ecdysone-stimulated axon pruning (Joiner and Wu 2004; Hoopfer et al. 2008). HOW is also an RNA binding protein. It is developmentally required and functions in muscle development and migration, adhesion, and glial migration and axon wrapping (Zaffran et al. 1997; Baehrecke 1997; Lo and Frasch 1997; Edenfeld et al. 2006). HOW is also required in the male germline to maintain the germline stem cell population and to permit mitotic divisions of spermatogonia (Monk et al. 2010).

Western blots to examine Bol levels were carried out using lysates of third instar larval testes that were treated with the proteasome inhibitor MG132 so that changes in protein level could be attributed to increased or decreased translation and not masked by changes in the amount of degradation. Although there was variability between replicates, expression of Bol appears to be decreased in *eIF4E-3*^{excision6} larval testes compared with *w*^{1118}/*Y* larval testes (Figure 24). In some replicates Bol was decreased while unchanged in others in *Mer*^{4}/*Y* larval testes. The amount of Bol protein was also decreased in *Mer*^{4}/*Y*;;*eIF4E-3*^{excision6} testes compared with control, but was not consistently higher or lower when compared with *eIF4E-3*^{excision6} alone. By IF analysis in testes, Bol expression does not appear different from the *w*^{1118}/*Y* control genotype in *Mer*^{4}/*Y* or *eIF4E-3*^{excision6} animals (Figure 25). Likewise, there is no apparent difference in *Mer*^{4}/*Y*;;*eIF4E-3*^{excision6} testes; in particular, Bol can accumulate in late spermatocytes in each of these genotypes (arrows in Figure 25). These data indicate that eIF4E-3 is

important, but not absolutely required, for translation of *bol* and that Merlin plays a minor role, if any, in *bol* translation.

Western blot analyses of HOW were carried out on lysates from third instar larval wing discs treated with MG132. Loss of eIF4E-3 results in an increase in the amount of HOW protein in wing discs (Figure 26). HOW levels were relatively unchanged, with observations of both slight increase and slight decrease, in Mer^{4}/Y wing discs, but were increased in Mer^{3}/Y wing discs in two of three experimental replicates. $Mer^{4}/Y;;eIF4E\text{-}3^{excision6}$ wing discs, like $eIF4E\text{-}3^{excision6}$, showed increased HOW expression. In adult testes, expression of HOW, as observed by immunofluorescence, does not appear to be altered by loss of eIF4E-3 or Merlin; HOW protein is seen in germline stem cells, gonialblasts, and early spermatogonia as reported previously (Monk et al. 2010) and observed in w^{1118}/Y control testes (Figure 27). However, $Mer^{4}/Y;;eIF4E\text{-}3^{excision6}$ testes frequently have fewer spermatogonia, identified by bright appearance of nuclei near the testis tip, compared with w^{1118}/Y (Figure 27D). An opposite phenotype of increased spermatogonial numbers was previously described when the long isoform of HOW was over-expressed in the male germline (Monk et al. 2010). Therefore eIF4E-3, and potentially Merlin, act to repress translation of *how* in the wing disc, and they interact to affect spermatogonial numbers which could be through regulation of *how* translation.

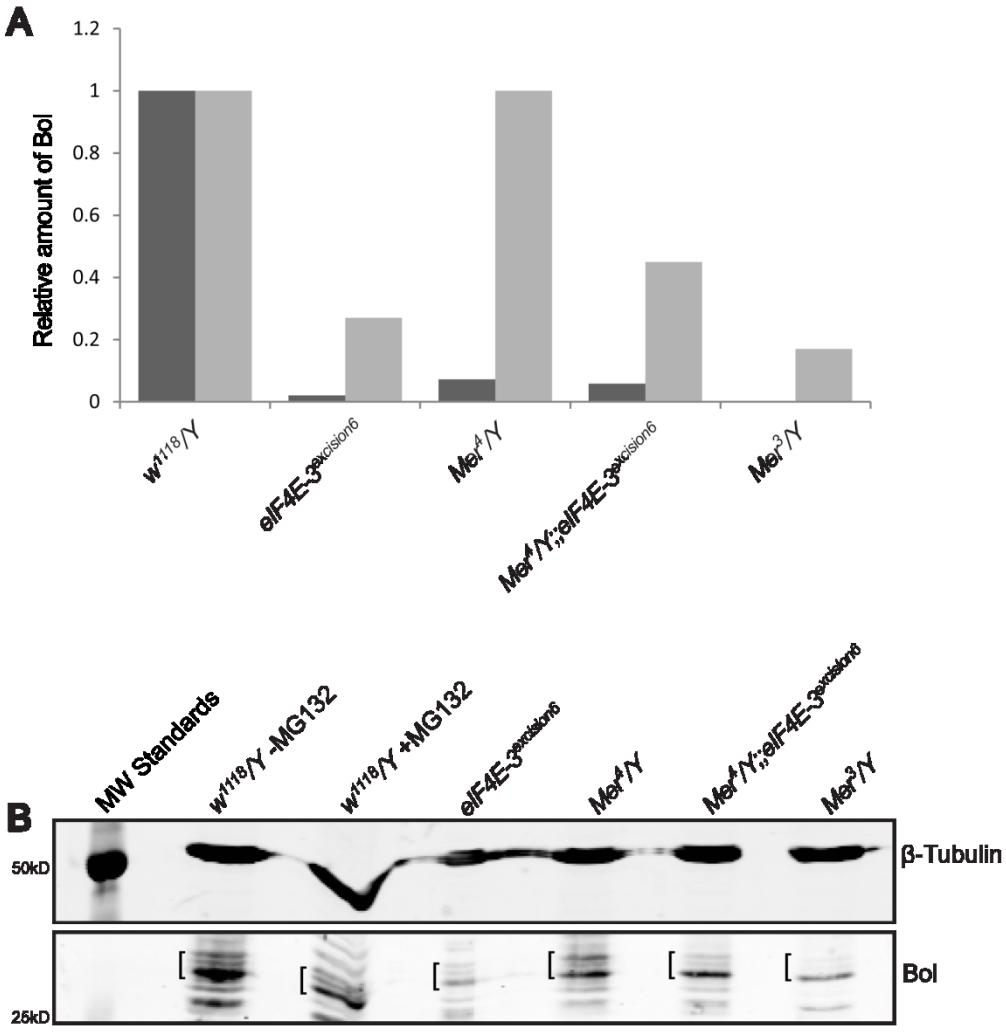
A
Relative amount of Bol
1.2
1
0.8
0.6
0.4
0.2
0
w1118/Y
eIF4E-3excision6
Mer4/Y
Mer4/Y;;eIF4E-3excision6
Mer3/Y
B
MW Standards
w1118/Y -MG132
w1118/Y +MG132
eIF4E-3excision6
Mer4/Y
Mer4/Y;;eIF4E-3excision6
Mer3/Y
50kD
β-Tubulin
25kD
Bol

Figure 24 | Protein levels of the target transcript *bol* are decreased with mutations in *eIF4E-3* and *Merlin*. (A) Expression of Bol in third instar larval testes treated with MG132 to inhibit proteasomal degradation and analysed by Western blot; two bars in each genotype represent two separate experiments. The intensity of bands corresponding to Bol was normalised to intensity of β-tubulin in the same lane, and is depicted for each genotype as a ratio to normalised intensity of Bol in w^{1118}/Y larval testes. In $eIF4E\text{-}3^{excision6}$ and $Mer^{4}/Y;;eIF4E\text{-}3^{excision6}$ larval testes, the amount of Bol protein is decreased. The effect of Merlin is less conclusive, as Bol was consistently decreased in Mer^{3}/Y animals, but may be either decreased or unaffected in Mer^{4}/Y animals. (B) Blot for Bol represented by the light grey bar in A. Bands indicated by the square bracket were measured as Bol protein.

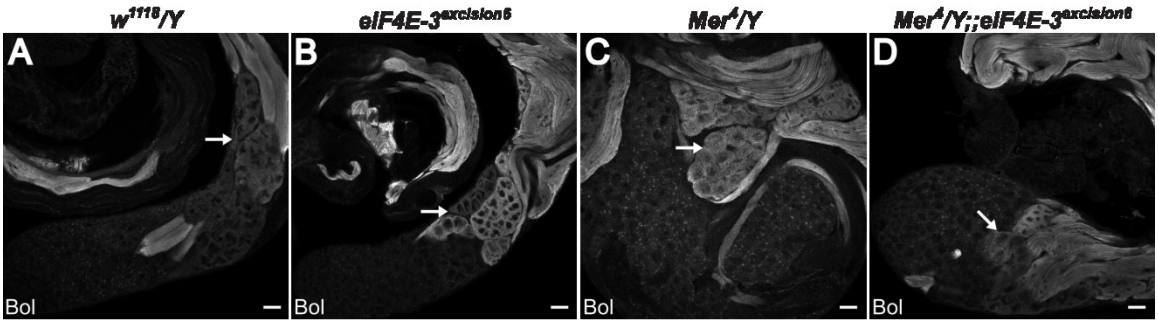

Figure 25 | Expression and localisation of Bol in testes does not appear to be altered in *eIF4E-3* or *Merlin* mutants. (A) In control w^{1118}/Y testes, Bol accumulates in the cytoplasm of late primary spermatocytes (arrow) and remains through spermatid stages. (B) Bol accumulates in late primary spermatocyte cytoplasm in $eIF4E\text{-}3^{excision6}$ testes as in the control (arrow), and in the spermatid stages that are present. (C) There is no observable difference in cytoplasmic Bol in spermatocytes of Mer^4/Y testes (arrow). (D) Loss of both Merlin and eIF4E-3 does not affect the cytoplasmic accumulation of Bol (arrow).

Scale bars: 20 μm

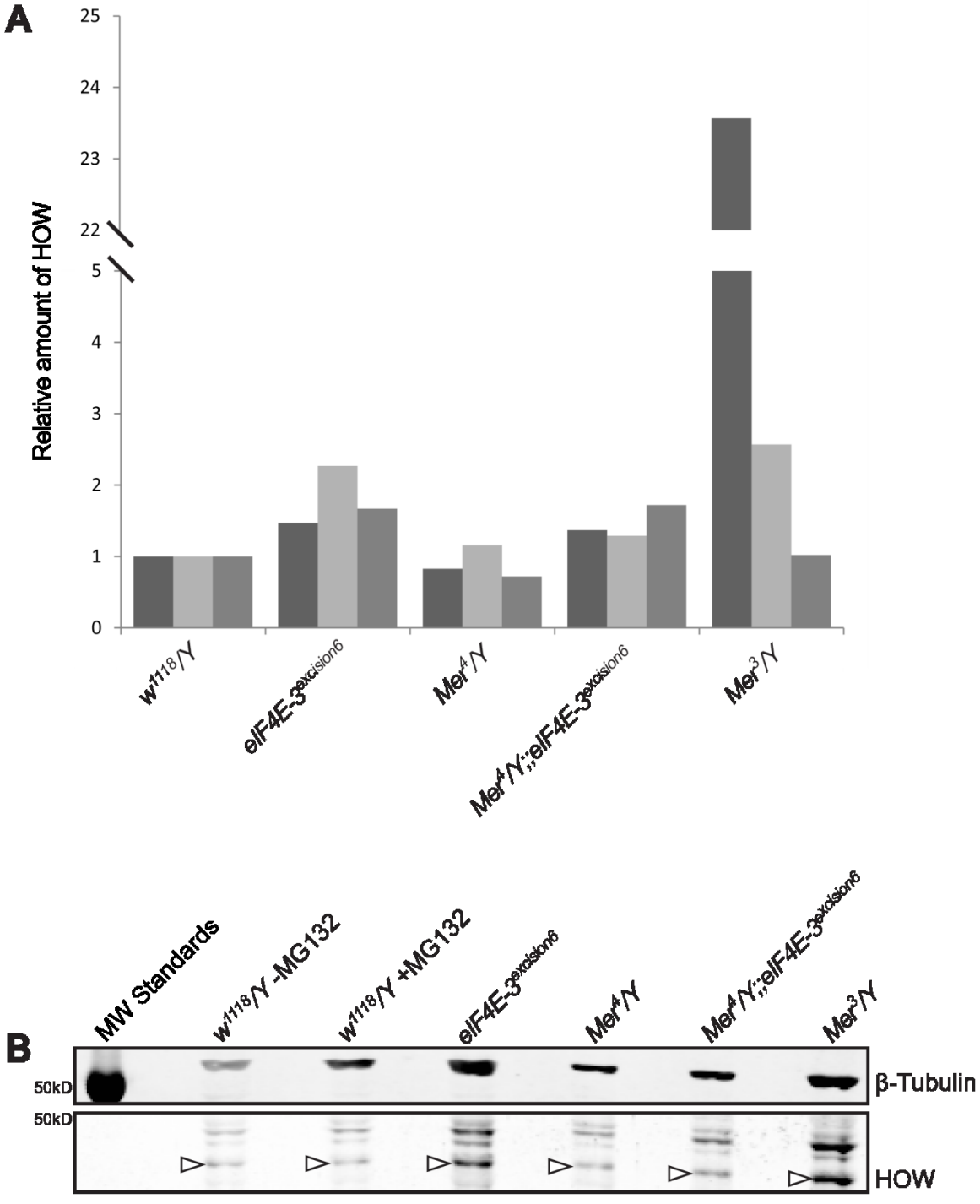
A
Relative amount of HOW
25
24
23
22
5
4
3
2
1
0
w1118/Y
eIF4E-3excision6
Mer4/Y
Mer4/Y;;eIF4E-3excision6
Mer3/Y
B
MW Standards
w1118/Y -MG132
w1118/Y +MG132
eIF4E-3excision6
Mer4/Y
Mer4/Y;;eIF4E-3excision6
Mer3/Y
50kD
50kD
β-Tubulin
HOW

Figure 26 | HOW protein is increased in wing discs with loss of eIF4E-3.

(A) Expression of HOW in third instar larval wing discs treated with MG132 to prevent degradation by the proteasome and analysed by Western blotting; three bars for each genotype represent separate experiments. For each genotype, the intensity of the HOW band was normalised to the intensity of the β-tubulin band. The protein levels are presented as a ratio relative to HOW in w^{1118}/Y wing discs. A modest increase in HOW protein was consistently observed with $eIF4E\text{-}3^{excision6}$ and $Mer^{4}/Y;;eIF4E\text{-}3^{excision6}$ genotypes. HOW was also increased in Mer^{3}/Y wing discs albeit with more variability as it was unchanged in one replicate. The effect of Mer^{4}/Y was not consistent with the Mer^{3} allele, and showed variable minor modifications of HOW protein level, wherein slightly reduced HOW was observed in two experimental replicates, but HOW was slightly increased in a third replicate. (B) Blot for HOW represented by the light grey bar in A. Bands indicated by arrowheads were measured as HOW.

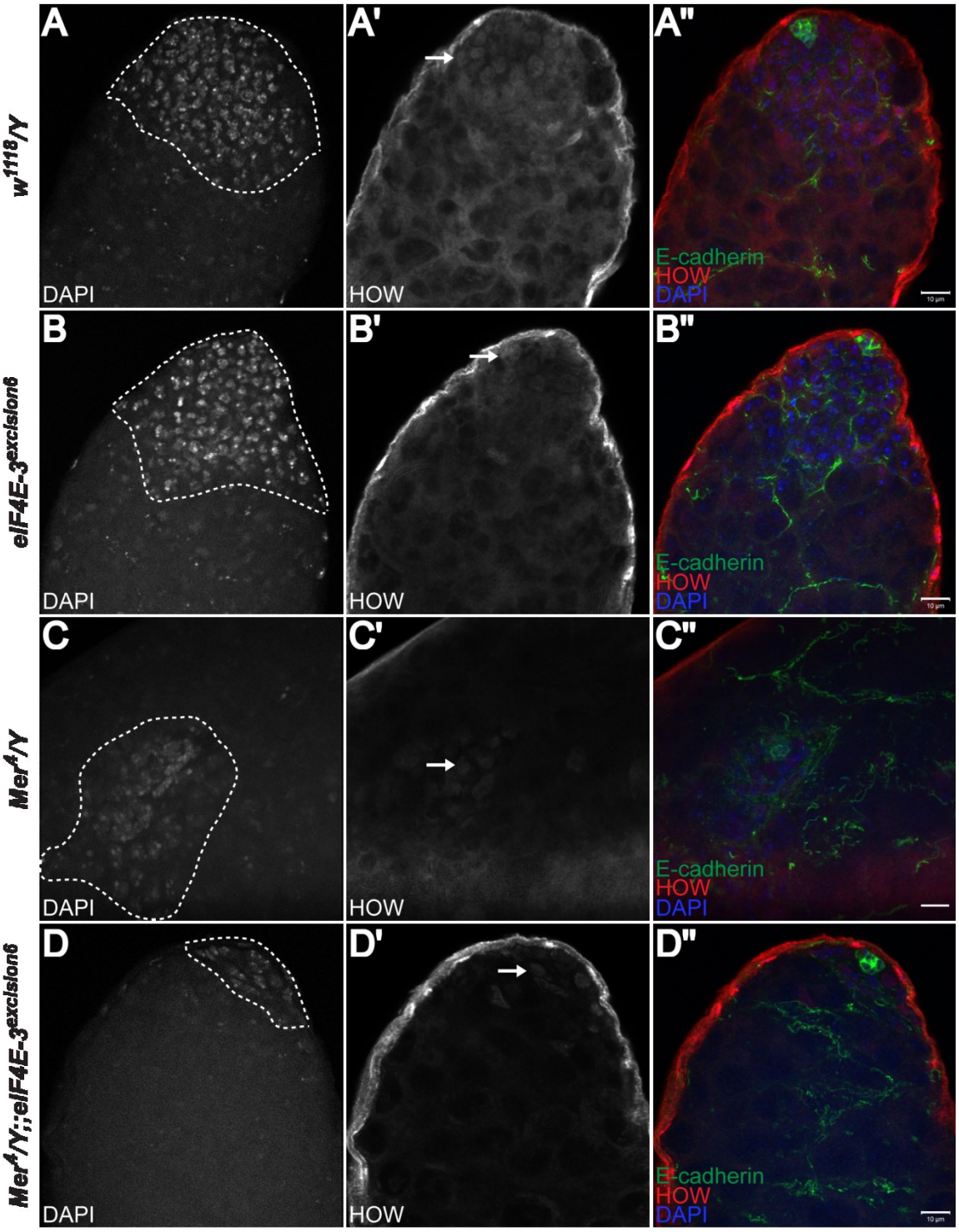
A
A'
A"
w1118/Y
DAPI
HOW
E-cadherin
HOW
DAPI
B
B'
B"
eIF4E-3excision6
DAPI
HOW
E-cadherin
HOW
DAPI
C
C'
C"
Mer4/Y
DAPI
HOW
E-cadherin
HOW
DAPI
D
D'
D"
Mer4/Y;;eIF4E-3excision6
DAPI
HOW
E-cadherin
HOW
DAPI

Figure 27 | Expression and localisation of HOW in testes is not obviously different in *eIF4E-3* or *Merlin* mutants, but loss of both Merlin and eIF4E-3 reduces the number of spermatogonia. (A-A'') HOW is expressed in hub cells (marked by E-cadherin, green in merge) and surrounding germline stem cells and gonialblasts (arrow). The population of spermatogonia, identified by bright DAPI staining, is outlined in A. (B-B'') No change is observed in expression of HOW in *eIF4E-3*^{excision6} testes (arrow), nor is the number of spermatogonia visibly different (outline in B). (C-C'') *Mer*^{4}*/Y* testes show HOW expression similar to control (arrow). Abundance of spermatogonia, outlined in C, does not appear to be altered compared to the control genotype. (D-D'') *Mer*^{4}*/Y;;eIF4E-3*^{excision6} double mutant testes do not have apparent alterations in HOW expression (arrow in D'); however, the population of spermatogonia appears reduced compared with w^{1118}/*Y* control testes.

Scale bars: 10 μm

Chapter 4 Discussion and Future Directions

4.1 | New alleles of *eIF4E-3*

In this study, two new alleles of *eIF4E-3* were created: $eIF4E\text{-}3^{excision6}$ and $eIF4E\text{-}3^{null,mCherry}$. Both were verified to be null mutations which are viable but cause sterility in males (Figure 5, Figure 11). These alleles will be useful for further study of eIF4E-3 function as they avoid the background lethality of the $eIF4E\text{-}3^{L0139}$ chromosome. By confirming that phenotypes previously reported as resulting from mutations in *eIF4E-3* are also observed in the $eIF4E\text{-}3^{excision6}$ and $eIF4E\text{-}3^{null,mCherry}$ alleles (Figure 6, Figure 7, Figure 11), it can be concluded that these effects – abnormal spermatogenesis resulting in infertility and absence of mature sperm, and enhancement of $Mer^{\Delta BB}$ overgrowth in the adult wing – are specific to loss of eIF4E-3 and not due to genetic background effects.

4.2 | Determining eIF4E-3 expression outside the male germline

Several approaches were undertaken in an effort to determine if eIF4E-3 is expressed in tissues other than spermatocytes, using this known expression pattern as a positive control. Each of the three antibodies tested shows specific recognition of eIF4E-3 demonstrated with Western blots and with IF, both by overlap with an antibody against a peptide tag in transgene-expressing animals and by absence of signal in eIF4E-3 null testes (Figure 8A-C''',F-G; Figure 9A-E; Figure 10A-E). However, in larval brains, each antibody uncovers a pattern different from the others that appears to be precise, in that only a few particular cells are labelled, but is not specific as eIF4E-3 null brains are identically labelled (Figure 8H-I; Figure 9F-G; Figure 10F-G). A similar trend was seen in other tissues examined, including pupal wings and embryonic nervous system, indicating that the patterns recognised are not specific to eIF4E-3. These antibodies might be recognising other epitopes. Precise but non-specific antibody signal in the *Drosophila* nervous system has been previously described (Saez and Young 1988), and was also observed in this study with other antibodies: α-dsRed was found to label some cells in negative control w^{1118} brains (see Figure 12E) and both α-dsRed and α-β-gal label cells in w^{1118} larval ventral nerve cords.

Using FISH to analyse distribution of *eIF4E-3* mRNA in larval tissue, expression was seen in wing and eye-antennal imaginal discs and in brains in addition to the spermatocyte positive control (Figure 13), although the high level of background signal makes precise interpretation somewhat difficult. Some attempts were made to improve signal to noise ratio, including addition of detergents to wash buffers as described to visualise transcripts with low expression in planaria (King and Newmark 2013), which helped reduce the background but also resulted in little to no signal. It would be helpful to continue optimisation of the protocol for a reliable overview of *eIF4E-3* transcript expression, or perhaps to try chromogenic visualisation of the probe (Tautz and Pfeifle 1989) rather than fluorescence, which is more readily monitored over time and can be stained for longer periods, potentially improving signal for low level expression.

β-gal from an *eIF4E-3* enhancer trap expresses in the positive control cells (spermatocytes) and in multiple separate areas of the larval brain lobe and optic stalk (Figure 14). The expression patterns seen by RNA FISH or with the mCherry reporter are not accounted for in this method; it is possible that the enhancer trap does not reflect all cells in which eIF4E-3 is normally expressed, as similar expression discrepancies have been noted with multiple enhancer traps in *Drosophila* (Calleja et al. 1996; Cabrera et al. 2002; Mayer et al. 2013).

Expression of the mCherry reporter, which replaces the eIF4E-3 coding region, was not seen in the spermatocytes, but was in the larval brain in the area of the lamina and medulla of the optic lobe (Figure 12). A conceivable reason no reporter expression was seen in spermatocytes despite evidence these cells highly express eIF4E-3 is because a regulatory element for *eIF4E-3* transcription is missing, maybe contained within an intron. It is therefore also possible that one or more regulatory elements for expression outside the male germline are absent and that the whole of eIF4E-3 endogenous expression is not captured by this reporter. This would align with the lack of congruence between mCherry expression and expression of the β-gal reporter or of the RNA FISH signal.

In addition to spermatocytes, eIF4E-3 appears to be expressed in the central nervous system of *Drosophila*. Although each method used to investigate eIF4E-3 expression pattern gives slightly different results, there is currently nothing known regarding the regulation of eIF4E-3 expression, so these discrepancies may simply reflect the capturing of different regulatory elements. Alternatively, because eIF4E-3 expression in the nervous system is likely at very low levels, as supported by the inability to detect it in larval brain lysates (Figure 15), it is possible that the sensitivity of some of these detection methods is not great enough to reflect the full pattern of expression. Taking into account all observed patterns of eIF4E-3 expression in the *Drosophila* larval brain, this translation factor appears to be expressed in, at minimum, cells associated with the visual region of the brain including adjacent to optic lobe neuroblasts, within the optic stalk, and in the medulla, as well as in an area at the anterior of the central brain and in an unidentified group of cells in the brain interior. Expression of eIF4E-3 specifically in the nervous system supports the idea that it may contribute to the nervous system specificity of NF2 tumours by adjusting Merlin activity in these cell types.

4.3 | Potential Merlin and eIF4E-3 interaction in photoreceptor axon guidance

The lamina plexus is formed by the termination of axon growth cones of photoreceptor neurons R1-R6, which occurs between a row of marginal glial cells and a row of epithelial glial cells (Winberg, Perez, and Steller 1992). These glia signal for the growth cones to stop at this stage (Poeck et al. 2001), where they pause before forming final synaptic connections (Fröhlich and Meinertzhagen 1982). This is necessary because the photoreceptor projections not only receive signals from the environment including glial cells, but they also influence the proliferation and differentiation of these cells in the brain environment (Huang and Kunes 1998; Huang, Shilo, and Kunes 1998). In *eIF4E-3*^{excision6} larvae, the size of the lamina plexus was found to be on average slightly, though not significantly, larger than that of w^{1118} larvae (Figure 16B). While the difference is not significant as measured over several replicates, it remains a possibility

that this is a true phenotype that is attenuated when Merlin is lost as well, and that the non-significance reflects either subtlety of the phenotype or incomplete penetrance. In larvae mutant for the activin receptor *babo*, the lamina plexus was found to be smaller and have fewer, less organised surrounding glia as a result of attenuated neuroblast proliferation and therefore a reduced pool of progenitor cells (Zhu et al. 2008). eIF4E-3 is potentially acting in an opposite manner, causing excess glia or lamina neuropil production and thereby affecting photoreceptor axon targeting. This could result from altered progenitor availability, as in *babo* mutants, or perhaps loss of eIF4E-3 changes the signalling capacity of the glia or of the axons in turn affecting the distribution of their synaptic targets. It would be interesting to examine the distribution of glia surrounding the lamina plexus by IF using an antibody to the glia marker repo. Appearance of glia in *eIF4E-3*^{excision6} larvae could be compared with a control to see if there is a difference in glial number or organisation, which may only be apparent in brains in which the lamina plexus is obviously longer than normal, and if so whether this difference is mitigated in animals null for both eIF4E-3 and Merlin. Cell type requirement for eIF4E-3 function could also be analysed using the *GAL4-UAS* system to generate either cell type specific knock-down or rescue of the *eIF4E-3*^{excision6} allele; however, this would likely be quite difficult to achieve considering the variability of the mutant phenotype.

4.4 | Merlin and eIF4E-3 interaction in central brain neuroblasts

Approximately 100 central brain neuroblasts for each brain lobe are specified from the procephalic neurogenic region of ectoderm by embryonic stage 11 (Urbach, Schnabel, and Technau 2003), and enter a quiescent state at the end of embryogenesis. Neuroblasts in the larval brain arise from the embryonically derived population by exiting quiescence beginning at the end of the first instar larval stage and reaching a peak of about 85 proliferating neuroblasts per brain lobe in third instar larvae (Ito and Hotta 1992). Within this population, eight neuroblasts are classified type II because they divide to produce intermediate neural progenitor cells, themselves having limited self-renewal capacity (Bello et al. 2008; Bowman et al. 2008; Boone and Doe 2008), and can

therefore generate large quantities of differentiated cells compared with type I neuroblasts, which produce ganglion mother cells that divide once and terminally differentiate (Boone and Doe 2008). However, this difference also makes type II lineages more prone to tumour formation, as deregulated self-renewal can occur in the neuroblast or intermediate neural progenitors (Kang and Reichert 2015). Interestingly, the canonical *Drosophila* eIF4E is important in progression of type II neuroblast-derived brain tumours, as neuroblast-specific depletion of eIF4E prevents tumour formation in mutant backgrounds that cause over-proliferation in type II lineages (Song and Lu 2011). However, eIF4E knock-down does not prevent tumour development in type I neuroblasts or alter the number of normal neuroblasts (Song and Lu 2011), so it is possible that one or more of the alternative eIF4E isoforms is more important in normal maintenance and division of neuroblasts. eIF4E-3 potentially participates in this process, as its loss caused a trend, albeit non-significant, toward more central brain neuroblasts (Figure 17B). Similarly, loss of Merlin trends toward a greater number of central brain neuroblasts, indicating it may also be involved in regulation of neuroblast maintenance. It is intriguing that the combination of the two mutations leads to a significantly reduced neuroblast count compared with either mutation on its own, more similar to the count in control brains. This suppressive interaction suggests that the functions of Merlin and eIF4E-3 in neuroblasts are linked, consistent with the idea that eIF4E-3 may enhance the tumour suppressor activity of Merlin in certain cell types.

Markers of mitosis and apoptosis were investigated to determine whether differences in cell division or cell death among *Merlin* and *eIF4E-3* mutant genotypes might account for the variation in overall neuroblast numbers. It was initially surprising that the brains of larvae which are null for both Merlin and eIF4E-3 had more dividing neuroblasts than the control genotype or loss of Merlin alone (Figure 17D), but a lower overall number of neuroblasts than loss of Merlin. However, as neuroblasts are normally specified in embryogenesis, an increased mitotic neuroblast population does not necessarily signify that more neuroblasts would be expected unless the divisions are symmetric. Given that

the overall neuroblast count is similar to that in control brains, it is more likely that these divisions are asymmetric. It is possible, therefore, that there is an increase in differentiated neurons/glia in *Mer*^{4}/*Y;;eIF4E-3*^{excision6} brains. The abundance and relatively non-distinct appearance of ELAV, the marker for differentiated neurons, in the larval brain makes it difficult to quantify the abundance of neurons accurately enough to determine what may be a subtle difference. On the other hand, differentiated glia could be quantified using repo as a marker in order to assess a potential increase in asymmetric divisions.

Neuroblasts are not found in normal adult brains as they cease dividing by the end of the pupal stage (Ito and Hotta 1992). In the central brain, some neuroblasts undergo apoptosis during the pupal stage (Cenci and Gould 2005), while others stop self-renewal and divide into two post-mitotic cells (Maurange, Cheng, and Gould 2008), and the mechanism of termination in type I neuroblasts that generate the mushroom body and in type II neuroblasts is unknown (Reichert 2011). Cleaved caspase-3 would therefore not be expected in Dpn^{+} neuroblasts in the central brain of third instar larvae as this is prior to the stage in which neuroblast divisions are terminated, and this corresponds to what was observed in control larval brains co-labelled with α-Dpn and α-casp-3. Neither the single nor the double mutant brains had casp-3^{+} neuroblasts either, demonstrating that the number of neuroblasts present in these genotypes is not being affected by apoptosis, at least at this developmental stage. It would be interesting to examine *Mer*^{4} and *eIF4E-3*^{excision6} adult brains to see whether any neuroblasts remain at this stage as a means of determining if stem cell termination might be defective. Since neither proliferation nor apoptosis seem to be influencing the neuroblast number in third instar larvae, *Mer*^{4} and *eIF4E-3*^{excision6} brains could be assessed for symmetric cell divisions as a source of extra neuroblasts by inducing single neuroblast mutant clones in larvae using the MARCM technique (Lee and Luo 1999): clones containing more than one neuroblast would be indicative of symmetric divisions producing an overabundance of cells. Alternatively, it is possible that an abnormal number of central brain neuroblasts are

specified during development, which could be determined by counting neuroblasts at late embryonic or early larval instar stages.

4.5 | Merlin and eIF4E-3 interact to alter testis morphology

Drosophila testes undergo a morphological change during the pupal life stage from the spherical larval gonad to the fully developed adult structure. This transformation begins around 30 hours after puparium formation (Stern 1941a; Gärtner et al. 2014), when contact is established between the seminal vesicle, which is derived from the genital disc, and the testis (Dobzhansky 1931; Stern 1941a; Stern 1941b). Contact induces a reciprocal cell migration: muscle cells originating in the genital disc migrate to encapsulate the testis, and pigment cells of the testis cover the seminal vesicle (Kozopas, Samos, and Nusse 1998) forming a bilayered sheath that encloses the testis and seminal vesicle. Both muscle cell migration and presence of pigment cells are required for shape change to occur, as testes have abnormal morphology if the testis fails to make contact with the genital disc (Stern 1941a), if muscle cell migration is defective (Kozopas, Samos, and Nusse 1998), or if the pigment cells are not specified (Kozopas, Samos, and Nusse 1998) or are lost during development (Nanda et al. 2009). In Mer^{4}/Y pharate adults, the testes are connected to seminal vesicles, indicating that their failure to elongate is not caused by failure to make contact with the genital disc. Mer^{4}/Y testes also have a population of pigment cells (Figure 19H), so the morphological defect does not result from absence of these cells; however, this does not preclude the possibility that they are functionally defective. More likely though, is that the failure of testes to elongate and coil when Merlin is lost is due to abnormalities in the muscle layer of the sheath, as some testes are not fully enclosed in muscle, and the muscle that is present lacks normal organisational integrity (Figure 19C). The muscle of the testis sheath is unique in *Drosophila* in that it is similar to vertebrate smooth muscle rather than striated muscle (Susic-Jung et al. 2012). Interestingly, Merlin is highly expressed in human smooth muscle (den Bakker, Riegman, et al. 1995), so there may be a particular requirement for its activity in this tissue type. Partial suppression of the testis morphological defect and

of fibre disorder in the muscle sheath when eIF4E-3 is lost in addition to Merlin indicates a genetic interaction between the two proteins. The phenotypes apparent when Merlin is lost could represent misregulated translation of one or more of the target transcripts identified by RIP-Chip. Perhaps Merlin interacts with eIF4E-3 to suppress translation of a certain transcript or transcripts, and in the absence of Merlin, eIF4E-3 is able to associate with other translation initiation factors and promote translation. If this is true, then when eIF4E-3 is lost in addition to Merlin translation would not occur, barring compensation by other eIF4Es, and the protein would not be expressed, similar to wild-type in which translation is actively repressed. Since loss of eIF4E-3 does not fully rescue the phenotypes seen, it is likely that there are other factors contributing to muscle sheath migration and organisation and testis morphology, including potential translational compensation by other eIF4E family members, or other functions of Merlin not related to translation. Knock-down of proteins involved in cellular adhesion including dumbfounded/kin of irre, sticks and stones, and hibris results in disorganised muscle filaments in addition to a normal underlying muscle sheath (Susic-Jung et al. 2012), a phenotype that is independent of the capacity for myoblast fusion (Kuckwa et al. 2016), indicating a role for adhesion in organisation of the testis muscle sheath. Merlin is known to localise and function at adherens junctions in both mammals and *Drosophila*, promoting cellular adhesion (McCartney and Fehon 1996; Lallemand et al. 2003; McLaughlin et al. 2007; Flaiz et al. 2008; Flaiz et al. 2009; Gladden et al. 2010); therefore, loss of Merlin function in adhesion may also contribute to the disorganisation of muscle fibres seen in Merlin null testes.

4.6 | Localisation of Merlin and eIF4E-3 in spermatocytes

When Merlin is lost, eIF4E-3 is redistributed such that it is less concentrated near the plasma membrane in late prophase spermatocytes (Figure 20B,C). Whether or not this is a direct effect was not determined, but Merlin is able to localise to the plasma membrane (den Bakker, Riegman, et al. 1995; Gonzalez-Agosti et al. 1996; McCartney and Fehon 1996; LaJeunesse, McCartney, and Fehon 1998), and it appears to be localised cortically

in spermatocytes (Dorogova et al. 2008), so it may be required to directly tether eIF4E-3 to the membrane. The functional significance of eIF4E-3 at the membrane is unclear. It may be that localised translation is required for some transcripts, or, alternatively, eIF4E-3 might be sequestered at the membrane to prevent activation of translation. Very little transcription occurs after meiosis, so most gene products required for post-meiotic stages are transcribed in spermatocytes and translationally silenced until needed (Schäfer et al. 1995). Possibly, Merlin association with eIF4E-3 and certain transcripts restricts them to the plasma membrane and prevents translation. It would be interesting to carry out RNA FISH/IF to see if any of the identified target mRNAs of Merlin and eIF4E-3 are localised near the spermatocyte membrane, and if so, whether the protein products are similarly localised as an indication of translational repression versus activation.

Conversely, loss of eIF4E-3 causes cortical Merlin localisation to change from an indistinct to a striated appearance (Figure 22B,C). Since eIF4E-3 does not appear to be specifically localised to the cortex, it is unlikely that Merlin cortical localisation depends on direct tethering by eIF4E-3. Perhaps association with eIF4E-3 is required for a particular conformation of Merlin that permits binding to partners causing it to be cortically localised whereas loss of eIF4E-3 leads to a different conformation of Merlin that binds different partners. For example, intramolecular binding leading to closed Merlin conformation is predicted to mask other binding sites in the FERM domain and prevent it from association with the actin cytoskeleton (James et al. 2001; Fehon, McClatchey, and Bretscher 2010). Alternatively, absence of eIF4E-3 may leave a site on Merlin that would normally be bound to it free to associate with another protein, potentially causing Merlin localisation to appear striated.

4.7 | Role of Merlin in post-meiotic spermatid cysts

Following meiosis of spermatocytes in *Drosophila*, the resulting 64 spermatids must polarise within the cyst, by gathering all nuclei to one side, and the cyst itself must polarise within the testis such that the nuclei are oriented toward the testis base (where

the seminal vesicle attaches) and the tails grow toward the testis tip (where the hub and stem cells are located). A defect in the former level of polarisation has been described for *Merlin* mutant cysts (Dorogova et al. 2008); although this was not observed in this study, it is possible that it is not as easily observed by the method used in this study (whole mount vs. squash). The second type of polarisation, however, could not be monitored by testes squash, but defects were observed in whole mount IF presented here (Figure 23B,D). Each cyst is enveloped by two somatic cells that correlate with the polarity of the cyst: one surrounds the nuclei, and the other extends around the sperm tails (Tokuyasu, Peacock, and Hardy 1972b). These somatic cyst cells become structurally divergent as the cyst matures – the tail cyst cell must grow much more than the head cyst cell in order to accommodate the lengthy sperm tails – and have differential gene expression (Gönczy, Viswanathan, and DiNardo 1992; Papagiannouli and Mechler 2009). Since they are distinguishable, the somatic cyst cells are plausible candidates for determining cyst polarity. Xu *et al.* (2014) have reported a requirement for atypical protein kinase C (aPKC) and the cytoplasmic polyadenylation element binding protein Orb2 at the tail end of elongating spermatid cysts to determine polarisation in terms of the tip-base axis of the testis. Hypomorphic alleles of these genes result in random orientation of spermatid cysts (Xu, Tyagi, and Schedl 2014). Similarly, arbitrary cyst polarisation was observed in Mer^{3}/Y testes (Figure 23B); however, Merlin does not localise to the tail end of the cyst as aPKC and Orb2. Instead, based on IF analysis of Mer^{4}/Y;*Act5C>Myc-Mer* testes, Merlin appears to be localised post-meiotically potentially to the tail cyst cell. A possible function for Merlin in determining spermatid cyst polarity with respect to the testis axis then, is as part of a signal upstream of Orb2 and aPKC, originating in the tail cyst cell. This possibility could be explored by observing whether aPKC is mislocalised in Mer^{3}/Y or Mer^{4}/Y cysts, or whether RNAi mediated knock-down of Merlin specifically in cyst cells, for example with *eya-GAL4* or *T155-GAL4* which express in late somatic cyst cells, is sufficient to cause the polarisation defect.

Merlin is also localised to the anterior of elongated spermatid nuclei (Figure 21D), which may correspond either to the acrosome or to the actin-enriched cap that develops in the head cyst cell to form projections that interdigitate with the elongated nuclei (Tokuyasu, Peacock, and Hardy 1972b; Desai, Shirolikar, and Ray 2009; Rotkopf et al. 2011). If the Merlin expression is in the head cyst cell, it should not affect the ability of Merlin to determine axis-base polarity from the tail cyst cell, as the head cyst cell expression does not appear to turn on until after the spermatid bundles have completed elongation and are preparing to individualise, at which point the polarity has long been determined. Merlin expression in the head cyst cell cap may nevertheless help explain another defect seen in sperm bundles: disorganisation of the nuclei and IC actin cones. Scattered nuclei and actin cones were reported in *Merlin* mutant cysts by Dorogova *et al.* (2008) by IF analysis of testes squashes, and were confirmed here by whole mount IF, but the mechanism by which loss of Merlin leads to scattering has not been determined. This phenotype has been described for a number of genes (Castrillon et al. 1993; Fabrizio et al. 1998; Ghosh-Roy, Desai, and Ray 2005; Robida et al. 2010) and has been termed the "expressway mutant" class (Fabrizio et al. 1998). It has been suggested that there are at least two possible mechanisms leading to this phenotype (Fabrizio et al. 1998): elongated spermatid nuclei begin in register but are pulled apart by a defective IC, or nuclei enter individualisation scattered and the actin cones form normally around each nucleus. Additionally, phenotypes may be either germ-cell intrinsic (Ghosh-Roy, Desai, and Ray 2005) or result from a flawed actin cap in the head cyst cell (Desai, Shirolikar, and Ray 2009). Like other ERM family proteins, merlin interacts with the actin cytoskeleton in mammalian cells (den Bakker et al. 1995; Sainio et al. 1997; den Bakker et al. 2000; James et al. 2001; Bashour et al. 2002; Cole et al. 2008), and *Drosophila* Merlin localises near the plasma membrane (McCartney and Fehon 1996; LaJeunesse, McCartney, and Fehon 1998) and appears to functionally interact with the actin cytoskeleton (Yin et al. 2013) and thus likely functions similarly to mammalian merlin. Therefore, Merlin could have a role in maintaining organisation of F-actin in the head cyst cell cap, which is required to

maintain a compact and in register bundle of nuclei (Desai, Shirolikar, and Ray 2009). Microfilaments and cellular adhesion proteins are also essential for cap maintenance (Rotkopf et al. 2011), which could also be related to the role of Merlin as it is known to localise to adherens and tight junctions (McCartney and Fehon 1996; Lallemand et al. 2003; Gladden et al. 2010). The potential effect of Merlin on the organisation of nuclear bundles and ICs as an organiser of the actin cap could be examined by specific knock-down or rescue in late cyst cells. To look at the role of Merlin more precisely in either the head or tail cyst cell, potentially an enhancer trap that is expressed only in either the head cyst cell or the tail cyst cell (Gönczy, Viswanathan, and DiNardo 1992) could be converted to a *GAL4* line (Sepp and Auld 1999) and then used to drive knock-down of Merlin by RNAi, or to rescue Mer^{3}/Y or Mer^{4}/Y phenotypes by expressing a wild-type *Merlin* transgene. It is of note that Merlin has also been implicated in spermatogenesis in mammals as its loss leads to defects in mature sperm, and is expressed in early and late germ cells and potentially also Sertoli cells, the mammalian equivalent of the somatic cyst cells in *Drosophila* (Zoch et al. 2015).

4.8 | Role of Merlin and eIF4E-3 in regulating translation

Loss of eIF4E-3 was previously shown to lead to an overall reduction in translation during *Drosophila* spermatogenesis based on incorporation of radiolabelled methionine and cysteine (Hernández et al. 2012). However, this same study found, by two-dimensional difference gel electrophoresis analysis of eIF4E-3 null testes lysates, that while a number of proteins were observed at lower levels, expression of some proteins were increased (Hernández et al. 2012). Similarly, both increase and decrease in protein levels of eIF4E-3 target transcripts selected in this study were observed (Figure 24, Figure 26). It was suggested that increased protein levels may be due to an indirect effect wherein the loss of eIF4E-3 reduces translation of a regulator of these genes, or these transcripts may be translated by other members of the eIF4E family, which may be expressed at higher levels to compensate for the loss of eIF4E-3 (Hernández et al. 2012). Alternatively, it is possible that the role of eIF4E-3 in translation is context-dependent, as

the *Drosophila* CPEB homologue Orb2 was recently shown to have both repressive and activating roles in translation depending on its status as a monomer or oligomer and on its interaction with partner proteins (Khan et al. 2015). Therefore, the proteins which eIF4E-3 complexes with may be either permissive or repressive of translation, potentially in a transcript-specific manner. In Western blot analyses of Merlin and eIF4E-3 target transcripts *how* and *bol*, loss of eIF4E-3 affected translation in opposite directions as HOW protein levels were increased, indicating de-repression of translation, and Bol protein levels were decreased, indicating loss of translation activation. The effect of loss of Merlin on *bol* translation is uncertain as it was decreased in one experiment and unchanged in another (Figure 24) – due to variability between blots, more replicates would be required to make a clear conclusion; however, Bol was consistently decreased in Mer^{3}/Y testes, suggesting Merlin may be involved in positive regulation of *bol* translation. Bol protein is decreased in $Mer^{4}/Y;;eIF4E\text{-}3^{excision6}$ larval testes compared with the control, but it is not clear if Merlin contributes to this loss of translation or if it is primarily due to loss of eIF4E-3. Merlin's effect on *how* translation is similarly ambiguous. Two of three experiments showed slightly decreased HOW protein in Mer^{4}/Y wing discs compared with w^{1118}/Y control, while in the third blot HOW was slightly increased (Figure 26). Mer^{3}/Y wing discs, on the other hand, had either increased or unchanged levels of HOW compared with the control. In the double null mutant, $Mer^{4}/Y;;eIF4E\text{-}3^{excision6}$, HOW protein was increased similarly to loss of eIF4E-3 alone. Overall, eIF4E-3 appears to be positively regulating translation of *bol* and negatively regulating translation of *how*, while the contribution of Merlin to translational regulation of these two transcripts is unclear. It is not unreasonable that eIF4E-3 may both enhance and repress translation, as it is able to bind proteins known to promote translation, eIF4G (Hernández et al. 2005) and Mextli (Hernández et al. 2013), and potentially the translation repressive 4E-BP Thor (Hernández et al. 2005). It is not known whether eIF4E-3 binds any of these proteins when it is complexed with Merlin, or how the Merlin/eIF4E-3 complex may be selecting specific transcripts. A possible reason that loss

of Merlin does not significantly affect protein levels is that the targets examined are not true targets for translational regulation by Merlin, as not all target transcripts identified in the RIP-Chip experiment have been confirmed. Individual target transcript candidates could be validated by immunoprecipitation of Merlin or eIF4E-3 together with qRT-PCR, or by RNA affinity purification, in which biotin-labelled mRNA would be synthesised, then incubated with lysate of either wild-type whole animals or specific tissues such as testes, and purified by streptavidin binding. eIF4E-3 and Merlin bound to the mRNA could then be assessed by Western blotting. It could also be that their association is tissue specific, since both *bol* and *how* are expressed in tissues other than testes and wing discs respectively, or that the role of Merlin associated with eIF4E-3 is connected more to localisation of translation rather than to the level of translation.

The differences in translation of *bol* and *how* were not readily apparent by IF analysis in adult or pharate adult testes as expression of both was seen in the same cells as in the control, and localisation did not appear to be altered (Figure 25, Figure 27). However, it was noted that *Mer*^{4}*;;eIF4E-3*^{excision6} testes appear to have fewer spermatogonia compared with the control genotype, which would be consistent with reduced levels of HOW as loss of HOW has been shown to result in loss of germline stem cells while its over-expression leads to an expansion of the spermatogonial population (Monk et al. 2010). Although this is not consistent with the Western blotting data, which showed increased HOW in *Mer*^{4}*/Y;;eIF4E-3*^{excision6} wing discs, it is possible that translation even of the same transcript is differentially regulated tissue-specifically potentially due to availability of different interacting partners. There may also be multiple modes of regulation on these transcripts, so the effect of loss of one part of a regulatory complex could be masked if other regulatory elements increase in response. Also, since Merlin and eIF4E-3 may be regulating translation of a number of transcripts including a group highly expressed in testes, possibly another of these targets affects either the regulation of others or phenotypes like the spermatogonial population.

4.9 | Conclusion and general future directions

The *Drosophila* alternative cap binding protein eIF4E-3 interacts with Merlin genetically and biochemically, and possibly modifies Merlin activity in specific cell types as it has a restricted expression pattern that includes the nervous system, where NF2 tumours develop in humans. Merlin and eIF4E-3 were each found to modify the other's localisation in spermatocytes and to interact to influence adult testis morphology. In the central nervous system, Merlin and eIF4E-3 interaction affects the number of neuroblasts in the larval central brain and potentially distribution of photoreceptor axons in the optic lobe. eIF4E-3 appears to be able to both positively and negatively regulate translation of specific transcripts, possibly with the involvement of Merlin although this interaction is not clear.

As Merlin lacks known RNA binding domains, and eIF4E-3 binds RNA via the m^7G cap, which is present on all cellular mRNAs, yet Merlin and eIF4E-3 associate with only a subset of transcripts, there is likely at least one additional protein in the complex that provides RNA recognition specificity. Further partners of Merlin and eIF4E-3 could be identified by determining what proteins can bind a particular mRNA that is known to be bound by Merlin and eIF4E-3. Transcripts identified as eIF4E-3/Merlin targets would be tagged, for example with biotin, and then captured on a streptavidin column. Subsequently, lysates of wild-type animals would be incubated with the bound column to allow interaction with potential binding proteins. This step could also be used to determine if there are differences in interacting proteins throughout development by using lysates of each developmental stage of *Drosphila*, or by using lysates from specific tissues. Finally, proteins binding the tagged mRNA would be eluted from the column and analysed by mass spectrometry, then confirmed with co-immunoprecipitations with Merlin and with eIF4E-3.

It would also be interesting to investigate biochemically how eIF4E-3 and Merlin interact, for example, whether eIF4E-3 preferentially binds either phosphorylated or non-phosphorylated Merlin or has equal affinity for both forms. Since

non-phosphorylated, closed conformation Merlin is generally considered to be active as a tumour suppressor (Shaw et al. 2001; Sherman et al. 1997), potential differences in binding affinity for eIF4E-3 could provide insight into how their association is regulated. This could be accomplished by co-immunoprecipitation of non-phosphorylable and phospho-mimetic forms of Merlin with eIF4E-3 and comparison of the two band intensities to determine the amount of associated protein. Additionally, determining which site of eIF4E-3 is bound by Merlin could yield insight into the mechanism of their association; for example, if Merlin binding blocks the site for eIF4G association, it would be acting in a similar manner to the 4E-BPs. The Merlin binding site of eIF4E-3 could be determined by creating constructs containing deletions or targeted mutation of segments of the protein, such as the site that binds eIF4G/4E-BP, and looking for loss of co-immunoprecipitation with full-length Merlin. Once the binding region is determined, the deletion construct could perhaps be used *in vivo* to confirm that physical interaction is necessary for genetic interaction phenotypes, such as rescue of testes morphology.

References

Abeysundara, N, A C Leung, D A Primrose, and S C Hughes. 2014. "Regulation of Cell Proliferation and Adhesion by Means of a Novel Region of Drosophila Merlin Interacting with Sip1." *Developmental Dynamics* 243 (12): 1554–70. doi:10.1002/dvdy.24187.

Algrain, M, O Turunen, A Vaheri, D Louvard, and M Arpin. 1993. "Ezrin Contains Cytoskeleton and Membrane Binding Domains Accounting for Its Proposed Role as a Membrane-Cytoskeletal Linker." *Journal of Cell Biology* 120 (1): 129–40. doi:10.1083/jcb.120.1.129.

Asthagiri, A R, D M Parry, J A Butman, H J Kim, E T Tsilou, Z Zhuang, and R R Lonser. 2009. "Neurofibromatosis Type 2." *The Lancet* 373 (9679): 1974–86. doi:10.1016/S0140-6736(09)60259-2.

Baehrecke, E H. 1997. "Who Encodes a KH RNA Binding Protein That Functions in Muscle Development." *Development* 124 (7). The Company of Biologists Ltd: 1323–32. doi:10.1016/S0168-9525(00)89030-7.

Baena-Lopez, L A, C Alexandre, A Mitchell, L Pasakarnis, and J-P Vincent. 2013. "Accelerated Homologous Recombination and Subsequent Genome Modification in Drosophila." *Development* 140 (23): 4818–25. doi:10.1242/dev.100933.

Baker, C C, and M T Fuller. 2007. "Translational Control of Meiotic Cell Cycle Progression and Spermatid Differentiation in Male Germ Cells by a Novel eIF4G Homolog." *Development* 134 (15): 2863–69. doi:10.1242/dev.003764.

Balasubramaniam, A, P Shannon, M Hodaie, N Laperriere, H Michaels, and A Guha. 2007. "Glioblastoma Multiforme after Stereotactic Radiotherapy for Acoustic Neuroma: Case Report and Review of the Literature." *Neuro-Oncology* 9 (4): 447–53. doi:10.1215/15228517-2007-027.

Barrangou, R, C Fremaux, H Deveau, M Richards, P Boyaval, S Moineau, D A Romero, and P Horvath. 2007. "CRISPR Provides Acquired Resistance Against Viruses in Prokaryotes." *Science* 315 (5819): 1709–12. doi:10.1126/science.1138140.

Baser, M E, D G Evans, R K Jackler, E Sujansky, and A Rubenstein. 2000. "Neurofibromatosis 2, Radiosurgery and Malignant Nervous System Tumours." *British Journal of Cancer* 82 (4): 998. doi:10.1054/bjoc.1999.1030.

Baser, M E, J M Friedman, D Aeschliman, H Joe, A J Wallace, R T Ramsden, and D G R Evans. 2002. "Predictors of the Risk of Mortality in Neurofibromatosis 2." *American Journal of Human Genetics* 71 (4): 715–23. doi:10.1086/342716.

Baser, M E, L Kuramoto, H Joe, J M Friedman, A J Wallace, J E Gillespie, R T Ramsden, and D G R Evans. 2004. "Genotype-Phenotype Correlations for Nervous System Tumors in Neurofibromatosis 2: A Population-Based Study." *American Journal of Human Genetics* 75 (2): 231–39. doi:10.1086/422700.

Baser, M E, L Kuramoto, R Woods, H Joe, J M Friedman, A J Wallace, R T Ramsden, et al. 2005. "The Location of Constitutional Neurofibromatosis 2 (NF2) Splice Site Mutations Is Associated with the Severity of NF2." *Journal of Medical Genetics* 42 (7): 540–46. doi:10.1136/jmg.2004.029504.

Bashour, A-M, J-J Meng, W Ip, M MacCollin, and N Ratner. 2002. "The Neurofibromatosis Type 2 Gene Product, Merlin, Reverses the F-Actin Cytoskeletal Defects in Primary Human Schwannoma Cells." *Molecular and Cellular Biology* 22 (4): 1150–57. doi:10.1128/MCB.22.4.1150-1157.2002.

Bassett, A R, C Tibbit, C P Ponting, and J-L Liu. 2013. "Highly Efficient Targeted Mutagenesis of Drosophila with the CRISPR/Cas9 System." *Cell Reports* 4 (1): 220–28. doi:10.1016/j.celrep.2013.06.020.

Bello, B C, N Izergina, E Caussinus, and H Reichert. 2008. "Amplification of Neural Stem Cell Proliferation by Intermediate Progenitor Cells in Drosophila Brain Development." *Neural Development* 3 (February). BioMed Central: 5. doi:10.1186/1749-8104-3-5.

Bernal, A, and D A Kimbrell. 2000. "Drosophila Thor Participates in Host Immune Defense and Connects a Translational Regulator with Innate Immunity." *PNAS* 97 (11): 6019–24. doi:10.1073/pnas.100391597.

Bianchi, A B, T Hara, V Ramesh, J Gao, A J P Klein-Szanto, F Morin, A G Menon, et al. 1994. "Mutations in Transcript Isoforms of the Neurofibromatosis 2 Gene in Multiple Human Tumour Types." *Nature Genetics* 6 (2): 185–92. doi:10.1038/ng0294-185.

Bianchi, A B, S I Mitsunaga, J Q Cheng, W M Klein, S C Jhanwar, B Seizinger, N Kley, A J P Klein-Szanto, and J R Testa. 1995. "High Frequency of Inactivating Mutations in the Neurofibromatosis Type 2 Gene (NF2) in Primary Malignant Mesotheliomas." *PNAS* 92 (24): 10854–58. doi:10.1073/pnas.92.24.10854.

Bier, E, H Vaessin, S Shepherd, K Lee, K McCall, S Barbel, L Ackerman, et al. 1989. "Searching for Pattern and Mutation in the Drosophila Genome with a P-lacZ Vector." *Genes & Development* 3 (9): 1273–87. doi:10.1101/gad.3.9.1273.

Bier, E, H Vaessin, S Younger-Shepherd, L Y Jan, and Y N Jan. 1992. "Deadpan, an Essential Pan-Neural Gene in Drosophila, Encodes a Helix-Loop-Helix Protein

Similar to the Hairy Gene Product." *Genes & Development* 6 (11): 2137–51. doi:10.1101/gad.6.11.2137.

Blakeley, J O, D G Evans, J Adler, D Brackmann, R Chen, R E Ferner, C O Hanemann, et al. 2012. "Consensus Recommendations for Current Treatments and Accelerating Clinical Trials for Patients with Neurofibromatosis Type 2." *American Journal of Medical Genetics* 158A (1): 24–41. doi:10.1002/ajmg.a.34359.

Bommer, U A, A Lazaris-Karatzas, A De Benedetti, P Nürnberg, R Benndorf, H Bielka, and N Sonenberg. 1994. "Translational Regulation of the Mammalian Growth-Related Protein P23: Involvement of eIF-4E." *Cellular & Molecular Biology Research* 40 (7-8): 633–41.

Boone, J Q, and C Q Doe. 2008. "Identification of Drosophila Type II Neuroblast Lineages Containing Transit Amplifying Ganglion Mother Cells." *Developmental Neurobiology* 68 (9): 1185–95. doi:10.1002/dneu.20648.

Bosch, M M, E Boltshauser, P Harpes, and K Landau. 2006. "Ophthalmologic Findings and Long-Term Course in Patients with Neurofibromatosis Type 2." *American Journal of Ophthalmology* 141 (6): 1068–77. doi:10.1016/j.ajo.2005.12.042.

Both, G W, A K Banerjee, and A J Shatkin. 1975. "Methylation-Dependent Translation of Viral Messenger RNAs in Vitro." *Proceedings of the National Academy of Sciences of the United States of America* 72 (3): 1189–93. doi:10.1073/pnas.72.3.1189.

Bouzas, E A, V Freidlin, D M Parry, R Eldridge, and M I Kaiser-Kupfer. 1993. "Lens Opacities in Neurofibromatosis 2: Further Significant Correlations." *The British Journal of Ophthalmology* 77 (6): 354–57. doi:10.1136/bjo.77.6.354.

Bowman, S K, V Rolland, J Betschinger, K A Kinsey, G Emery, and J A Knoblich. 2008. "The Tumor Suppressors Brat and Numb Regulate Transit-Amplifying Neuroblast Lineages in Drosophila." *Developmental Cell* 14 (4): 535–46. doi:10.1016/j.devcel.2008.03.004.

Bretscher, A, K Edwards, and R G Fehon. 2002. "ERM Proteins and Merlin: Integrators at the Cell Cortex." *Nature Reviews Molecular Cell Biology* 3 (8): 586–99. doi:10.1038/nrm882.

Bruder, C E, K Ichimura, E Blennow, T Ikeuchi, T Yamaguchi, Y Yuasa, V P Collins, and J P Dumanski. 1999. "Severe Phenotype of Neurofibromatosis Type 2 in a Patient with a 7.4-MB Constitutional Deletion on Chromosome 22: Possible Localization of a Neurofibromatosis Type 2 Modifier Gene?" *Genes, Chromosomes & Cancer* 25 (2): 184–90. doi:10.1002/(SICI)1098-2264(199906)25:2<184::AID-GCC15>3.0.CO;2-B.

Cabrera, G R, D Godt, P-Y Fang, J-L Couderc, and F A Laski. 2002. "Expression Pattern of Gal4 Enhancer Trap Insertions into the Bric À Brac Locus Generated by P Element Replacement." *Genesis* 34 (1-2): 62–65. doi:10.1002/gene.10115.

Cačev, T, G Aralica, B Lončar, and S Kapitanović. 2014. "Loss of NF2/Merlin Expression in Advanced Sporadic Colorectal Cancer." *Cellular Oncology* 37 (1): 69–77. doi:10.1007/s13402-013-0164-2.

Calleja, M, E Moreno, S Pelaz, and G Morata. 1996. "Visualization of Gene Expression in Living Adult Drosophila." *Science* 274 (5285): 252–55. doi:10.1126/science.274.5285.252.

Campbell, D S, and C E Holt. 2001. "Chemotropic Responses of Retinal Growth Cones Mediated by Rapid Local Protein Synthesis and Degradation." *Neuron* 32 (6): 1013–26. doi:10.1016/S0896-6273(01)00551-7.

Campbell, L, B Jasani, D F R Griffiths, and M Gumbleton. 2015. "Phospho-4e-BP1 and eIF4E Overexpression Synergistically Drives Disease Progression in Clinically Confined Clear Cell Renal Cell Carcinoma." *American Journal of Cancer Research* 5 (9): 2838–48.

Campos-Ortega, J A. 1993. "Early Neurogenesis in Drosophila Melanogaster." In *The Development of Drosophila Melanogaster*, edited by M Bate and M Martinez-Arias, 1091–1129. Cold Spring Harbor, NY: Cold Spring Harbor Laboratory Press.

Carberry, S E, D E Friedland, R E Rhoads, and D J Goss. 1992. "Binding of Protein Synthesis Initiation Factor 4E to Oligoribonucleotides: Effects of Cap Accessibility and Secondary Structure." *Biochemistry* 31 (5): 1427–32.

Carvalho, G B, W W Ja, and S Benzer. 2009. "Non-Lethal PCR Genotyping of Single Drosophila." *BioTechniques* 46 (4): 312–14. doi:10.2144/000113088.

Castrillon, D H, P Gönczy, S Alexander, R Rawson, C G Eberhart, S Viswanathan, S DiNardo, and S A Wasserman. 1993. "Toward a Molecular Genetic Analysis of Spermatogenesis in Drosophila Melanogaster: Characterization of Male-Sterile Mutants Generated by Single P Element Mutagenesis." *Genetics* 135 (2): 489–505.

Cenci, C, and A P Gould. 2005. "Drosophila Grainyhead Specifies Late Programmes of Neural Proliferation by Regulating the Mitotic Activity and Hox-Dependent Apoptosis of Neuroblasts." *Development* 132 (17): 3835–45. doi:10.1242/dev.01932.

Cenci, G, S Bonaccorsi, C Pisano, F Verni, and M Gatti. 1994. "Chromatin and Microtubule Organization during Premeiotic, Meiotic and Early Postmeiotic Stages of Drosophila Melanogaster Spermatogenesis." *Journal of Cell Science* 107 (Pt 1 (December): 3521–34.

Chagnovich, D, and R Lehmann. 2001. "Poly(A)-Independent Regulation of Maternal Hunchback Translation in the Drosophila Embryo." *PNAS* 98 (20): 11359–64. doi:10.1073/pnas.201284398.

Cheng, M H, J Z Maines, and S A Wasserman. 1998. "Biphasic Subcellular Localization of the DAZL-Related Protein Boule in Drosophila Spermatogenesis." *Developmental Biology* 204 (2): 567–76. doi:10.1006/dbio.1998.9098.

Chiasson-MacKenzie, C, Z S Morris, Q Baca, B Morris, J K Coker, R Mirchev, A E Jensen, et al. 2015. "NF2/Merlin Mediates Contact-Dependent Inhibition of EGFR Mobility and Internalization via Cortical Actomyosin." *The Journal of Cell Biology*, 1–15. doi:10.1083/jcb.201503081.

Cho, P F, C Gamberi, Y A Cho-Park, I B Cho-Park, P Lasko, and N Sonenberg. 2006. "Cap-Dependent Translational Inhibition Establishes Two Opposing Morphogen Gradients in Drosophila Embryos." *Current Biology* 16 (20): 2035–41. doi:10.1016/j.cub.2006.08.093.

Cho, P F, F Poulin, Y A Cho-Park, I B Cho-Park, J D Chicoine, P Lasko, and N Sonenberg. 2005. "A New Paradigm for Translational Control: Inhibition via 5'-3' mRNA Tethering by Bicoid and the eIF4E Cognate 4EHP." *Cell* 121 (3): 411–23. doi:10.1016/j.cell.2005.02.024.

Clouse, K N, S B Ferguson, and T Schüpbach. 2008. "Squid, Cup, and PABP55B Function Together to Regulate Gurken Translation in Drosophila." *Developmental Biology* 313 (2): 713–24. doi:10.1016/j.ydbio.2007.11.008.

Cole, B K, M Curto, A W Chan, and A I McClatchey. 2008. "Localization to the Cortical Cytoskeleton Is Necessary for Nf2/merlin-Dependent Epidermal Growth Factor Receptor Silencing." *Mol Cell Biol* 28 (4): 1274–84. doi:10.1128/MCB.01139-07.

Curto, M, B K Cole, D Lallemand, C H Liu, and A I McClatchey. 2007. "Contact-Dependent Inhibition of EGFR Signaling by Nf2/Merlin." *Journal of Cell Biology* 177 (5): 893–903. doi:10.1083/jcb.200703010.

Dahanukar, A, J A Walker, and R P Wharton. 1999. "Smaug, a Novel RNA-Binding Protein That Operates a Translational Switch in Drosophila." *Molecular Cell* 4 (2): 209–18. doi:10.1016/S1097-2765(00)80368-8.

Darnell, J C, S J van Driesche, C Zhang, K Y S Hung, A Mele, C E Fraser, E F Stone, et al. 2011. "FMRP Stalls Ribosomal Translocation on mRNAs Linked to Synaptic Function and Autism." *Cell* 146 (2): 247–61. doi:10.1016/j.cell.2011.06.013.

De Benedetti, A, and J R Graff. 2004. "eIF-4E Expression and Its Role in Malignancies and Metastases." *Oncogene* 23 (18): 3189–99. doi:10.1038/sj.onc.1207545.

den Bakker, M A, P H Riegman, R A Hekman, W Boersma, P J Janssen, T H van der Kwast, and E C Zwarthoff. 1995. "The Product of the NF2 Tumour Suppressor Gene Localizes near the Plasma Membrane and Is Highly Expressed in Muscle Cells." *Oncogene* 10 (4): 757–63.

den Bakker, M A, P H Riegman, A P Suurmeijer, C J Vissers, M Sainio, O Carpén, and E C Zwarthoff. 2000. "Evidence for a Cytoskeleton Attachment Domain at the N-Terminus of the NF2 Protein." *Journal of Neuroscience Research* 62 (6): 764–71. doi:10.1002/1097-4547(20001215)62:6<764::AID-JNR2>3.0.CO;2-V.

den Bakker, M A, M Tascilar, P H J Riegman, A C P Hekman, W Boersma, P J A Janssen, T A W de Jong, W Hendriks, T H van der Kwast, and E C Zwarthoff. 1995. "Neurofibromatosis Type 2 Protein Co-Localizes with Elements of the Cytoskeleton." *The American Journal of Pathology* 147 (5): 1339–49.

Desai, B S, S Shirolikar, and K Ray. 2009. "F-Actin-Based Extensions of the Head Cyst Cell Adhere to the Maturing Spermatids to Maintain Them in a Tight Bundle and Prevent Their Premature Release in Drosophila Testis." *BMC Biology* 7: 19. doi:10.1186/1741-7007-7-19.

Dever, T E. 2002. "Gene-Specific Regulation by General Translation Factors." *Cell* 108 (4): 545–56. doi:10.1016/S0092-8674(02)00642-6.

Dobzhansky, T. 1931. "Interaction between Female and Male Parts in Gynandromorphs of Drosophila Simulans." *Wilhelm Roux' Archiv Fur Entwicklungsmechanik Der Organismen* 123 (3-4): 719–46. doi:10.1007/BF01380651.

Dorogova, N V, E M Akhmametyeva, S A Kopyl, N V Gubanova, O S Yudina, L V Omelyanchuk, and L-S Chang. 2008. "The Role of Drosophila Merlin in Spermatogenesis." *BMC Cell Biology* 9: 1. doi:10.1186/1471-2121-9-1.

Doudna, J A, and E Charpentier. 2014. "The New Frontier of Genome Engineering with CRISPR-Cas9." *Science* 346 (6213). doi:10.1126/science.1258096.

Dumanski, J P, E Carlbom, V P Collins, and M Nordenskjöld. 1987. "Deletion Mapping of a Locus on Human Chromosome 22 Involved in the Oncogenesis of Meningioma." *PNAS* 84 (24): 9275–79.

Edenfeld, G, G Volohonsky, K Krukkert, E Naffin, U Lammel, A Grimm, D Engelen, A Reuveny, T Volk, and C Klämbt. 2006. "The Splicing Factor Crooked Neck Associates with the RNA-Binding Protein HOW to Control Glial Cell Maturation in Drosophila." *Neuron* 52 (6): 969–80. doi:10.1016/j.neuron.2006.10.029.

Egger, B, J Q Boone, N R Stevens, A H Brand, and C Q Doe. 2007. "Regulation of Spindle Orientation and Neural Stem Cell Fate in the Drosophila Optic Lobe." *Neural Development* 2 (January): 1. doi:10.1186/1749-8104-2-1.

Evans, D G R, A Moran, A King, S Saeed, N Gurusinghe, and R Ramsden. 2005. "Incidence of Vestibular Schwannoma and Neurofibromatosis 2 in the North West of England over a 10-Year Period: Higher Incidence than Previously Thought." *Otology & Neurotology* 26 (1): 93–97.

Evans, D G R, R T Ramsden, A Shenton, C Gokhale, N L Bowers, S M Huson, G Pichert, and A Wallace. 2007. "Mosaicism in Neurofibromatosis Type 2: An Update of Risk Based on Uni/bilaterality of Vestibular Schwannoma at Presentation and Sensitive Mutation Analysis Including Multiple Ligation-Dependent Probe Amplification." *Journal of Medical Genetics* 44 (7): 424–28. doi:10.1136/jmg.2006.047753.

Evans, D G, L Trueman, A Wallace, S Collins, and T Strachan. 1998. "Genotype/phenotype Correlations in Type 2 Neurofibromatosis (NF2): Evidence for More Severe Disease Associated with Truncating Mutations." *Journal of Medical Genetics* 35 (6): 450–55. doi:10.1136/jmg.35.6.450.

Evans, D G, A J Wallace, C L Wu, L Trueman, R T Ramsden, and T Strachan. 1998. "Somatic Mosaicism: A Common Cause of Classic Disease in Tumor-Prone Syndromes? Lessons from Type 2 Neurofibromatosis." *American Journal of Human Genetics* 63 (3): 727–36. doi:10.1086/512074.

Evsikov, A V, and C M de Evsikova. 2009. "Evolutionary Origin and Phylogenetic Analysis of the Novel Oocyte-Specific Eukaryotic Translation Initiation Factor 4E in Tetrapoda." *Development Genes and Evolution* 219 (2): 111–18. doi:10.1007/s00427-008-0268-2.

Fabrizio, J J, G Hime, S K Lemmon, and C Bazinet. 1998. "Genetic Dissection of Sperm Individualization in Drosophila Melanogaster." *Development* 125 (10): 1833–43. doi:10.1101/gad.3.9.1273.

Fehon, R G, A I McClatchey, and A Bretscher. 2010. "Organizing the Cell Cortex: The Role of ERM Proteins." *Nature Reviews Molecular Cell Biology* 11 (4): 276–87. doi:10.1038/nrm2866.

Fehon, R G, T Oren, D R LaJeunesse, T E Melby, and B M McCartney. 1997. "Isolation of Mutations in the Drosophila Homologues of the Human Neurofibromatosis 2 and Yeast CDC42 Genes Using a Simple and Efficient Reverse-Genetic Method." *Genetics* 146: 245–52.

Fernandez-Valle, C, Y Tang, J Ricard, A Rodenas-Ruano, A Taylor, E Hackler, J Biggerstaff, and J Iacovelli. 2002. "Paxillin Binds Schwannomin and Regulates Its Density-Dependent Localization and Effect on Cell Morphology." *Nature Genetics* 31 (4): 354–62. doi:10.1038/ng930.

Fischbach, K-F, and P R Hiesinger. 2008. "Optic Lobe Development." In *Brain Development in Drosophila Melanogaster*, 628:115–36. New York, NY: Springer New York. doi:10.1007/978-0-387-78261-4_8.

Flaiz, C, S Ammoun, A Biebl, and C O Hanemann. 2009. "Altered Adhesive Structures and Their Relation to RhoGTPase Activation in Merlin-Deficient Schwannoma." *Brain Pathology* 19 (1): 27–38. doi:10.1111/j.1750-3639.2008.00165.x.

Flaiz, C, K Kaempchen, C Matthies, and C O Hanemann. 2007. "Actin-Rich Protrusions and Nonlocalized GTPase Activation in Merlin-Deficient Schwannomas." *Journal of Neuropathology and Experimental Neurology* 66 (7): 608–16. doi:10.1097/nen.0b013e318093e555.

Flaiz, C, T Utermark, D B Parkinson, A Poetsch, and C O Hanemann. 2008. "Impaired Intercellular Adhesion and Immature Adherens Junctions in Merlin-Deficient Human Primary Schwannoma Cells." *GLIA* 56 (5): 506–15. doi:10.1002/glia.20629.

Franklin-Dumont, T M, C Chatterjee, S A Wasserman, and S Dinardo. 2007. "A Novel eIF4G Homolog, Off-Schedule, Couples Translational Control to Meiosis and Differentiation in Drosophila Spermatocytes." *Development* 134 (15): 2851–61. doi:10.1242/dev.003517.

Fröhlich, A, and I A Meinertzhagen. 1982. "Synaptogenesis in the First Optic Neuropile of the Fly's Visual System." *Journal of Neurocytology* 11 (1): 159–80.

Fuller, M T. 1993. "Spermatogenesis." In *The Development of Drosophila Melanogaster*, edited by M Bate and A Martinez-Arias, 71–147. Cold Spring Harbor, NY: Cold Spring Harbor Laboratory Press.

Garrity, P A, C-H Lee, I Salecker, H C Robertson, C J Desai, K Zinn, and S L Zipursky. 1999. "Retinal Axon Target Selection in Drosophila Is Regulated by a Receptor Protein Tyrosine Phosphatase." *Neuron* 22 (4): 707–17. doi:10.1016/S0896-6273(00)80730-8.

Gärtner, S M K, C Rathke, R Renkawitz-Pohl, and S Awe. 2014. "Ex Vivo Culture of Drosophila Pupal Testis and Single Male Germ-Line Cysts: Dissection, Imaging, and Pharmacological Treatment." *Journal of Visualized Experiments : JoVE*, no. 91 (September): 51868. doi:10.3791/51868.

Gary, R, and A Bretscher. 1995. "Ezrin Self-Association Involves Binding of an N-Terminal Domain to a Normally Masked C-Terminal Domain That Includes the F-Actin Binding Site." *Molecular Biology of the Cell* 6 (8): 1061–75. doi:10.1091/mbc.E12-02-0152.

Gavilan, H S, R M Kulikauskas, D H Gutmann, and R G Fehon. 2014. "In Vivo Functional Analysis of the Human NF2 Tumor Suppressor Gene in Drosophila." *PloS One* 9 (3): e90853. doi:10.1371/journal.pone.0090853.

Ghosh, S, and P Lasko. 2015. "Loss-of-Function Analysis Reveals Distinct Requirements of the Translation Initiation Factors eIF4E, eIF4E-3, eIF4G and eIF4G2 in Drosophila Spermatogenesis." *Plos One* 10 (4): e0122519. doi:10.1371/journal.pone.0122519.

Ghosh-Roy, A, B S Desai, and K Ray. 2005. "Dynein Light Chain 1 Regulates Dynamin-Mediated F-Actin Assembly during Sperm Individualization in Drosophila." *Molecular Biology of the Cell* 16 (7): 3107–16. doi:10.1091/mbc.E05-02-0103.

Gingold, H, D Tehler, N R Christoffersen, M M Nielsen, F Asmar, S M Kooistra, N S Christophersen, et al. 2014. "A Dual Program for Translation Regulation in Cellular Proliferation and Differentiation." *Cell* 158 (6): 1281–92. doi:10.1016/j.cell.2014.08.011.

Gingras, A C, B Raught, and N Sonenberg. 2001. "Regulation of Translation Initiation by FRAP/mTOR." *Genes and Development* 15 (7): 807–26. doi:10.1101/gad.887201.

Gkogkas, C G, A Khoutorsky, I Ran, E Rampakakis, T Nevarko, D B Weatherill, C Vasuta, et al. 2013. "Autism-Related Deficits via Dysregulated eIF4E-Dependent Translational Control." *Nature* 493 (7432): 371–77. doi:10.1038/nature11628.

Gladden, A B, A M Hebert, E E Schneeberger, and A I McClatchey. 2010. "The NF2 Tumor Suppressor, Merlin, Regulates Epidermal Development through the Establishment of a Junctional Polarity Complex." *Developmental Cell* 19 (5): 727–39. doi:10.1016/j.devcel.2010.10.008.

Gönczy, P, S Viswanathan, and S DiNardo. 1992. "Probing Spermatogenesis in Drosophila with P-Element Enhancer Detectors." *Development* 114 (1): 89–98.

Gonzalez-Agosti, C, T Wiederhold, M E Herndon, J Gusella, and V Ramesh. 1999. "Interdomain Interaction of Merlin Isoforms and Its Influence on Intermolecular Binding to NHE-RF." *Journal of Biological Chemistry* 274 (48): 34438–42. doi:10.1074/jbc.274.48.34438.

Gonzalez-Agosti, C, L Xu, D Pinney, R Beauchamp, W Hobbs, J Gusella, and V Ramesh. 1996. "The Merlin Tumor Suppressor Localizes Preferentially in Membrane Ruffles." *Oncogene* 13 (6): 1239–47.

Gonzalez-Gomez, P, M J Bello, M E Alonso, J Lomas, D Arjona, J M de Campos, J Vaquero, et al. 2003. "CpG Island Methylation in Sporadic and Neurofibromatis Type 2-Associated Schwannomas." *Clinical Cancer Research* 9 (15): 5601–6.

Gould-Somero, M, and L Holland. 1974. "The Timing of RNA Synthesis for Spermiogenesis in Organ Cultures of Drosophila Melanogaster Testes." *Wilhelm Roux' Archiv Für Entwicklungsmechanik Der Organismen* 174 (2): 133–48. doi:10.1007/BF00573626.

Gratz, S J, A M Cummings, J N Nguyen, D C Hamm, L K Donohue, M M Harrison, J Wildonger, and K M O'connor-Giles. 2013. "Genome Engineering of Drosophila with the CRISPR RNA-Guided Cas9 Nuclease." *Genetics*. doi:10.1534/genetics.113.152710.

Graveley, B R, A N Brooks, J W Carlson, M O Duff, J M Landolin, L Yang, C G Artieri, et al. 2011. "The Developmental Transcriptome of Drosophila Melanogaster." *Nature* 471 (7339): 473–79. doi:10.1038/nature09715.

Green, P, A Y Hartenstein, and V Hartenstein. 1993. "The Embryonic Development of the Drosophila Visual System." *Cell & Tissue Research* 273 (3): 583–98. doi:10.1007/BF00333712.

Grifo, J A, S M Tahara, M A Morgan, A J Shatkin, and W C Merrick. 1983. "New Initiation Factor Activity Required for Globin mRNA Translation." *The Journal of Biological Chemistry* 258 (9): 5804–10.

Grönholm, M, M Sainio, F Zhao, L Heiska, A Vaheri, and O Carpén. 1999. "Homotypic and Heterotypic Interaction of the Neurofibromatosis 2 Tumor Suppressor Protein Merlin and the ERM Protein Ezrin." *Journal of Cell Science* 112 (Pt 6 (March): 895–904.

Gutmann, D H, M J Giordano, A S Fishback, and A Guha. 1997. "Loss of Merlin Expression in Sporadic Meningiomas, Ependymomas and Schwannomas." *Neurology* 49 (1): 267–70.

Gutmann, DH, L Sherman, L Seftor, C Haipek, K Hoang Lu, M Hendrix, and KH Lu. 1999. "Increased Expression of the NF2 Tumor Suppressor Gene Product, Merlin, Impairs Cell Motility, Adhesion and Spreading." *Human Molecular Genetics* 8 (2): 267–75. doi:ddc028 [pii].

Hall, A. 1998. "Rho GTPases and the Actin Cytoskeleton." *Science* 279 (5350): 509–14. doi:10.1126/science.279.5350.509.

Hamaratoglu, F, M Willecke, M Kango-Singh, R Nolo, E Hyun, C Tao, H Jafar-Nejad, and G Halder. 2006. "The Tumour-Suppressor Genes NF2/Merlin and Expanded Act through Hippo Signalling to Regulate Cell Proliferation and Apoptosis." *Nature Cell Biology* 8 (1): 27–36. doi:10.1038/ncb1339.

Hanemann, C O, R Diebold, and D Kaufmann. 2007. "Role of NF2 Haploinsufficiency in NF2-Associated Polyneuropathy." *Brain Pathology* 17 (4): 371–76. doi:10.1111/j.1750-3639.2007.00086.x.

Hardy, R W, K T Tokuyasu, D L Lindsley, and M Garavito. 1979. "The Germinal Proliferation Center in the Testis of Drosophila Melanogaster." *Journal of Ultrasructure Research* 69 (2): 180–90. doi:10.1016/S0022-5320(79)90108-4.

Hernández, G, M Altmann, J M Sierra, H Urlaub, R Diez del Corral, P Schwartz, and R Rivera-Pomar. 2005. "Functional Analysis of Seven Genes Encoding Eight Translation Initiation Factor 4E (eIF4E) Isoforms in Drosophila." *Mechanisms of Development* 122 (4): 529–43. doi:10.1016/j.mod.2004.11.011.

Hernández, G, H Han, V Gandin, L Fabian, T Ferreira, J Zuberek, N Sonenberg, J A Brill, and P Lasko. 2012. "Eukaryotic Initiation Factor 4E-3 Is Essential for Meiotic Chromosome Segregation, Cytokinesis and Male Fertility in Drosophila." *Development* 139 (17): 3211–20. doi:10.1242/dev.073122.

Hernández, G, M Miron, H Han, N Liu, J Magescas, G Tettweiler, F Frank, N Siddiqui, N Sonenberg, and P Lasko. 2013. "Mextli Is a Novel Eukaryotic Translation Initiation Factor 4E-Binding Protein That Promotes Translation in Drosophila Melanogaster." *Molecular and Cellular Biology* 33 (15): 2854–64. doi:10.1128/MCB.01354-12.

Hernandez, G, and J M Sierra. 1995. "Translation Initiation Factor eIF-4E from Drosophila: cDNA Sequence and Expression of the Gene." *Biochim Biophys Acta* 1261 (3): 427–31.

Hikasa, H, Y Sekido, and A Suzuki. 2016. "Merlin/NF2-Lin28B-Let-7 Is a Tumor-Suppressive Pathway That Is Cell-Density Dependent and Hippo Independent." *Cell Reports* 14 (12): 2950–61. doi:10.1016/j.celrep.2016.02.075.

Hilton, D A, N Ristic, and C O Hanemann. 2009. "Activation of ERK, AKT and JNK Signalling Pathways in Human Schwannomas in Situ." *Histopathology* 55 (6): 744–49. doi:10.1111/j.1365-2559.2009.03440.x.

Homem, C C F, and J A Knoblich. 2012. "Drosophila Neuroblasts: A Model for Stem Cell Biology." *Development* 139 (23): 4297–4310. doi:10.1242/dev.080515.

Hoopfer, E D, A Penton, R J Watts, and L Luo. 2008. "Genomic Analysis of Drosophila Neuronal Remodeling: A Role for the RNA-Binding Protein Boule as a Negative Regulator of Axon Pruning." *The Journal of Neuroscience* 28 (24): 6092–6103. doi:10.1523/JNEUROSCI.0677-08.2008.

Huang, A M, E J Rehm, and G M Rubin. 2009. "Quick Preparation of Genomic DNA from Drosophila." *Cold Spring Harbor Protocols* 2009 (4). doi:10.1101/pdb.prot5198.

Huang, Z, and S Kunes. 1998. "Signals Transmitted along Retinal Axons in Drosophila: Hedgehog Signal Reception and the Cell Circuitry of Lamina Cartridge Assembly." *Development* 125 (19): 3753–64. doi:10.1016/S0092-8674(00)80094-X.

Huang, Zhen, B Z Shilo, and Sam Kunes. 1998. "A Retinal Axon Fascicle Uses Spitz, an EGF Receptor Ligand, to Construct a Synaptic Cartridge in the Brain of Drosophila." *Cell* 95 (5): 693–703. doi:10.1016/S0092-8674(00)81639-6.

Hughes, S C, and R G Fehon. 2006. "Phosphorylation and Activity of the Tumor Suppressor Merlin and the ERM Protein Moesin Are Coordinately Regulated by the Slik Kinase." *The Journal of Cell Biology* 175 (2): 305–13. doi:10.1083/jcb.200608009.

Hummel, T, and C Klämbt. 2008. *Drosophila*. Edited by Christian Dahmann. *Methods in Molecular Biology: Drosophila: Methods and Protocols*. Vol. 420. Methods in Molecular Biology. Totowa, NJ: Humana Press. doi:10.1007/978-1-59745-583-1.

Huynh, D P, T Nechiporuk, and S M Pulst. 1994. "Alternative Transcripts in the Mouse Neurofibromatosis Type 2 (NF2) Gene Are Conserved and Code for Schwannomins with Distinct C-Terminal Domains." *Human Molecular Genetics* 3 (7): 1075–79. doi:10.1093/hmg/3.7.1075.

Insco, M L, A S Bailey, J Kim, G H Olivares, O L Wapinski, C H Tam, and M T Fuller. 2012. "A Self-Limiting Switch Based on Translational Control Regulates the Transition from Proliferation to Differentiation in an Adult Stem Cell Lineage." *Cell Stem Cell* 11 (5): 689–700. doi:10.1016/j.stem.2012.08.012.

Ito, Kei, and Yoshiki Hotta. 1992. "Proliferation Pattern of Postembryonic Neuroblasts in the Brain of Drosophila Melanogaster." *Developmental Biology* 149 (1): 134–48. doi:10.1016/0012-1606(92)90270-Q.

Jacob, A, T X Lee, B A Neff, S Miller, B Welling, and L-S Chang. 2008. "Phosphatidylinositol 3-kinase/AKT Pathway Activation in Human Vestibular Schwannoma." *Otology & Neurotology* 29 (1): 58–68. doi:10.1097/mao.0b013e31816021f7.

James, M F, S Han, C Polizzano, S R Plotkin, B D Manning, A O Stemmer-Rachamimov, J F Gusella, and V Ramesh. 2009. "NF2/merlin Is a Novel Negative Regulator of mTOR Complex 1, and Activation of mTORC1 Is Associated with Meningioma and Schwannoma Growth." *Molecular and Cellular Biology* 29 (15): 4250–61. doi:10.1128/MCB.01581-08.

James, M F, N Manchanda, C Gonzalez-Agosti, J H Hartwig, and V Ramesh. 2001. "The Neurofibromatosis 2 Protein Product Merlin Selectively Binds F-Actin but Not G-Actin, and Stabilizes the Filaments through a Lateral Association." *The Biochemical Journal* 356 (June): 377–86. doi:10.1042/0264-6021:3560377.

Jankovics, F, R Sinka, T Lukácsovich, and M Erdélyi. 2002. "MOESIN Crosslinks Actin and Cell Membrane in Drosophila Oocytes and Is Required for OSKAR Anchoring." *Current Biology* 12 (23): 2060–65. doi:10.1016/S0960-9822(02)01256-3.

Jinek, M, K Chylinski, I Fonfara, M Hauer, J A Doudna, and E Charpentier. 2012. "A Programmable Dual-RNA–Guided DNA Endonuclease in Adaptive Bacterial Immunity." *Science* 337 (6096): 816–21. doi:10.1126/science.1225829.

Johnson, K C, J L Kissil, J L Fry, and T Jacks. 2002. "Cellular Transformation by a FERM Domain Mutant of the Nf2 Tumor Suppressor Gene." *Oncogene* 21 (39): 5990–97. doi:10.1038/sj.onc.1205693.

Joiner, M-L, and C-F Wu. 2004. "Nervous System Function for the Testis RNA-Binding Protein Boule in Drosophila." *Journal of Neurogenetics* 18 (1): 341–63. doi:10.1080/01677060490477435.

Joshi, B, A-L Cai, B D Keiper, W B Minich, R Mendez, C M Beach, J Stepinski, R Stolarski, E Darzynkiewicz, and R E Rhoads. 1995. "Phosphorylation of Eukaryotic Protein Synthesis Initiation Factor 4E at Ser-209." *Journal of Biological Chemistry* 270 (24): 14597–603. doi:10.1074/jbc.270.24.14597.

Joshi, B, A Cameron, and R Jagus. 2004. "Characterization of Mammalian eIF4E-Family Members." *European Journal of Biochemistry* 271 (11): 2189–2203. doi:10.1111/j.1432-1033.2004.04149.x.

Jung, H, C G Gkogkas, N Sonenberg, and C E Holt. 2014. "Remote Control of Gene Function by Local Translation." *Cell* 157 (1): 26–40. doi:10.1016/j.cell.2014.03.005.

Jung, M-Y, L Lorenz, and J D Richter. 2006. "Translational Control by Neuroguidin, a Eukaryotic Initiation Factor 4E and CPEB Binding Protein." *Molecular and Cellular Biology* 26 (11): 4277–87. doi:10.1128/MCB.02470-05.

Kang, B S, D R Cooper, Y Devedjiev, U Derewenda, and Z S Derewenda. 2002. "The Structure of the FERM Domain of Merlin, the Neurofibromatosis Type 2 Gene

Product." *Acta Crystallographica Section D: Biological Crystallography* 58 (3): 381–91. doi:10.1107/S0907444901021175.

Kang, Kyung Hwa, and Heinrich Reichert. 2015. "Control of Neural Stem Cell Self-Renewal and Differentiation in Drosophila." *Cell and Tissue Research* 359 (1): 33–45. doi:10.1007/s00441-014-1914-9.

Kerekatte, V, K Smiley, B Hu, A Smith, F Gelder, and A De Benedetti. 1995. "The Proto-Oncogene/translation Factor eIF4E: A Survey of Its Expression in Breast Carcinomas." *International Journal of Cancer* 64 (1): 27–31. doi:10.1002/ijc.2910640107.

Kevil, C G, A De Benedetti, D K Payne, L L Coe, F S Laroux, and J S Alexander. 1996. "Translational Regulation of Vascular Permeability Factor by Eukaryotic Initiation Factor 4E: Implications for Tumor Angiogenesis." *International Journal of Cancer* 65 (6): 785–90. doi:10.1002/(SICI)1097-0215(19960315)65:6<785::AID-IJC14>3.0.CO;2-3.

Khan, M R, L Li, C Pérez-Sánchez, A Saraf, L Florens, B D Slaughter, J R Unruh, and K Si. 2015. "Amyloidogenic Oligomerization Transforms Drosophila Orb2 from a Translation Repressor to an Activator." *Cell* 163 (6): 1468–83. doi:10.1016/j.cell.2015.11.020.

Kim-Ha, J, K Kerr, and P M Macdonald. 1995. "Translational Regulation of Oskar mRNA by Bruno, an Ovarian RNA-Binding Protein, Is Essential." *Cell* 81 (3): 403–12. doi:10.1016/0092-8674(95)90393-3.

King, Ryan S, and Phillip a Newmark. 2013. "In Situ Hybridization Protocol for Enhanced Detection of Gene Expression in the Planarian Schmidtea Mediterranea." *BMC Developmental Biology* 13 (1): 8. doi:10.1186/1471-213X-13-8.

Kluwe, L, and V F Mautner. 1996. "A Missense Mutation in the NF2 Gene Results in Moderate and Mild Clinical Phenotypes of Neurofibromatosis Type 2." *Human Genetics* 97 (2): 224–27. doi:10.1007/BF02265270.

Kluwe, L, V Mautner, B Heinrich, R Dezube, L B Jacoby, R E Friedrich, and M MacCollin. 2003. "Molecular Study of Frequency of Mosaicism in Neurofibromatosis 2 Patients with Bilateral Vestibular Schwannomas." *Journal of Medical Genetics* 40 (2): 109–14.

Knudson, A G. 1971. "Mutation and Cancer: Statistical Study of Retinoblastoma." *PNAS* 68 (4): 820–23.

Koromilas, A E, A Lazaris-Karatzas, and N Sonenberg. 1992. "mRNAs Containing Extensive Secondary Structure in Their 5′ Non-Coding Region Translate Efficiently in Cells Overexpressing Initiation Factor eIF-4E." *The EMBO Journal* 11 (11): 4153–58. doi:10.1126/science.1382315.

Kozopas, Karen M, Cindy Harryman Samos, and Roel Nusse. 1998. "DWnt-2, a Drosophila Wnt Gene Required for the Development of the Male Reproductive Tract, Specifies a Sexually Dimorphic Cell Fate." *Genes and Development* 12 (8): 1155–65. doi:10.1101/gad.12.8.1155.

Kubacka, D, R N Miguel, N Minshall, E Darzynkiewicz, N Standart, and J Zuberek. 2015. "Distinct Features of Cap Binding by eIF4E1b Proteins." *Journal of Molecular Biology* 427 (2): 387–405. doi:10.1016/j.jmb.2014.11.009.

Kuckwa, J, K Fritzen, D Buttgereit, S Rothenbusch-Fender, and R Renkawitz-Pohl. 2016. "A New Level of Plasticity: Drosophila Smooth-like Testes Muscles Compensate Failure of Myoblast Fusion." *Development* 143 (2): 329–38. doi:10.1242/dev.126730.

LaJeunesse, D R, B M McCartney, and R G Fehon. 1998. "Structural Analysis of Drosophila Merlin Reveals Functional Domains Important for Growth Control and Subcellular Localization." *Journal of Cell Biology* 141 (7): 1589–99. doi:10.1083/jcb.141.7.1589.

———. 2001. "A Systematic Screen for Dominant Second-Site Modifiers of Merlin/NF2 Phenotypes Reveals an Interaction With blistered/DSRF and Scribbler." *Genetics* 158: 667–79.

Lallemand, D, M Curto, I Saotome, M Giovannini, and A I McClatchey. 2003. "NF2 Deficiency Promotes Tumorigenesis and Metastasis by Destabilizing Adherens Junctions." *Genes and Development* 17 (9): 1090–1100. doi:10.1101/gad.1054603.

Lallemand, D, A L Saint-Amaux, and M Giovannini. 2009. "Tumor-Suppression Functions of Merlin Are Independent of Its Role as an Organizer of the Actin Cytoskeleton in Schwann Cells." *Journal of Cell Science* 122 (22): 4141–49. doi:10.1242/jcs.045914.

Lamphear, B J, and R Panniers. 1990. "Cap Binding Protein Complex That Restores Protein Synthesis in Heat-Shocked Ehrlich Cell Lysates Contains Highly Phosphorylated eIF-4E*." *The Journal of Biological Chemistry* 265 (10): 5333–36.

Landon, A L, P A Muniandy, A C Shetty, E Lehrmann, L Volpon, S Houng, Y Zhang, et al. 2014. "MNKs Act as a Regulatory Switch for eIF4E1 and eIF4E3 Driven mRNA Translation in DLBCL." *Nature Communications* 5 (May): 5413. doi:10.1038/ncomms6413.

Lazaris-Karatzas, A, KS Montine, and N Sonenberg. 1990. "Malignant Transformation by a Eukaryotic Initiation Factor Subunit That Binds to mRNA 5'cap." *Nature* 345 (6275): 544–47. doi:10.1038/345544a0.

Lazaris-Karatzas, A, M R Smith, R M Frederickson, M L Jaramillo, Y L Liu, H F Kung, and N Sonenberg. 1992. "Ras Mediates Translation Initiation Factor 4E-Induced Malignant Transformation." *Genes and Development* 6 (9): 1631–42. doi:10.1101/gad.6.9.1631.

Lee, J Y, H Kim, C H Ryu, J Y Kim, B H Choi, Y Lim, P W Huh, et al. 2004. "Merlin, a Tumor Suppressor, Interacts with Transactivation-Responsive RNA-Binding Protein and Inhibits Its Oncogenic Activity." *Journal of Biological Chemistry* 279 (29): 30265–73. doi:10.1074/jbc.M312083200.

Lee, J Y, H J Moon, W K Lee, H J Chun, C W Han, Y-W Jeon, Y Lim, et al. 2006. "Merlin Facilitates Ubiquitination and Degradation of Transactivation-Responsive RNA-Binding Protein." *Oncogene* 25 (8): 1143–52. doi:10.1038/sj.onc.1209150.

Lee, T, and L Luo. 1999. "Mosaic Analysis with a Repressible Neurotechnique Cell Marker for Studies of Gene Function in Neuronal Morphogenesis." *Neuron* 22: 451–61.

Li, S, J Fu, C Lu, M Y Mapara, S Raza, U Hengst, and S Lentzsch. 2016. "Elevated Translation Initiation Factor eIF4E Is an Attractive Therapeutic Target in Multiple Myeloma." *Molecular Cancer Therapeutics* 15 (4): 711–19. doi:10.1158/1535-7163.MCT-15-0798.

Li, W, J Cooper, L Zhou, C Yang, H Erdjument-Bromage, D Zagzag, M Snuderl, et al. 2014. "Merlin/NF2 Loss-Driven Tumorigenesis Linked to CRL4DCAF1-Mediated Inhibition of the Hippo Pathway Kinases Lats1 and 2 in the Nucleus." *Cancer Cell* 26 (1): 48–60. doi:10.1016/j.ccr.2014.05.001.

Li, W, L You, J Cooper, G Schiavon, A Pepe-Caprio, L Zhou, R Ishii, et al. 2010. "Merlin/NF2 Suppresses Tumorigenesis by Inhibiting the E3 Ubiquitin Ligase CRL4DCAF1 in the Nucleus." *Cell* 140 (4): 477–90. doi:10.1016/j.cell.2010.01.029.

Li, Y, G I Tennekoon, M Birnbaum, M A Marchionni, and J L Rutkowski. 2001. "Neuregulin Signaling through a PI3K/Akt/Bad Pathway in Schwann Cell Survival." *Molecular and Cellular Neuroscience* 17 (4): 761–67. doi:10.1006/mcne.2000.0967.

Li, Y, H Zhou, F Li, S W Chan, Z Lin, Z Wei, Z Yang, et al. 2015. "Angiomotin Binding-Induced Activation of Merlin/NF2 in the Hippo Pathway." *Cell Research* 25 (7): 801–17. doi:10.1038/cr.2015.69.

Lim, C K, and R L Kelley. 2012. "Autoregulation of the Drosophila Noncoding roX1 RNA Gene." *PLoS Genetics* 8 (3): 23–29. doi:10.1371/journal.pgen.1002564.

Lin, T, X Kong, T Haystead, A Pause, G J Belsham, N Sonenberg, and J C Lawrence Jr. 1994. "PHAS-I as a Link between Mitogen-Activated Protein Kinase and Translation Initiation." *Science* 266 (5185): 653–56. doi:10.1126/science.7939721.

Lo, P C H, and M Frasch. 1997. "A Novel KH-Domain Protein Mediates Cell Adhesion Processes in Drosophila." *Developmental Biology* 190 (2): 241–56. doi:10.1006/dbio.1997.8699.

Lomas, J, M J Bello, D Arjona, M E Alonso, V Martinez-Glez, I Lopez-Marin, C Amiñoso, et al. 2005. "Genetic and Epigenetic Alteration of the NF2 Gene in Sporadic Meningiomas." *Genes, Chromosomes & Cancer* 42 (3): 314–19. doi:10.1002/gcc.20141.

Lopez-Lago, M A, T Okada, M M Murillo, N Socci, and F G Giancotti. 2009. "Loss of the Tumor Suppressor Gene NF2, Encoding Merlin, Constitutively Activates Integrin-Dependent mTORC1 Signaling." *Molecular and Cellular Biology* 29 (15): 4235–49. doi:10.1128/MCB.01578-08.

Louvet, S, J Aghion, A Santa-Maria, P Mangeat, and B Maro. 1996. "Ezrin Becomes Restricted to Outer Cells Following Asymmetrical Division in the Preimplantation Mouse Embryo." *Developmental Biology* 177 (2): 568–79. doi:10.1006/dbio.1996.0186.

Lutchman, M, and G A Rouleau. 1995. "The Neurofibromatosis Type 2 Gene Product, Schwannomin, Suppresses Growth of NIH 3T3 Cells." *Cancer Research* 55 (11): 2270–74.

Mader, S, H Lee, A Pause, and N Sonenberg. 1995. "The Translation Initiation Factor eIF-4E Binds to a Common Motif Shared by the Translation Factor eIF-4 Gamma and the Translational Repressors 4E-Binding Proteins." *Molecular and Cellular Biology* 15 (9): 4990–97. doi:10.1128/MCB.15.9.4990.

Maeda, Masato, Takeshi Matsui, Masayuki Imamura, Sachiko Tsukita, and Sachiko Tsukita. 1999. "Expression Level, Subcellular Distribution and Rho-GDI Binding Affinity of Merlin in Comparison with Ezrin/Radixin/Moesin Proteins." *Oncogene* 18 (34): 4788–97. doi:10.1038/sj.onc.1202871.

Maines, J Z, and S A Wasserman. 1999. "Post-Transcriptional Regulation of the Meiotic Cdc25 Protein Twine by the Dazl Orthologue Boule." *Nature Cell Biology* 1 (3): 171–74. doi:10.1038/11091.

Maitra, S, R M Kulikauskas, H Gavilan, and R G Fehon. 2006. "The Tumor Suppressors Merlin and Expanded Function Cooperatively to Modulate Receptor Endocytosis and Signaling." *Current Biology* 16 (7): 702–9. doi:10.1016/j.cub.2006.02.063.

Manchanda, N, A Lyubimova, H-Y H Ho, M F James, J F Gusella, N Ramesh, S B Snapper, and V Ramesh. 2005. "The NF2 Tumor Suppressor Merlin and the ERM Proteins Interact with N-WASP and Regulate Its Actin Polymerization Function." *Journal of Biological Chemistry* 280 (13): 12517–22. doi:10.1074/jbc.C400583200.

Marcotrigiano, J, A C Gingras, N Sonenberg, and S K Burley. 1997. "Cocrystal Structure of the Messenger RNA 5′ Cap-Binding Protein (eIF4E) Bound to 7-Methyl-GDP." *Cell* 89 (6): 951–61. doi:10.1016/S0092-8674(00)80280-9.

———. 1999. "Cap-Dependent Translation Initiation in Eukaryotes Is Regulated by a Molecular Mimic of eIF4G." *Molecular Cell* 3 (6): 707–16. doi:10.1016/S1097-2765(01)80003-4.

Matsuo, H, H Li, A M McGuire, C M Fletcher, A C Gingras, N Sonenberg, and G Wagner. 1997. "Structure of Translation Factor eIF4E Bound to m7GDP and Interaction with 4E-Binding Protein." *Nature Structural Biology* 4 (9): 717–24. doi:10.1038/nsb0997-717.

Matsuo, H, T Moriguchi, T Takagi, T Kusakabe, S Buratowski, M Sekine, Y Kyogoku, and G Wagner. 2000. "Efficient Synthesis of 13 C , 15 N-Labeled RNA Containing the Cap Structure M 7 GpppA." *Journal of the American Chemical Society* 122 (11): 2417–21. doi:10.1021/ja9926820.

Maurange, C, L Cheng, and A P Gould. 2008. "Temporal Transcription Factors and Their Targets Schedule the End of Neural Proliferation in Drosophila." *Cell* 133 (5): 891–902. doi:10.1016/j.cell.2008.03.034.

Mautner, V F, M E Baser, and L Kluwe. 1996. "Phenotypic Variability in Two Families with Novel Splice-Site and Frameshift NF2 Mutations." *Human Genetics* 98 (2): 203–6. doi:10.1007/s004390050191.

Mautner, V F, M Lindenau, M E Baser, L Kluwe, and J Gottschalk. 1997. "Skin Abnormalities in Neurofibromatosis 2." *Archives of Dermatology* 133 (12): 1539–43. doi:10.1001/archderm.1997.03890480059008.

Mayer, L R, S Diegelmann, Y Abassi, F Eichinger, and G O Pflugfelder. 2013. "Enhancer Trap Infidelity in Drosophila Optomotor-Blind." *Fly* 7 (2): 118–28. doi:10.4161/fly.23657.

McCartney, B M, and R G Fehon. 1996. "Distinct Cellular and Subcellular Patterns of Expression Imply Distinct Functions for the Drosophila Homologues of Moesin and the Neurofibromatosis Tumor Suppressor, NF2." *Journal of Cell Biology* 133 (4): 843–52.

McCartney, B M, R M Kulikauskas, D R LaJeunesse, and R G Fehon. 2000. "The Neurofibromatosis-2 Homologue, Merlin, and the Tumor Suppressor Expanded Function Together in Drosophila to Regulate Cell Proliferation and Differentiation." *Development* 127 (6): 1315–24. doi:10.1002/(sici)1096-8628(19960906)64:4<563::aid-ajmg7>3.0.co.

McClatchey, A I. 2007. "Neurofibromatosis." *Annual Review of Pathology* 2 (January): 191–216. doi:10.1146/annurev.pathol.2.010506.091940.

McClatchey, A I, I Saotome, V Ramesh, J F Gusella, and T Jacks. 1997. "The Nf2 Tumor Suppressor Gene Product Is Essential for Extraembryonic Development Immediately prior to Gastrulation." *Genes and Development* 11 (10): 1253–65. doi:10.1101/gad.11.10.1253.

McLaughlin, M E, G M Kruger, K L Slocum, D Crowley, N A Michaud, J Huang, M Magendantz, and T Jacks. 2007. "The Nf2 Tumor Suppressor Regulates Cell-Cell Adhesion during Tissue Fusion." *PNAS* 104 (9): 3261–66. doi:10.1073/pnas.0700044104.

Meinertzhagen, I A, and T E Hanson. 1993. "The Development of the Optic Lobe." In *The Development of Drosophila Melanogaster*, edited by M Bate and A Martinez-Arias, 1363–1491. Cold Spring Harbor, NY: Cold Spring Harbor Laboratory Press.

Minich, W B, M L Balasta, D J Goss, and R E Rhoads. 1994. "Chromatographic Resolution of in Vivo Phosphorylated and Nonphosphorylated Eukaryotic Translation Initiation Factor eIF-4E: Increased Cap Affinity of the Phosphorylated Form." *PNAS* 91 (16): 7668–72. doi:10.1073/pnas.91.16.7668.

Minshall, N, M H Reiter, D Weil, and N Standart. 2007. "CPEB Interacts with an Ovary-Specific eIF4E and 4E-T in Early Xenopus Oocytes." *Journal of Biological Chemistry* 282 (52): 37389–401. doi:10.1074/jbc.M704629200.

Miron, M, P Lasko, and N Sonenberg. 2003. "Signaling from Akt to FRAP/TOR Targets Both 4E-BP and S6K in Drosophila Melanogaster." *Molecular and Cellular Biology* 23 (24): 9117–26. doi:10.1128/MCB.23.24.9117-9126.2003.

Miron, M, J Verdú, P E D Lachance, M J Birnbaum, P F Lasko, and N Sonenberg. 2001. "The Translational Inhibitor 4E-BP Is an Effector of PI(3)K/Akt Signalling and Cell Growth in Drosophila." *Nature Cell Biology* 3 (6): 596–601. doi:10.1038/35078571.

Miyagi, Y, A Sugiyama, A Asai, T Okazaki, Y Kuchino, and S J Kerr. 1995. "Elevated Levels of Eukaryotic Translation Initiation Factor eIF-4E, mRNA in a Broad Spectrum of Transformed Cell Lines." *Cancer Letters* 91 (2): 247–52. doi:10.1016/0304-3835(95)03737-H.

Monk, A C, N A Siddall, T Volk, B Fraser, L M Quinn, E A McLaughlin, and G R Hime. 2010. "HOW Is Required for Stem Cell Maintenance in the Drosophila Testis and for the Onset of Transit-Amplifying Divisions." *Cell Stem Cell* 6 (4): 348–60. doi:10.1016/j.stem.2010.02.016.

Moreno, J A, H Radford, D Peretti, J R Steinert, N Verity, M G Martin, M Halliday, et al. 2012. "Sustained Translational Repression by eIF2α-P Mediates Prion Neurodegeneration." *Nature* 485 (7399): 507–11. doi:10.1038/nature11058.

Morita, M, L W Ler, M R Fabian, N Siddiqui, M Mullin, V C Henderson, T Alain, et al. 2012. "A Novel 4EHP-GIGYF2 Translational Repressor Complex Is Essential for Mammalian Development." *Molecular and Cellular Biology* 32 (17): 3585–93. doi:10.1128/MCB.00455-12.

Morrison, H, LS Sherman, J Legg, F Banine, C Isacke, CA Haipek, DH Gutmann, H Ponta, and P Herrlich. 2001. "The NF2 Tumor Suppressor Gene Product, Merlin, Mediates Contact Inhibition of Growth through Interactions with CD44." *Genes and Development* 15 (8): 968–80. doi:10.1101/gad.189601.

Morrison, H, T Sperka, J Manent, M Giovannini, H Ponta, and P Herrlich. 2007. "Merlin/neurofibromatosis Type 2 Suppresses Growth by Inhibiting the Activation of Ras and Rac." *Cancer Research* 67 (2): 520–27. doi:10.1158/0008-5472.CAN-06-1608.

Murray, L B, Y-K I Lau, and Q Yu. 2012. "Merlin Is a Negative Regulator of Human Melanoma Growth." Edited by Keiran Smalley. *PloS One* 7 (8): e43295. doi:10.1371/journal.pone.0043295.

Nabel-Rosen, H, N Dorevitch, A Reuveny, and T Volk. 1999. "The Balance between Two Isoforms of the Drosophila RNA-Binding Protein How Controls Tendon Cell Differentiation." *Molecular Cell* 4 (4): 573–84. doi:10.1016/S1097-2765(00)80208-7.

Nakamura, A, K Sato, and K Hanyu-Nakamura. 2004. "Drosophila Cup Is an eIF4E Binding Protein That Associates with Bruno and Regulates Oskar mRNA Translation in Oogenesis." *Developmental Cell* 6 (1): 69–78. doi:10.1016/S1534-5807(03)00400-3.

Nanda, S, T J DeFalco, S H Y Loh, N Phochanukul, N Camara, M van Doren, and S Russell. 2009. "Sox100B, a Drosophila Group E Sox-Domain Gene, Is Required for Somatic Testis Differentiation." *Sexual Development* 3 (1): 26–37. doi:10.1159/000200079.

Napoli, I, V Mercaldo, P P Boyl, B Eleuteri, F Zalfa, S De Rubeis, D Di Marino, et al. 2008. "The Fragile X Syndrome Protein Represses Activity-Dependent Translation through CYFIP1, a New 4E-BP." *Cell* 134 (6): 1042–54. doi:10.1016/j.cell.2008.07.031.

Nathan, C A O, L Liu, B D Li, F W Abreo, I Nandy, and A DeBenedetti. 1997. "Detection of the Proto-Oncogene eIF4E in Surgical Margins May Predict Recurrence in Head and Neck Cancer." *Oncogene* 15 (5): 579–84. doi:Doi 10.1038/Sj.Onc.1201216.

Nelson, M R, A M Leidal, and C A Smibert. 2004. "Drosophila Cup Is an eIF4E-Binding Protein That Functions in Smaug-Mediated Translational Repression." *The EMBO Journal* 23 (1): 150–59. doi:10.1038/sj.emboj.7600026.

Neves-Pereira, M, B Müller, D Massie, J H G Williams, P C M O'Brien, A Hughes, S-B Shen, D S Clair, and Z Miedzybrodzka. 2009. "Deregulation of EIF4E: A Novel Mechanism for Autism." *Journal of Medical Genetics* 46 (11): 759–65. doi:10.1136/jmg.2009.066852.

Niedzwiecka, A, J Marcotrigiano, J Stepinski, M Jankowska-Anyszka, A Wyslouch-Cieszynska, M Dadlez, A C Gingras, et al. 2002. "Biophysical Studies of eIF4E Cap-Binding Protein: Recognition of mRNA 5′ Cap Structure and Synthetic Fragments of eIF4G and 4E-BP1 Proteins." *Journal of Molecular Biology* 319 (3): 615–35. doi:10.1016/S0022-2836(02)00328-5.

Obremski, VJ, AM Hall, and C Fernandez-Valle. 1998. "Merlin, the Neurofibromatosis Type 2 Gene Product, and beta1 Integrin Associate in Isolated and Differentiating Schwann Cells." *Journal of Neurobiology* 37 (4): 487–501. doi:10.1002/(SICI)1097-4695(199812)37:4<487::AID-NEU1>3.0.CO;2-B.

Olivieri, G, and A Olivieri. 1965. "Autoradiographic Study of Nucleic Acid Synthesis during Spermatogenesis in Drosophila Melanogaster." *Mutation Research/Fundamental and Molecular Mechanisms of Mutagenesis* 2 (4): 366–80. doi:10.1016/0027-5107(65)90072-2.

Osborne, M J, L Volpon, J A Kornblatt, B Culjkovic-Kraljacic, A Baguet, and K L Borden. 2013. "eIF4E3 Acts as a Tumor Suppressor by Utilizing an Atypical Mode of Methyl-7-Guanosine Cap Recognition." *Proceedings of the National Academy of Sciences of the United States of America* 110 (10): 3877–82. doi:10.1073/pnas.1216862110.

Papagiannouli, Fani, and Bernard M Mechler. 2009. "Discs Large Regulates Somatic Cyst Cell Survival and Expansion in Drosophila Testis." *Cell Research* 19 (10): 1139–49. doi:10.1038/cr.2009.71.

Parry, D M, R Eldridge, M I Kaiser-Kupfer, E A Bouzas, A Pikus, and N Patronas. 1994. "Neurofibromatosis 2 (NF2): Clinical Characteristics of 63 Affected Individuals and Clinical Evidence for Heterogeneity." *American Journal of Medical Genetics* 52 (4): 450–61. doi:10.1002/ajmg.1320520411.

Parry, D M, M M MacCollin, M I Kaiser-Kupfer, K Pulaski, H S Nicholson, M Bolesta, R

Eldridge, and J F Gusella. 1996. “Germ-Line Mutations in the Neurofibromatosis 2 Gene: Correlations with Disease Severity and Retinal Abnormalities.” *American Journal of Human Genetics* 59 (3): 529–39.

Pattatucci, A M, and T C Kaufman. 1991. “The Homeotic Gene Sex Combs Reduced of Drosophila Melanogaster Is Differentially Regulated in the Embryonic and Imaginal Stages of Development.” *Genetics* 129 (2): 443–61.

Pause, A, G J Belsham, A C Gingras, O Donzé, T A Lin, J C Lawrence Jr, and N Sonenberg. 1994. “Insulin-Dependent Stimulation of Protein Synthesis by Phosphorylation of a Regulator of 5’-cap Function.” *Nature* 371 (6500): 762–67. doi:10.1038/371762a0.

Pearson, M A, D Reczek, A Bretscher, and P A Karplus. 2000. “Structure of the ERM Protein Moesin Reveals the FERM Domain Fold Masked by an Extended Actin Binding Tail Domain.” *Cell* 101 (3): 259–70. doi:10.1016/S0092-8674(00)80836-3.

Pellock, B J, E Buff, K White, and I K Hariharan. 2007. “The Drosophila Tumor Suppressors Expanded and Merlin Differentially Regulate Cell Cycle Exit, Apoptosis, and Wingless Signaling.” *Developmental Biology* 304 (1): 102–15. doi:10.1016/j.ydbio.2006.12.021.

Pelton, P D, L S Sherman, T A Rizvi, M A Marchionni, P Wood, R A Friedman, and N Ratner. 1998. “Ruffling Membrane, Stress Fiber, Cell Spreading and Proliferation Abnormalities in Human Schwannoma Cells.” *Oncogene* 17 (17): 2195–2209. doi:10.1038/sj.onc.1202141.

Pestonjamasp, K, M R Amieva, C P Strassel, W M Nauseef, H Furthmayr, and E J Luna. 1995. “Moesin, Ezrin, and p205 Are Actin-Binding Proteins Associated with Neutrophil Plasma Membranes.” *Molecular Biology of the Cell* 6 (3): 247–59. doi:10.1091/mbc.6.3.247.

Petricoin, E F, V Espina, R P Araujo, B Midura, C Yeung, X Wan, G S Eichler, et al. 2007. “Phosphoprotein Pathway Mapping: Akt/mammalian Target of Rapamycin Activation Is Negatively Associated with Childhood Rhabdomyosarcoma Survival.” *Cancer Research* 67 (7): 3431–40. doi:10.1158/0008-5472.CAN-06-1344.

Piper, M, S Salih, C Weinl, C E Holt, and W A Harris. 2005. “Endocytosis-Dependent Desensitization and Protein Synthesis-Dependent Resensitization in Retinal Growth Cone Adaptation.” *Nature Neuroscience* 8 (2). Nature Publishing Group: 179–86. doi:10.1038/nn1380.

Poeck, B, S Fischer, D Gunning, S L Zipursky, and I Salecker. 2001. “Glial Cells Mediate

Target Layer Selection of Retinal Axons in the Developing Visual System of Drosophila." *Neuron* 29 (1): 99–113. doi:10.1016/S0896-6273(01)00183-0.

Polesello, C, I Delon, P Valenti, P Ferrer, and F Payre. 2002. "Dmoesin Controls Actin-Based Cell Shape and Polarity during Drosophila Melanogaster Oogenesis." *Nature Cell Biology* 4 (10): 782–89. doi:10.1038/ncb856.

Poulin, F, A C Gingras, H Olsen, S Chevalier, and N Sonenberg. 1998. "4E-BP3, a New Member of the Eukaryotic Initiation Factor 4E-Binding Protein Family." *Journal of Biological Chemistry* 273 (22): 14002–7. doi:10.1074/jbc.273.22.14002.

Prokop, A, and G M Technau. 1991. "The Origin of Postembryonic Neuroblasts in the Ventral Nerve Cord of Drosophila Melanogaster." *Development (Cambridge, England)* 111 (1): 79–88.

Ptushkina, M, T von der Haar, M M Karim, J M X Hughes, and J E G McCarthy. 1999. "Repressor Binding to a Dorsal Regulatory Site Traps Human eIF4E in a High Cap-Affinity State." *EMBO Journal* 18 (14): 4068–75. doi:10.1093/emboj/18.14.4068.

Qu, Y, R Zhao, H Wang, K Chang, X Yang, X Zhou, B Dai, et al. 2016. "Phosphorylated 4EBP1 Is Associated with Tumor Progression and Poor Prognosis in Xp11.2 Translocation Renal Cell Carcinoma." *Scientific Reports* 6 (March): 23594. doi:10.1038/srep23594.

Reczek, D, M Berryman, and A Bretscher. 1997. "Identification of EPB50: A PDZ-Containing Phosphoprotein That Associates with Members of the Ezrin-Radixin-Moesin Family." *Journal of Cell Biology* 139 (1): 169–79. doi:10.1083/jcb.139.1.169.

Reddy, B V V G, and K D Irvine. 2011. "Regulation of Drosophila Glial Cell Proliferation by Merlin-Hippo Signaling." *Development* 138 (23): 5201–12. doi:10.1242/dev.069385.

Reichert, Heinrich. 2011. "Drosophila Neural Stem Cells: Cell Cycle Control of Self-Renewal, Differentiation, and Termination in Brain Development." *Results and Problems in Cell Differentiation* 53: 529–46. doi:10.1007/978-3-642-19065-0_21.

Richter, J D, and N Sonenberg. 2005. "Regulation of Cap-Dependent Translation by eIF4E Inhibitory Proteins." *Nature* 433 (7025): 477–80. doi:10.1038/nature03205.

Riemenschneider, M.J., A. Perry, and G. Reifenberger. 2006. "Histological Classification and Molecular Genetics of Meningiomas." *The Lancet Neurology* 5 (12): 1045–54. doi:10.1016/S1474-4422(06)70625-1.

Rivera-Pomar, R, D Niessing, U Schmidt-Ott, W J Gehring, and H Jäckle. 1996. "RNA

Binding and Translational Suppression by Bicoid." *Nature* 379 (6567): 746–49. doi:10.1038/379746a0.

Robida, Mark, Vinod Sridharan, Sheridan Morgan, Timsi Rao, and Ravinder Singh. 2010. "Drosophila Polypyrimidine Tract-Binding Protein Is Necessary for Spermatid Individualization." *PNAS* 107 (28): 12570–75. doi:10.1073/pnas.1007935107.

Rojo, F, L Najera, J Lirola, J Jiménez, M Guzmán, M D Sabadell, J Baselga, and S R y Cajal. 2007. "4E-Binding Protein 1, a Cell Signaling Hallmark in Breast Cancer That Correlates with Pathologic Grade and Prognosis." *Clinical Cancer Research* 13 (1): 81–89. doi:10.1158/1078-0432.CCR-06-1560.

Rom, E, H C Kim, A C Gingras, J Marcotrigiano, D Favre, H Olsen, S K Burley, and N Sonenberg. 1998. "Cloning and Characterization of 4EHP, a Novel Mammalian eIF4E-Related Cap-Binding Protein." *Journal of Biological Chemistry* 273 (21): 13104–9. doi:10.1074/jbc.273.21.13104.

Rong, R, X Tang, D H Gutmann, and K Ye. 2004. "Neurofibromatosis 2 (NF2) Tumor Suppressor Merlin Inhibits Phosphatidylinositol 3-Kinase through Binding to PIKE-L." *PNAS* 101 (52): 18200–205. doi:0405971102 [pii]\n10.1073/pnas.0405971102.

Rose, J K. 1975. "Heterogeneous 5′-Terminal Structures Occur on Vesicular Stomatitis Virus mRNAs." *The Journal of Biological Chemistry* 250 (20): 8098–8104.

Rosenwald, I B, A Lazaris-Karatzas, N Sonenberg, and E V Schmidt. 1993. "Elevated Levels of Cyclin D1 Protein in Response to Increased Expression of Eukaryotic Initiation Factor 4E." *Molecular and Cellular Biology* 13 (12): 7358–63.

Rotkopf, S, Y Hamberg, T Aigaki, S B Snapper, B-Z Shilo, and E D Schejter. 2011. "The WASp-Based Actin Polymerization Machinery Is Required in Somatic Support Cells for Spermatid Maturation and Release." *Development* 138: 2729–39. doi:10.1242/dev.059865.

Rouleau, G A, P Merel, M Lutchman, M Sanson, J Zucman, C Marineau, K Hoang-Xuan, S Demczuk, C Desmaze, and B Plougastel. 1993. "Alteration in a New Gene Encoding a Putative Membrane-Organizing Protein Causes Neuro-Fibromatosis Type 2." *Nature* 363 (6429): 515–21. doi:10.1038/363515a0.

Ruggero, D, L Montanaro, L Ma, W Xu, P Londei, C Cordon-Cardo, and P P Pandolfi. 2004. "The Translation Factor eIF-4E Promotes Tumor Formation and Cooperates with c-Myc in Lymphomagenesis." *Nature Medicine* 10 (5): 484–86. doi:10.1038/nm1042.

Ruttledge, M H, A A Andermann, C M Phelan, J O Claudio, F Y Han, N Chretien, S Rangaratnam, et al. 1996. "Type of Mutation in the Neurofibromatosis Type 2 Gene (NF2) Frequently Determines Severity of Disease." *American Journal of Human Genetics* 59 (2): 331–42. http://www.ncbi.nlm.nih.gov/pubmed/8755919.

Saez, L, and M W Young. 1988. "In Situ Localization of the per Clock Protein during Development of Drosophila Melanogaster." *Molecular and Cellular Biology* 8 (12): 5378–85.

Sainio, M, F Zhao, L Heiska, O Turunen, M den Bakker, E Zwarthoff, M Lutchman, et al. 1997. "Neurofibromatosis 2 Tumor Suppressor Protein Colocalizes with Ezrin and CD44 and Associates with Actin-Containing Cytoskeleton." *Journal of Cell Science* 110 (Pt 1 (September): 2249–60. http://www.ncbi.nlm.nih.gov/pubmed/9378774.

Saotome, I, M Curto, and A I McClatchey. 2004. "Ezrin Is Essential for Epithelial Organization and Villus Morphogenesis in the Developing Intestine." *Developmental Cell* 6 (6): 855–64. doi:10.1016/j.devcel.2004.05.007.

Schäfer, M, D Börsch, A Hülster, and U Schäfer. 1993. "Expression of a Gene Duplication Encoding Conserved Sperm Tail Proteins Is Translationally Regulated in Drosophila Melanogaster." *Molecular and Cellular Biology* 13 (3): 1708–18. doi:10.1128/MCB.13.3.1708.Updated.

Schäfer, M, K Nayernia, W Engel, and U Schäfer. 1995. "Translational Control in Spermatogenesis." *Developmental Biology* 172 (2): 344–52. doi:10.1006/dbio.1995.8049.

Schulz, A, S L Baader, M Niwa-Kawakita, M J Jung, R Bauer, C Garcia, A Zoch, et al. 2013. "Merlin Isoform 2 in Neurofibromatosis Type 2-Associated Polyneuropathy." *Nature Neuroscience* 16 (4): 426–33. doi:10.1038/nn.3348.

Schwarz, S, Z Durisko, and R Dukas. 2014. "Food Selection in Larval Fruit Flies: Dynamics and Effects on Larval Development." *Die Naturwissenschaften* 101 (1): 61–68. doi:10.1007/s00114-013-1129-z.

Scoles, D R. 2008. "The Merlin Interacting Proteins Reveal Multiple Targets for NF2 Therapy." *Biochimica et Biophysica Acta* 1785 (1): 32–54. doi:10.1016/j.bbcan.2007.10.001.

Scoles, D R, W H Yong, Y Qin, K Wawrowsky, and S M Pulst. 2006. "Schwannomin Inhibits Tumorigenesis through Direct Interaction with the Eukaryotic Initiation Factor Subunit c (eIF3c)." *Human Molecular Genetics* 15 (7): 1059–70. doi:10.1093/hmg/ddl021.

Seki, N, T Takasu, K Mandai, M Nakata, H Saeki, Y Heike, I Takata, Y Segawa, T Hanafusa, and K Eguchi. 2002. "Expression of Eukaryotic Initiation Factor 4E in Atypical Adenomatous Hyperplasia and Adenocarcinoma of the Human Peripheral Lung." *Clinical Cancer Research* 8 (10): 3046–53. doi:10.1002/1097-0142(19950101)75:1+<191::aid-cncr2820751307>3.0.co.

Sekido, Y, H I Pass, S Bader, D. J Y Mew, M F Christman, A F Gazdar, and J D Minna. 1995. "Neurofibromatosis Type 2 (NF2) Gene Is Somatically Mutated in Mesothelioma but Not in Lung Cancer." *Cancer Research* 55 (6): 1227–31. doi:10.1016/0169-5002(95)90162-0.

Selleck, S B, C Gonzalez, D M Glover, and K White. 1992. "Regulation of the G1-S Transition in Postembryonic Neuronal Precursors by Axon Ingrowth." *Nature* 355 (6357): 253–55. doi:10.1038/355253a0.

Selleck, S B, and H Steller. 1991. "The Influence of Retinal Innervation on Neurogenesis in the First Optic Ganglion of Drosophila." *Neuron* 6 (1): 83–99. doi:10.1016/0896-6273(91)90124-I.

Sepp, K J, and V J Auld. 1999. "Conversion of lacZ Enhancer Trap Lines to GAL4 Lines Using Targeted Transposition in Drosophila Melanogaster." *Genetics* 151 (3): 1093–1101.

Shatkin, A J. 1976. "Capping of Eucaryotic mRNAs." *Cell* 9 (4 PART 2): 645–53. doi:10.1016/0092-8674(76)90128-8.

Shaw, R J, J G Paez, M Curto, A Yaktine, W M Pruitt, I Saotome, J P O'Bryan, et al. 2001. "The Nf2 Tumor Suppressor, Merlin, Functions in Rac-Dependent Signaling." *Developmental Cell* 1 (1): 63–72. doi:10.1016/S1534-5807(01)00009-0.

Sherman, L, H M Xu, R T Geist, S Saporito-Irwin, N Howells, H Ponta, P Herrlich, and D H Gutmann. 1997. "Interdomain Binding Mediates Tumor Growth Suppression by the NF2 Gene Product." *Oncogene* 15 (20): 2505–9. doi:10.1038/sj.onc.1201418.

Sjöblom, T, S Jones, L D Wood, D Parsons, J Lin, T D Barber, D Mandelker, et al. 2006. "The Consensus Coding Sequences of Human Breast and Colorectal Cancers." *Science* 314 (5797): 268–74. doi:10.1126/science.1133427.

Slattery, W H. 2015. "Neurofibromatosis Type 2." *Otolaryngologic Clinics of North America* 48 (3): 443–60. doi:10.1016/j.otc.2015.02.005.

Smibert, C A, Y S Lie, W Shillinglaw, W J Henzel, and P M Macdonald. 1999. "Smaug, a Novel and Conserved Protein, Contributes to Repression of Nanos mRNA Translation in Vitro." *RNA* 5 (12): 1535–47. doi:10.1017/S1355838299991392.

Smibert, C A, J E Wilson, K Kerr, and P M Macdonald. 1996. “Smaug Protein Represses Translation of Unlocalized Nanos mRNA in the Drosophila Embryo.” *Genes and Development* 10 (20): 2600–2609. doi:10.1101/gad.10.20.2600.

Sonenberg, N, M A Morgan, W C Merrick, and A J Shatkin. 1978. “A Polypeptide in Eukaryotic Initiation Factors That Crosslinks Specifically to the 5′-terminal Cap in mRNA.” *PNAS* 75 (10): 4843–47. doi:10.1073/pnas.75.10.4843.

Song, Yan, and Bingwei Lu. 2011. “Regulation of Cell Growth by Notch Signaling and Its Differential Requirement in Normal vs. Tumor-Forming Stem Cells in Drosophila.” *Genes and Development* 25 (24): 2644–58. doi:10.1101/gad.171959.111.

Sonoda, J, and R P Wharton. 2001. “Drosophila Brain Tumor Is a Translational Repressor.” *Genes and Development* 15 (6): 762–73. doi:10.1101/gad.870801.

Speck, O, S C Hughes, N K Noren, R M Kulikauskas, and R G Fehon. 2003. “Moesin Functions Antagonistically to the Rho Pathway to Maintain Epithelial Integrity.” *Nature* 421 (6918): 83–87. doi:10.1038/nature01295.

Stebbins-Boaz, B, Q Cao, C H de Moor, R Mendez, and J D Richter. 1999. “Maskin Is a CPEB-Associated Factor That Transiently Interacts with eIF-4E.” *Molecular Cell* 4 (6): 1017–27. doi:10.1016/S1097-2765(00)80230-0.

Stern, Curt. 1941a. “The Growth of Testes in Drosophila. I. The Relation between Vas Deferens and Testis within Various Species.” *Journal of Experimental Zoology* 87 (1): 113–58. doi:10.1002/jez.1400870109.

———. 1941b. “The Growth of Testes in Drosophila II. The Nature of Interspecific Differences.” *Journal of Experimental Zoology* 87 (1): 159–80. doi:10.1002/jez.1400870110.

Susic-Jung, Loreen, Christina Hornbruch-Freitag, Jessica Kuckwa, Karl Heinz Rexer, Uwe Lammel, and Renate Renkawitz-Pohl. 2012. “Multinucleated Smooth Muscles and Mononucleated as Well as Multinucleated Striated Muscles Develop during Establishment of the Male Reproductive Organs of Drosophila Melanogaster.” *Developmental Biology* 370 (1): 86–97. doi:10.1016/j.ydbio.2012.07.022.

Tautz, D, and C Pfeifle. 1989. “A Non-Radioactive in Situ Hybridization Method for the Localization of Specific RNAs in Drosophila Embryos Reveals Translational Control of the Segmentation Gene Hunchback.” *Chromosoma* 98 (2): 81–85.

Taylor, A M, J Wu, H-C Tai, and E M Schuman. 2013. “Axonal Translation of β-Catenin Regulates Synaptic Vesicle Dynamics.” *Journal of Neuroscience* 33 (13): 5584–89. doi:10.1523/JNEUROSCI.2944-12.2013.

Tikoo, A, M Varga, V Ramesh, J Gusella, and H Maruta. 1994. "An Anti-Ras Function of Neurofibromatosis Type 2 Gene Product (NF2/Merlin)." *The Journal of Biological Chemistry* 269 (38): 23387–90.

Tokuyasu, K T. 1975. "Dynamics of Spermiogenesis in Drosophila Melanogaster. VI. Significance Of 'onion' nebenkern Formation." *Journal of Ultrasructure Research* 53 (1): 93–112. doi:10.1016/S0022-5320(75)80089-X.

Tokuyasu, K T, W J Peacock, and R W Hardy. 1972a. "Dynamics of Spermiogenesis in Drosophila Melanogaster. I. Individualization Process." *Zeitschrift Fuïr Zellforschung Und Mikroskopische Anatomie* 124 (4): 479–506. doi:10.1007/BF00335253.

———. 1972b. "Dynamics of Spermiogenesis in Drosophila Melanogaster - II. Coiling Process." *Zeitschrift Für Zellforschung Und Mikroskopische Anatomie* 127 (4): 492–525. doi:10.1007/BF00306868.

Toledano, H, C D'Alterio, M Loza-Coll, and D L Jones. 2012. "Dual Fluorescence Detection of Protein and RNA in Drosophila Tissues." *Nature Protocols* 7 (10): 1808–17. doi:10.1038/nprot.2012.105.

Tomoo, K, X Shen, K Okabe, Y Nozoe, S Fukuhara, S Morino, M Sasaki, et al. 2003. "Structural Features of Human Initiation Factor 4E, Studied by X-Ray Crystal Analyses and Molecular Dynamics Simulations." *Journal of Molecular Biology* 328 (2): 365–83. doi:10.1016/S0022-2836(03)00314-0.

Topisirovic, I, M Ruiz-Gutierrez, and K L B Borden. 2004. "Phosphorylation of the Eukaryotic Translation Initiation Factor eIF4E Contributes to Its Transformation and mRNA Transport Activities." *Cancer Research* 64 (23): 8639–42. doi:10.1158/0008-5472.CAN-04-2677.

Troca-Marín, J A, A Alves-Sampaio, and M L Montesinos. 2012. "Deregulated mTOR-Mediated Translation in Intellectual Disability." *Progress in Neurobiology* 96 (2): 268–82. doi:10.1016/j.pneurobio.2012.01.005.

Trofatter, J A, M M MacCollin, J L Rutter, J R Murrell, M P Duyao, D M Parry, R Eldridge, N Kley, A G Menon, and K Pulaski. 1993. "A Novel Moesin-, Ezrin-, Radixin-like Gene Is a Candidate for the Neurofibromatosis 2 Tumor Suppressor." *Cell* 72 (5): 791–800. doi:10.1016/0092-8674(93)90406-G.

Truman, J W, and M Bate. 1988. "Spatial and Temporal Patterns of Neurogenesis in the Central Nervous System of Drosophila Melanogaster." *Developmental Biology* 125 (1): 145–57. doi:10.1016/0012-1606(88)90067-X.

Tsukita, S, K Oishi, N Sato, J Sagara, A Kawai, and S Tsukita. 1994. "ERM Family Members as Molecular Linkers between the Cell Surface Glycoprotein CD44 and Actin-Based Cytoskeletons." *Journal of Cell Biology* 126 (2): 391–401. doi:10.1083/jcb.126.2.391.

Tulina, N, and E Matunis. 2001. "Control of Stem Cell Self-Renewal in Drosophila Spermatogenesis by JAK-STAT Signaling." *Science* 294 (5551): 2546–49. doi:10.1126/science.1066700.

Turunen, Ossi, Torsten Wahlström, and Antti Vaheri. 1994. "Ezrin Has a COOH-Terminal Actin-Binding Site That Is Conserved in the Ezrin Protein Family." *Journal of Cell Biology* 126 (6): 1445–53. doi:10.1083/jcb.126.6.1445.

Urbach, R, R Schnabel, and G M Technau. 2003. "The Pattern of Neuroblast Formation, Mitotic Domains and Proneural Gene Expression during Early Brain Development in Drosophila." *Development* 130 (16): 3589–3606. doi:10.1242/dev.00528.

Valzania, L, H Ono, M Ignesti, V Cavaliere, F Bernardi, C Gamberi, P Lasko, and G Gargiulo. 2016. "Drosophila 4EHP Is Essential for the Larval-Pupal Transition and Required in the Prothoracic Gland for Ecdysone Biosynthesis." *Developmental Biology* 410 (1): 14–23. doi:10.1016/j.ydbio.2015.12.021.

Villaescusa, J C, C Buratti, D Penkov, L Mathiasen, J Planagumà, E Ferretti, and F Blasi. 2009. "Cytoplasmic Prep1 Interacts with 4EHP Inhibiting Hoxb4 Translation." Edited by Michael Polymenis. *PLoS ONE* 4 (4): e5213. doi:10.1371/journal.pone.0005213.

von der Haar, T, J D Gross, G Wagner, and J E G McCarthy. 2004. "The mRNA Cap-Binding Protein eIF4E in Post-Transcriptional Gene Expression." *Nature Structural & Molecular Biology* 11 (6): 503–11. doi:10.1038/nsmb779.

Wang, D O, S M Kim, Y Zhao, H Hwang, S K Miura, W S Sossin, and K C Martin. 2009. "Synapse- and Stimulus-Specific Local Translation during Long-Term Neuronal Plasticity." *Science* 324 (5934): 1536–40. doi:10.1126/science.1173205.

Wang, S, I B Rosenwald, M J Hutzler, G A Pihan, L Savas, J-J Chen, and B A Woda. 1999. "Expression of the Eukaryotic Translation Initiation Factors 4E and 2α in Non-Hodgkin's Lymphomas." *The American Journal of Pathology* 155 (1): 247–55. doi:10.1016/S0002-9440(10)65118-8.

Waskiewicz, A J, A Flynn, C G Proud, and J A Cooper. 1997. "Mitogen-Activated Protein Kinases Activate the Serine/threonine Kinases Mnk1 and Mnk2." *EMBO Journal* 16 (8): 1909–20. doi:10.1093/emboj/16.8.1909.

Wharton, R P, and G Struhl. 1991. "RNA Regulatory Elements Mediate Control of Drosophila Body Pattern by the Posterior Morphogen Nanos." *Cell* 67 (5): 955–67. doi:10.1016/0092-8674(91)90368-9.

White, K, M E Grether, J M Abrams, L Young, K Farrell, and H Steller. 1994. "Genetic Control of Programmed Cell Death in Drosophila." *Science* 264 (5159): 677–83. doi:10.1126/science.8171319.

Wilk, R, S U M Murthy, H Yan, and H M Krause. 2010. "In Situ Hybridization: Fruit Fly Embryos and Tissues." In *Current Protocols Essential Laboratory Techniques*, 1–24. Hoboken, NJ, USA: John Wiley & Sons, Inc. doi:10.1002/9780470089941.et0903s04.

Winberg, M L, S E Perez, and H Steller. 1992. "Generation and Early Differentiation of Glial Cells in the First Optic Ganglion of Drosophila Melanogaster." *Development* 115 (4): 903–11. http://www.ncbi.nlm.nih.gov/pubmed/1451666.

Wong, HK, A Shimizu, ND Kirkpatrick, I Garkavtsev, AW Chan, E di Tomaso, M Klagsbrun, and RK Jain. 2012. "Merlin/NF2 Regulates Angiogenesis in Schwannomas through a Rac1/semaphorin 3F-Dependent Mechanism." *Neoplasia* 14 (2): 84–94. doi:10.1593/neo.111600.

Xu, H M, and D H Gutmann. 1998. "Merlin Differentially Associates with the Microtubule and Actin Cytoskeleton." *Journal of Neuroscience Research* 51 (3): 403–15. doi:10.1002/(SICI)1097-4547(19980201)51:3<403::AID-JNR13>3.0.CO;2-7.

Xu, Shuwa, Sanjay Tyagi, and Paul Schedl. 2014. "Spermatid Cyst Polarization in Drosophila Depends upon Apkc and the CPEB Family Translational Regulator orb2." *PLoS Genetics* 10 (5). doi:10.1371/journal.pgen.1004380.

Xu, T, Y Zong, L Peng, S Kong, M Zhou, J Zou, J Liu, R Miao, X Sun, and L Li. 2016. "Overexpression of eIF4E in Colorectal Cancer Patients Is Associated with Liver Metastasis." *Onco Targets and Therapy* 9: 815–22. doi:10.2147/OTT.S98330.

Xu, X, J Vatsyayan, C Gao, C J Bakkenist, and J Hu. 2010. "Sumoylation of eIF4E Activates mRNA Translation." *EMBO Reports* 11 (4): 299–304. doi:10.1038/embor.2010.18.

Yaegashi, S, R Sachse, N Ohuchi, S Mori, and T Sekiya. 1995. "Low Incidence of a Nucleotide Sequence Alteration of the Neurofibromatosis 2 Gene in Human Breast Cancers." *Jpn J Cancer Res* 86 (10): 929–33. doi:0910505095967876 [pii].

Yamashita, Y M, D L Jones, and M T Fuller. 2003. "Orientation of Asymmetric Stem Cell Division by the APC Tumor Suppressor and Centrosome." *Science* 301 (5639): 1547–50. doi:10.1126/science.1087795.

Yang, G, C A Smibert, D R Kaplan, and F D Miller. 2014. "An eIF4E1/4E-T Complex Determines the Genesis of Neurons from Precursors by Translationally Repressing a Proneurogenic Transcription Program." *Neuron* 84 (4): 723–39. doi:10.1016/j.neuron.2014.10.022.

Yang, Y, D A Primrose, A C Leung, R B Fitzsimmons, M C McDermand, A Missellbrook, J Haskins, A S Smylie, and S C Hughes. 2012. "The PP1 Phosphatase Flapwing Regulates the Activity of Merlin and Moesin in Drosophila." *Developmental Biology* 361 (2): 412–26. doi:10.1016/j.ydbio.2011.11.007.

Yarunin, A, R E Harris, M P Ashe, and H L Ashe. 2011. "Patterning of the Drosophila Oocyte by a Sequential Translation Repression Program Involving the d4EHP and Belle Translational Repressors." *RNA Biology* 8 (5): 904–12. doi:10.4161/rna.8.5.16325.

Yi, C, S Troutman, D Fera, A Stemmer-Rachamimov, J L Avila, N Christian, N L Persson, et al. 2011. "A Tight Junction-Associated Merlin-Angiomotin Complex Mediates Merlin's Regulation of Mitogenic Signaling and Tumor Suppressive Functions." *Cancer Cell* 19 (4): 527–40. doi:10.1016/j.ccr.2011.02.017.

Yin, F, J Yu, Y Zheng, Q Chen, N Zhang, and D Pan. 2013. "Spatial Organization of Hippo Signaling at the Plasma Membrane Mediated by the Tumor Suppressor merlin/NF2." *Cell* 154 (6): 1342–55. doi:10.1016/j.cell.2013.08.025.

Yonemura, S, M Hirao, Y Doi, N Takahashi, T Kondo, S Tsukita, and S Tsukita. 1998. "Ezrin/radixin/moesin (ERM) Proteins Bind to a Positively Charged Amino Acid Cluster in the Juxta-Membrane Cytoplasmic Domain of CD44, CD43, and ICAM-2." *Journal of Cell Biology* 140 (4): 885–95. doi:10.1083/jcb.140.4.885.

Yu, F X, B Zhao, and K L Guan. 2015. "Hippo Pathway in Organ Size Control, Tissue Homeostasis, and Cancer." *Cell* 163 (4): 811–28. doi:10.1016/j.cell.2015.10.044.

Zaffran, S, M Astier, D Gratecos, and M Sémériva. 1997. "The Held out Wings (How) Drosophila Gene Encodes a Putative RNA-Binding Protein Involved in the Control of Muscular and Cardiac Activity." *Development* 124 (10): 2087–98. http://www.ncbi.nlm.nih.gov/pubmed/9169854.

Zhan, Y, N Modi, A M Stewart, R I Hieronimus, J Liu, D H Gutmann, and D N Chadee. 2011. "Regulation of Mixed Lineage Kinase 3 Is Required for Neurofibromatosis-2-Mediated Growth Suppression in Human Cancer." *Oncogene* 30 (7): 781–89. doi:10.1038/onc.2010.453.Regulation.

Zhang, N, H Bai, K K David, J Dong, Y Zheng, J Cai, M Giovannini, P Liu, R A Anders, and D Pan. 2010. "The Merlin/NF2 Tumor Suppressor Functions through the YAP Oncoprotein to Regulate Tissue Homeostasis in Mammals." *Developmental Cell* 19 (1): 27–38. doi:10.1016/j.devcel.2010.06.015.

Zhu, C C, J Q Boone, P A Jensen, S Hanna, L Podemski, J Locke, C Q Doe, and M B O'Connor. 2008. "Drosophila Activin- and the Activin-like Product Dawdle Function Redundantly to Regulate Proliferation in the Larval Brain." *Development* 135 (3): 513–21. doi:10.1242/dev.010876.

Zoch, A, S Mayerl, A Schulz, T Greither, L Frappart, J Rübsam, H Heuer, M Giovannini, and H Morrison. 2015. "Merlin Isoforms 1 and 2 Both Act as Tumour Suppressors and Are Required for Optimal Sperm Maturation." Edited by Stefan Schlatt. *PloS One* 10 (8): e0129151. doi:10.1371/journal.pone.0129151.

Zuberek, J, K Kuchta, G Hernández, N Sonenberg, and K Ginalski. 2016. "Diverse Cap-Binding Properties of Drosophila eIF4E Isoforms." *Biochimica et Biophysica Acta (BBA) - Proteins and Proteomics* 1864 (10): 1292–1303. doi:10.1016/j.bbapap.2016.06.015.

Appendix

Additional IF labelling observed with α-eIF4E-3 antibodies #23 and #968

In addition to embryos, testes, third instar larval brains, and pupal wings, labelling by Ab#23 was observed in brains and retinae of w^{1118} animals beginning in third instar larvae, throughout pupal development, and in adults. In the larval eye disc, Ab#23 signal is observed at the membrane of photoreceptor cells (Figure A1A), and this localisation is preserved in pupae 13h APF (Figure A1C) and 25h APF (Figure A1E). In eyes 48h APF and in the adult retina, Ab#23 signal shifts to accessory cells (Figure A1G,I). The two most prominent cells and their axons observed with Ab#23 in third instar larval brains (arrows in Figure A1B) are seen throughout pupal development (arrows in Figure A1D,F,G) and in adult brains (arrows in Figure A1J). Additional labelling is seen in 24h APF and 48h APF brains and in adult brains, most notably at the anterior of the brain and the distal tip of the ventral nerve cord. With the exception of third instar larval brains, tissues described here were not examined for specificity of the labelling by IF using tissue from eIF4E-3 null animals.

Embryos 12-16h AEL were observed to be labelled by Ab#23 in a pattern of two cells per segment within the ventral nerve cord (Figure A2A-B'), but these cells were also labelled in eIF4E-3 null embryos, indicating that the pattern is non-specific (see Figure 8D-E'). With Ab#968, embryos 12-16h AEL were labelled similarly, although more than two cells appeared to be labelled in each segment (Figure A2C-D'). This antibody was not tested against eIF4E-3 null embryos. IF with Ab#53 was also attempted with embryos of the same age, but no signal was observed. In larval brains, labelling with Ab#53 was not seen except when a PLP fix was used, so potentially the antibody is not compatible with the standard fix used for embryo IF, but no additional fixation methods were tested. Additionally, the embryo IF protocol was carried out with embryos 12-16h AEL, incubating with rabbit pre-immune serum instead of an α-eIF4E-3 primary antibody as a negative control. No labelling above background was observed (Figure

A2E-E'), indicating that the precise but non-specific pattern seen with Ab#23 is not caused by a factor particular to normal rabbit serum.

Before the labelling seen in third instar larval brains and in embryos with Ab#23 was determined to be non-specific by pattern retention in confirmed null mutants, identification of the apparent cell bodies labelled by Ab#23 was attempted (Table A1). For some markers an antibody was available, so IF was carried out on w^{1118} larval brains or embryos 12-16h AEL, incubating with both Ab#23 and the antibody marker tested, and tissues were observed for overlap in fluorescent signal. For other markers, *GAL4* lines were used to drive expression of GFP in specific cells, and IF was carried out on embryos or dissected brains with Ab#23 to look for overlap between the antibody and GFP signals. Some of the tests using driver lines were inconclusive as GFP did not appear to be expressed where it was expected to be, and may have been more successful if an α-GFP antibody was used or if crosses were kept at 29°C.

In the male germline, eIF4E-3 expression has been previously reported to be in spermatocytes and early spermatids based on IF analysis with Ab#968 (Hernández et al. 2012). This expression pattern was observed with all antibodies tested and by FISH; however, with Ab#23 additional localisation of eIF4E-3 was observed associated with individualising spermatid bundles (Figure A3). In cells at this stage in spermatogenesis, Ab#23 signal was observed at the front of the actin cones as the individualisation complex moves away from the needle-shaped nuclei. Furthermore, when observed from an angle directly facing the front of the individualisation complex, Ab#23 labelling is restricted to a ring on each actin cone. As eIF4E-3 null animals have defective spermatogenesis that does not progress to the individualisation stage, it was not possible to test the specificity of this localisation by examination of *eIF4E-3* mutants. Perhaps if *eIF4E-3* could be specifically knocked down post-meiosis, the lack of localisation in individualising spermatid bundles could be confirmed and its effect determined.

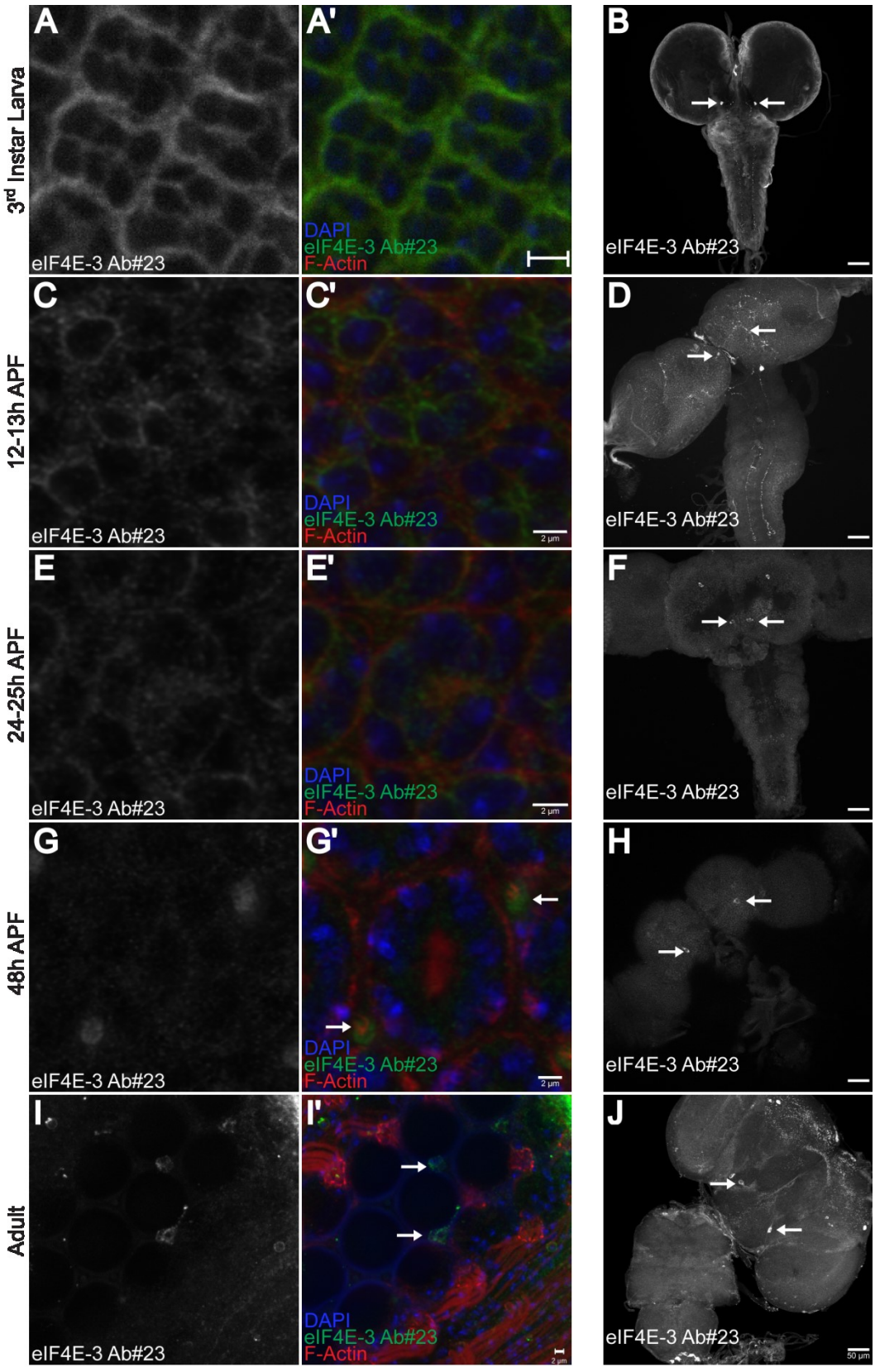
3rd Instar Larva
12-13h APF
24-25h APF
48h APF
Adult
A
A'
B
C
C'
D
E
E'
F
G
G'
H
I
I'
J
eIF4E-3 Ab#23
DAPI
eIF4E-3 Ab#23
F-Actin
2 µm
50 µm

Figure A1 | IF analysis with Ab#23 in larval, pupal, and adult retinae and brains. (A-A') Ab#23 signal is seen at the membrane of photoreceptor cells in the eye disc of third instar larvae. (B) Two cell bodies (arrows) and apparent axon projections down the length of the ventral nerve cord are labelled by Ab#23 in the central nervous system of third instar larvae. (C-C') Fluorescent signal corresponding to Ab#23 is seen at photoreceptor cell membranes in 13h APF eyes. (D) The two cell bodies seen in larval brains are also labelled in the 12h APF brain (arrows). (E-E') In 25h APF eyes, signal for Ab#23 continues to be observed at photoreceptor cell membranes. (F) In the 24h APF brain, Ab#23 labels two cell bodies as seen in larval and 12h APF brains (arrows), as well as two additional cell bodies at a more anterior position. (G-G') Ab#23 labelling in the retina is altered compared with previous developmental stages at 48h APF; rather than photoreceptor cell membranes, Ab#23 appears to be labelling accessory cells. (H) Ab#23 continues to label two prominent cell bodies (arrows) in brains 48h APF. (I-I') IF in the adult retina shows labelling of accessory cells, as in the 48h APF retina. (J) Two cell bodies are still labelled in the adult brain (arrows). Additional signal is seen toward the anterior of the adult brain, and in cell bodies at the tip of the ventral nerve cord. Scale bars in A',C',E',G',I': 2 μm ; scale bars in B,D,F,H,J: 50 μm

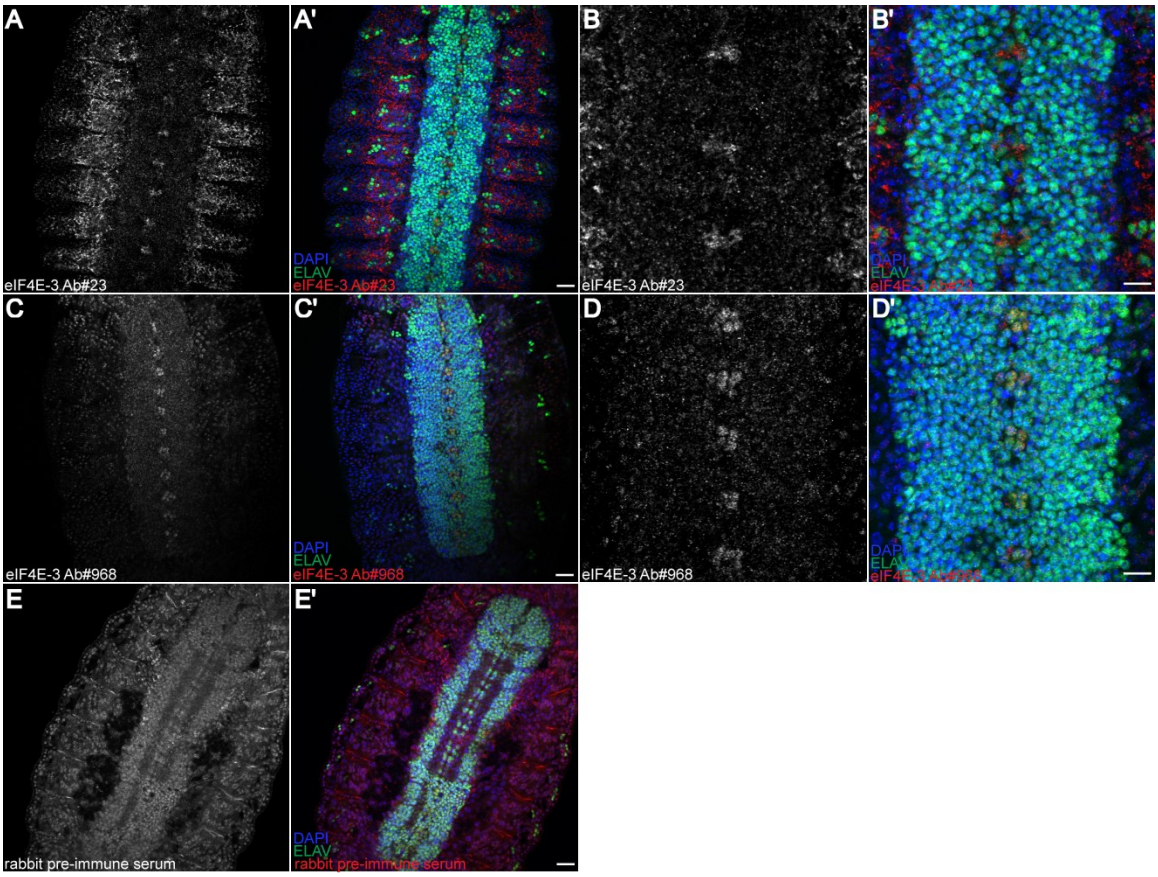

Figure A2 | IF of embryos 12-16h AEL shows similar signal with two peptide antibodies, Ab#23 and Ab#968. (A-A') Ab#23 labels two cells per segment in the ventral nerve cord of embryos. (B-B') Higher magnification of A-A'. (C-C') Ab#968 signal is very similar to that of Ab#23, but up to four cells per segment are labelled. (D-D') Higher magnification of C-C'. (E-E') Embryos incubated with rabbit pre-immune serum rather than primary antibody, as a negative control, have high background but no specific signal.

Scale bars in A',C',E': 20 μm ; scale bars in B',D': 10 μm

Table A1 | Markers tested for identification of cells labelled by Ab#23 in embryos 12-16h AEL and third instar larval brains.

Marker/Driver	Antibody / Fly Stock	12-16h Embryos	Larval Brains
Chaoptin	DSHB 24B10	not tested	overlap
Engrailed	DSHB 4D9	no overlap	not tested
Futsch	DSHB 22C10	no overlap	not tested
Pericardin	DSHB EC11	inconclusive	not tested
Single-Minded	DSHB	no overlap	not tested
Wrapper	DSHB 10D3	no overlap	no overlap
Ilp2	*Ilp2-GAL4*	not tested	potential overlap
dMP2	*dMP2-GAL4*	not tested	no overlap
Mz97-GAL4	*Mz97-GAL4* (BL9488)	not tested	no overlap
Per	*Per-GAL4* (BL7127)	not tested	no overlap
Ple	*Ple-GAL4* (BL8848)	inconclusive	no overlap
Vglut	*Vglut-GAL4* (BL24635)	not tested	no overlap
R15E08	Janelia line BL47324	not tested	inconclusive
R20D07	Janelia line BL49848	not tested	no overlap
R22G09	Janelia line BL48040	not tested	inconclusive
R32F03	Janelia line BL45588	not tested	inconclusive
R33G09	Janelia line BL49365	not tested	inconclusive
R41D06	Janelia line BL38876	not tested	no overlap
R42B10	Janelia line BL50146	not tested	no overlap
R73H06	Janelia line BL47396	not tested	inconclusive

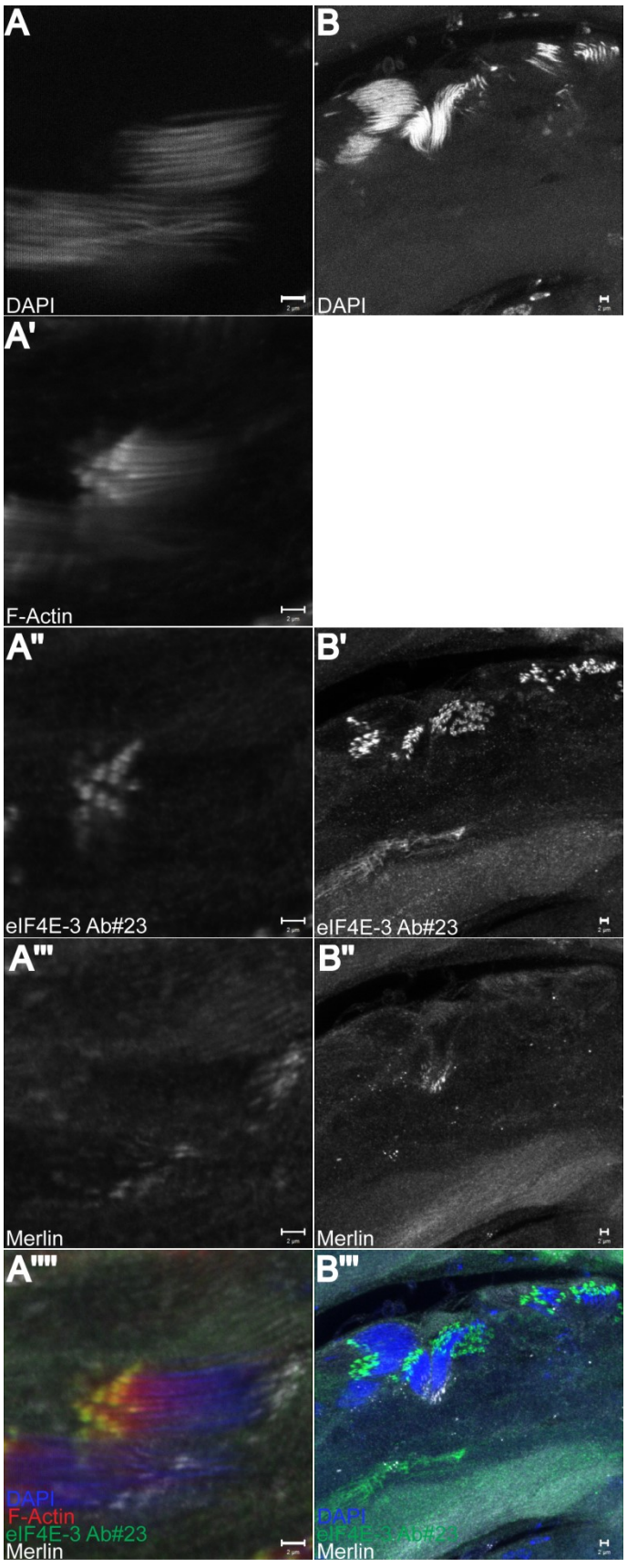
A
DAPI
B
DAPI
A'
F-Actin
A"
eIF4E-3 Ab#23
B'
eIF4E-3 Ab#23
A'''
Merlin
B"
Merlin
A''''
DAPI
F-Actin
eIF4E-3 Ab#23
Merlin
B'''
DAPI
Merlin

Figure A3 | IF analysis of the male germline with α-eIF4E-3 Ab#23 shows labelling of individualising spermatid bundles. (A-A'''') Ab#23 labels individualising spermatid bundles, identified by presence of the actin-based individualisation complex, at the advancing end of the individualisation complex. (B-B''') When spermatid bundles are viewed end-on, Ab#23 labelling is restricted to a ring at the front of each actin cone in the individualisation complex.
Scale bars: 2 μm

Potential alteration of eIF4E-3 post-translational modification in eIF4E-3^{IIIa239} and eIF4E-3^{IIIa278}

Western blot analysis was carried out with lysates of testes and ovaries from animals with the alleles *eIF4E-3^{L0139}*, *eIF4E-3^{IIIa239}*, and *eIF4E-3^{IIIa278}* in trans with *Df(3L)BSC732* alongside *w^{1118}* control tissues to confirm absence of detectable eIF4E-3 expression in ovaries, and to determine if eIF4E-3 is expressed in the male germline with each allele. As observed previously, eIF4E-3 is recognised as a double band in *w^{1118}* testes lysates (Figure A1). No eIF4E-3 band is recognised in lysates of ovaries or in *eIF4E-3^{L0139}/Df(3L)BSC732* testes lysates. Lysates of *eIF4E-3^{IIIa239}/Df(3L)BSC732* testes show an absence of the higher molecular weight band, while the lower band is missing in *eIF4E-3^{IIIa278}/Df(3L)BSC732*. The two group IIIa alleles in trans with each other have a double band as in the control; however, the upper band is more prominent than the lower, which is opposite of what is observed in *w^{1118}* lysates. Potentially the appearance of two bands indicates post-translational modification, as phosphorylation or sumoylation of eIF4E has been shown to occur and to affect its function (Joshi et al. 1995; Xu et al. 2010), and the group IIIa alleles affect the capacity to be modified. Although *Drosophila* eIF4E-3 lacks the phosphorylation site equivalent to mammalian S209 (Hernández et al. 2005), it is not known if eIF4E-3 is post-translationally modified.

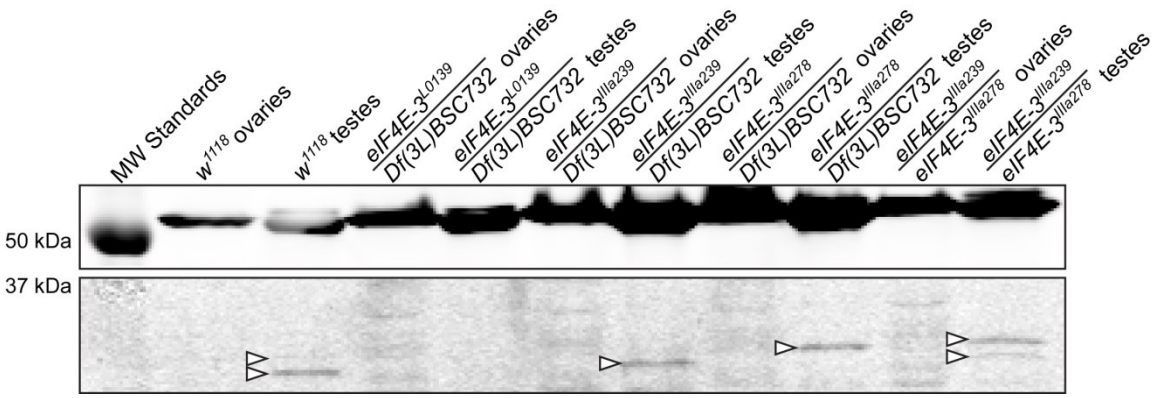

Figure A4 | *eIF4E-3^{IIIa239}* and *eIF4E-3^{IIIa278}* alleles each cause loss of part of the eIF4E-3 band doublet in Western blot analysis of testes lysates. Lysates of adult testes and ovaries of each genotype were analysed by Western blot with Ab#53 to determine presence or absence of protein in each tissue and in each genotype. A double band near the predicted molecular weight of eIF4E-3 (28.5 kDa) is observed in lysate of *w^{1118}* testes, but not ovaries. Similarly, no bands are observed in ovary lysates from any other genotype. No bands are present in *eIF4E-3^{L0139}/Df(3L)BSC732* testes lysate, indicating absence of protein with the *eIF4E-3^{L0139}* allele. With the *eIF4E-3^{IIIa239}* allele, protein is not absent, but only a single band is observed, apparently corresponding to the lower molecular weight band of the doublet observed in *w^{1118}* testes lysate. Only the higher molecular weight band is observed in *eIF4E-3^{IIIa278}/Df(3L)BSC732* testes lysate. When the two group IIIa alleles are together in trans, two bands are present in the testes lysate, but the band at a higher molecular weight is more prominent whereas the lower molecular weight band is more prominent in *w^{1118}*.